DISSOLUTION OF NON-FUNCTIONALIZED AND FUNCTIONALIZED NANOMATERIALS IN SIMULATED BIOLOGICAL AND ENVIRONMENTAL FLUIDS

Odwa Mbanga

A thesis submitted to the Faculty of Science, University of the Witwatersrand, Johannesburg, in fulfilment of the requirements for the degree of Doctor of philosophy

University of the Witwatersrand

Johannesburg

2023

Declaration

I declare that this dissertation is my own unaided work. It is being submitted for the degree of Doctor of Philosophy at the University of the Witwatersrand, Johannesburg. It has not been submitted before for any degree or examination at any university.

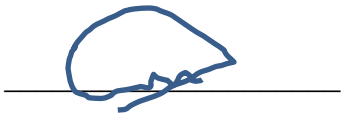

(Signature of candidate)

19/ June/2023

List of publications

1. **Dissolution of citrate stabilized, polyethylene glycol coated carboxyl and amine functionalized gold nanoparticles in simulated biological fluids and environmental media.** Odwa Mbanga, Ewa Cukrowska, Mary Gulumian. Published in the Journal of Nanoparticle Research (2021). https://doi.org/10.1007/s11051-020-05132-x

2. **Dissolution kinetics of silver nanoparticles: Behaviour in simulated biological fluids and synthetic environmental media.** Odwa Mbanga, Ewa Cukrowska, Mary Gulumian. Published in Toxicology Reports (2022). https://doi.org/10.1016/j.toxrep.2022.03.044

3. **Dissolution of titanium dioxide nanoparticles in synthetic biological and environmental media to predict their biodurability and persistence.** Odwa Mbanga, Ewa Cukrowska, Mary Gulumian. Published in Toxicology in Vitro (2022). https://doi.org/10.1016/j.tiv.2022.105457

4. **A comparative study of the biodurability and persistence of gold, silver and titanium dioxide nanoparticles using the continuous flow through system.** Odwa Mbanga, Ewa Cukrowska, Mary Gulumian. Published in Nanomaterials MDPI (2023). https://doi.org/10.3390/nano13101653

Contribution of authors

The principal author, Odwa Mbanga contributed to the conceptualization, methodology, validation, formal analysis, investigation and writing the original draft of all the manuscripts and published articles presented in this thesis. The co-authors who are also the supervisors of the PhD study assisted with editing the drafted manuscripts and made suggestions for improvement.

Abstract

The incorporation of nanoparticles in consumer products is exponentially high, however, research into their behaviour in biological and environmental surroundings is still very limited. In the present study, the static system and the continuous flow-through dissolution protocols were utilized to evaluate and elucidate the dissolution behaviour of gold, silver, and titanium dioxide nanoparticles. The behaviour of these particles was studied in a range of artificial physiological fluids and environmental media, to obtain a more precise comprehension of how they would react in the human body and the environment. The biodurability and persistence were estimated by calculating the dissolution kinetics of the nanoparticles in artificial physiological fluids and environmental media. The details of the current research are described as follows:

An investigation into the dissolution of non-functionalized and functionalized gold nanoparticles was conducted as the first component of the research, examining the effect of surface functionalization on dissolution. The study determined the dissolution rates of functionalized and non-functionalized gold nanoparticles. Dissolution was observed to be significantly higher in acidic media than in alkaline media. The nanoparticle surface modification, particle aggregation, and chemical composition of the simulated fluid significantly affected the dissolution rate. It was concluded that gold nanoparticles are biodurable and have the potential to cause long-term health effect as well as high environmental persistency. This work has been published in the Journal of Nanoparticle Research and is presented in this thesis as **Paper 1**.

Silver nanoparticles were also included in this study because they have many applications and industrial purposes. Therefore, their risk assessment was also of utmost importance. The results indicated that silver nanoparticle solubility was influenced by the alkalinity and acidity of artificial media. Low pH values and high ionic strength encouraged silver nanoparticle dissolution and accelerated the dissolution rate. The agglomeration state and reactivity of the particles changed upon exposure to simulated fluids, though their shape remained the same. The fast

dissolution rates in most fluids indicated that the release of silver ions would cause short-term effects. This work has been published in Toxicology Reports and has been presented in this thesis as **Paper 2**.

Although titanium dioxide nanoparticles are insoluble and undergo negligible dissolution, it was of utmost importance to investigate their behaviour in biological and environmental surroundings. This is as a result of the incorporation of these particles in everyday consumer products, in the nanosized range which raises concerns about their safety. Therefore, in Paper 3 presented in this thesis the dissolution kinetics of titanium dioxide nanoparticles in simulated body fluids representative of the lungs, stomach, blood plasma and media representing the aquatic ecosystem were investigated to anticipate how they behave *in vivo*. This work has been published in Toxicology *In Vitro* and presented in this thesis as **Paper 3**. The results indicated that titanium dioxide nanoparticles were very insoluble, and their dissolution was limited in all simulated fluids. Acidic media such as the synthetic stomach fluids were most successful in dissolving the particles, while alkaline media had lower dissolution. High ionic strength seawater also had a higher dissolution rate than freshwater. The dissolution rates of the particles were low, and their half-times were long. The results indicated that these particles could potentially cause health issues in the long term, as well as remain unchanged in the environment. This work has been published in Toxicology *In Vitro* and presented in this thesis as **Paper 3**.

The last component of the research compared the dissolution kinetics of gold, silver and titanium dioxide nanoparticles through the use of the continuous flow-through system. The findings indicated that titanium dioxide nanoparticles were the most biodurable and persistent, followed by gold and silver nanoparticles. Therefore, it was suggested that product developers should use the OECD's guidelines for testing before releasing their product to the market to ensure its safety. This work has been published in Nanomaterials MDPI and presented in this thesis as **Paper 4**.

Dedication

This thesis is dedicated to my grandfather, who did everything he could to invest in my education. It is also dedicated to my parents, siblings, and extended family members for their unwavering support.

Acknowledgements

First and foremost, I would like to thank my supervisors, Prof. Ewa Cukrowska and Prof. Mary Gulumian, for providing me with the opportunity to develop and hone my research skills and abilities through this research project. Weekly meetings and monthly progress reports kept me focused and created a productive environment. My supervisors' financial support enabled the smooth execution of this research project, for which I will be eternally grateful.

Secondly, I would like to thank Prof. Luke Chimuka and Prof. Hlanganani Tutu for always being ready and willing to offer extra help and guidance when it was needed. Outside of my academic work, I appreciate the humility and support shown to me.

I have learned so much from everyone in the Environmental Analytical Chemistry Research Group, both past and present. I truly and humbly thank you all for being the pillars of strength that I needed, from overnight study sessions to group work on projects, for always reminding me why I started this journey in the first place, and for always lending your ears regarding the progress of my research.

I will never be able to thank the Toxicology Department at the National Institute for Occupational Health (NIOH) enough for accommodating me in their offices for the duration of my research. My transition into the institute would not have been as smooth without your assistance. From the laboratory orientation to navigating the office space and teamwork, you all have played a commendable and unforgettable role in my growth, and for that I thank you from the bottom of my heart. I would also like to thank North-West University for ensuring the smooth conclusion of this research project.

I would also like to express my gratitude to my family, friends, and university colleagues for their unwavering support throughout my PhD journey.

Contents

List of figures

List of tables

Abbreviations

ABDC	Alkylbenzyldimethylammonium chloride
AuNPs	Gold nanoparticles
BP	Blood plasma
$CaCl_2$	Calcium chloride
$CaCl_2 \cdot 2H_2O$	Calcium chloride dehydrate
$C_6H_9Na_3O_9$	Sodium citrate trihydrate
$[-C_6H_8O_7]$	Citrate
$C_8H_5O_4K$	Potassium hydrogen phthalate
CH_3COONa	Sodium acetate trihydrate
[-COOH]	Carboxylic acids
$d\text{-}H_2O$	De-ionized water
FTIR	Fourier transform infrared spectroscopy
FW	Freshwater
GF	Gamble's fluid
GIF	Gastrointestinal fluid
HCl	Hydrochloric acid
HNO_3	Nitric acid
ICP-MS	Inductively coupled mass spectroscopy
LSPR	Localized surface plasmon resonance
IF	Intestinal fluid
In	Indium
KBr	Potassium bromide
KCl	Potassium chloride
$k_{dis\text{-}}$	Dissolution rate constant

$K_2HPO_4 \cdot 3H_2O$	Potassium phosphate dibasic trihydrate
$MgCl_2$	Magnesium chloride
$MgCl_2 \cdot 6H_2O$	Magnesium chloride hexahydrate
$MgSO_4$	Magnesium sulphate
[-NH2]-	Amine
NH_2CH_2COOH	Glycine
NMs	Nanomaterials
NP	Nanoparticles
PEG	Polyethylene-glycol
PSF	Artificial alveolar lysosomal fluid
Re	Rhenium
SW	Artificial sea water
NaHCO	Sodium bicarbonate
NaCl	Sodium chloride
Na_2HPO_4	Sodium phosphate dibasic
Na_2SO_4	Sodium sulphate anhydrous
$(NH_2C(CH_2OH)_3)$	tris (hydroxymethyl) aminomethane
$SrCl_2$	Strontium chloride
$t_{1/2}$	Half-time
TEM	Transmission Electron Microscopy
UV-vis	Ultraviolet Visible spectroscopy

CHAPTER 1

1 Introduction

1.1 Background

Nanotechnology is the engineering and construction of materials with a specific structure at the nanoscale, generally smaller than 100 nm (Abbasi et al. 2023; Kerin et al.2023). Nanomaterials (NMs) are used to make nanotechnology products. These are small materials that can be natural, accidental, or manufactured and comprise of particles that can be present as agglomerates or aggregates and have an exterior diameter of a hundred nanometers or less (Abbasi et al. 2023; Joseph et al. 2023; Kerin et al. 2023). The production of NMs involves the manipulation of individual atoms or molecules at the nanoscale to create materials containing very small structures (Abbasi et al. 2023; Joseph et al. 2023). These have different physical and chemical properties as shown in Figure 1.1. Nanoparticles (NPs) on the other hand are small particles between the sizes of 1 nm to 100 nm and are used as building blocks of NMs (Joseph et al. 2023).

NPs come in different shapes, sizes, compositions, and functionality depending on their intended use in vivo as represented in Figure 1.1 (Abbasi et al. 2023; Joseph et al. 2023; Kerin et al. 2023). They are made up of a myriad of substances, including metals, metal oxides, semiconductors, polymers and liposomes (Abbasi et al. 2023; Joseph et al. 2023; Kerin et al. 2023). These particles can be easily modified to create specific surface properties such as charged surfaces, hydrophobic or incorporation of targeting agents for specific applications (Abbasi et al. 2023; Joseph et al. 2023; Kerin et al. 2023). The ability to customize and alter the design

of NPs makes them highly versatile and capable of performing complex tasks within the body.

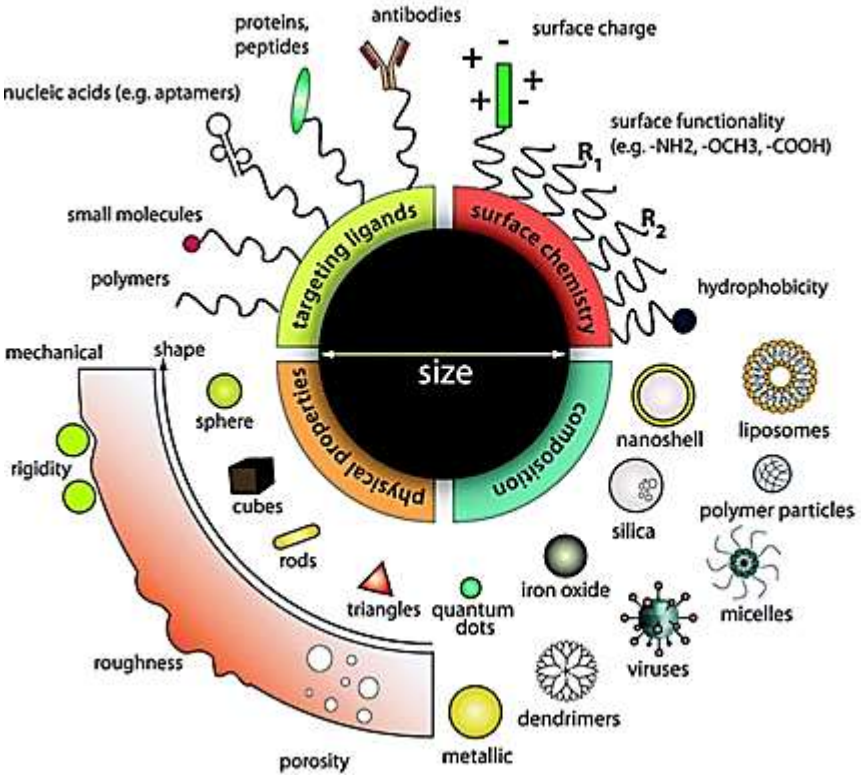

Figure 1.1: Representation of various physicochemical properties of NPs. Image obtained from Zhang, (2015).

1.2 Broader view of nanoparticles

NPs possess unique physicochemical properties such as high percentage of atoms on their surfaces making them highly reactive due to the large surface-area-to-volume-ratio, surface biocompatibility which may confer NPs with many desirable characteristics including antimicrobial properties (Mathur et al. 2018). As a result, there is an exponential growth in the manufacturing, production, and application of NPs in a myriad of consumer products. The current study focused on two metallic particles, namely gold nanoparticles (AuNPs) and silver nanoparticles (AgNPs), and one metallic oxide nanoparticle namely titanium dioxide nanoparticles (TiO_2 NPs). These particles were selected for their inherent properties, widespread applications, and incorporation into consumer products (Ganasan et al. 2023).

For example, over the last two decades AuNPs have found a great deal of application in a wide variety of areas including the field of biomedical nanotechnology (Ganasan et al. 2023; Hieu, 2017). The use AgNPs extends to various industries including agriculture, food, food packaging and cosmetics owing to their antimicrobial properties (Ganasan et al. 2023; Gottardo et al. 2021). Due to their ability to be bright and opacifying strength (Musial et al. 2020), TiO_2 NPs are incorporated in many commercial products including food items, paper and ink (Freyre-Fonseca et al. 2016).

Even though there are great benefits that the world may gain from using NPs on both the laboratory scale all the way to industrial scale, there is a considerable number of unanswered questions about their safety on biological systems and environmental surroundings. Furthermore, as the use and incorporation of NPs exponentially increases, there is an urgency to elucidate their effects in biological systems and environmental surroundings (Hieu, 2017; Kraegeloh et al. 2018; Lin et al. 2016; Oh & Park, 2014). This will translate into a need to conduct research which will assess potential risks that might be caused by NPs on biological systems and environmental surroundings, to minimize these risks or eliminate them.

Dissolution influences the behaviour of NPs in biological surroundings and in the environment (Klaessig, 2018; Sauer et al. 2021). It can be defined as the process whereby a particle enters the solution phase to create a homogenous mixture and releases ions and other species into the surrounding environment (Innes et al. 2021; Sohal et al. 2018). Dissolution influences the biodurability and persistence of nanoparticles. Biodurability is a term used to describe the particles' propensity to resist structural change by chemical decomposition, dissolution and/or catalytic disintegration in biological media (Utembe et al. 2015). Persistence refers to a particles' ability to remain unreactive in its surroundings for a prolonged time span (Sohal et al. 2018; Utembe et al. 2015). Dissolution tests may demonstrate a nanoparticle's resistance to physical, chemical and enzymatic degradation, allowing for the assessment of nanoparticles' potential toxicity over short and long time periods, as well as their ability to cause diseases (Innes et al. 2021). For instance, if

a particle has a fast rate of dissolution, there is a greater chance of immediate health impacts and its environmental consequences can be observed much quicker (Laux et al. 2017). However, particles that take a long time to dissolve are biodurable, meaning these particles can have both immediate and lasting impacts on health and can remain in the environment for extended periods of time (OECD, 2018). It has been proven that the most significant source of toxicity for NPs containing metals is the release of metal ions (Innes et al. 2021; OECD, 2018; Utembe et al. 2015).

1.3 Problem statement

Concerns have been raised about the ability of NPs to cause negative health effects and environmental harm due to their increasing prevalence in consumer items. Furthermore, the development of NPs is much faster than the understanding of the effects they may cause when they are released into the environment. The effects of NPs on living organisms have not been studied in depth, although some research on rats has been done (Gulumian & Cassee, 2021). It is still unclear if these particles will alter biological systems or if they will remain unchanged in the body until they are eliminated or metabolized.

It is therefore crucial to conduct research which will assess potential risks that might be caused by NPs in biological systems and environmental surroundings. Additionally, safety assessment of NPs should be incorporated in the early developmental stages of nano-enabled products rather than later when a nanoparticle has reached the market (Gulumian & Cassee, 2021).

This research was conducted to assess the dissolution behaviour and kinetics of gold, silver, and titanium dioxide NPs immersed in artificial physiological and environmental fluids to predict their dissolution kinetics**.**

CHAPTER 2

2 Literature review

2.1 Application of nanoparticles

2.1.1 Gold nanoparticles

Over the last two decades AuNPs have found extensive use in a wide range of fields including the biomedical field where they are used to target tumours, photothermal therapies and anti-inflammatory treatments as shown in Figure 2.1.1 (Abbasi et al. 2023; Carabineiro, 2017; Carlander et al. 2019; Fratoddi et al. 2015; Hieu, 2017). This is due to the fact that AuNPs have distinct intrinsic properties such as their optical, electronic, thermal and mechanical (Bailly et al. 2019; Elahi et al. 2018; Sani et al. 2021). Moreover, they are useful for drug delivery, medical imaging, diagnosis, chemical and biological sensing, photothermal therapy, and radiation therapy (Abbasi et al. 2023; Breitner et al.2015; Carabineiro, 2017; Elahi et al. 2018; Hieu, 2017; Sani et al. 2021). These inherent properties make them excellent biotechnology tools. Furthermore, AuNPs are increasingly being utilized in an expansive range of industries, from beverage production to environmental remediation (Elahi et al. 2018; Sani et al. 2021). For example, they are used in the oxidation of carbon monoxide, to mitigate pollution and in the purification of hydrogen and water (Sani et al. 2021).

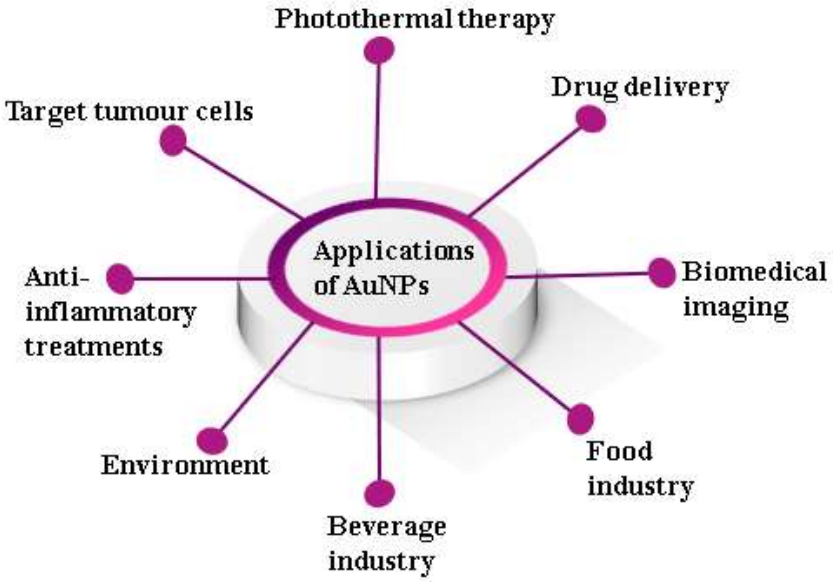

Figure 2.1.1: Applications of gold nanoparticles

2.1.2 Silver nanoparticles

AgNPs are used in a myriad of applications because of their antimicrobial activity as shown in Figure 2.1.2 including fields such as biomedical and environmental remediation (Abbasi et al. 2023; Abdelghany et al. 2018; Agrawal et al. 2018; León-Silva et al. 2016). In the field of catalysis AgNPs are incorporated in automotive catalysts, photocatalysts, solar & fuel cells and propellants (Agrawal et al. 2018; Joseph et al. 2023). They are used in these fields precisely because of their intrinsic properties such as the optical, chemical, electronic and thermal conductivity (Abbasi et al. 2023; Agrawal et al. 2018; Foldbjerg et al. 2015; Yaqoob et al. 2020). As a result, they are utilized in various industries including photonics, microelectronics and catalysis (Deshmukh et al. 2019; León-Silva et al. 2016; Yaqoob et al. 2020). Due to these properties, they are also used in the biomedical filed for imaging, bio-detection, drug delivery and bio-magnetic separations (Agrawal et al. 2018; Sharma et al. 2014). Due to their antimicrobial properties their use extends to various industrial application including water treatment, home appliances and decontamination of medical devices (Beer et al. 2012; Pareek et al. 2018; Zhang et al. 2019). For example, household products such as toys, sunscreen,

water purification systems, washing machines and surface coatings all contain AgNPs (Joseph et al. 2023). They are also used in the textile industry including a wide range of applications, ranging from food packaging materials to odour-resistant fabrics and cosmetics (Badawy et al. 2010; Behra et al. 2013; Deshmukh et al. 2019; Gottardo et al. 2021; Yaqoob et al. 2020). Lastly, medical products that contain AgNPs include wound dressing materials, surgical equipment, urinary catheters, bone prostheses etc (Hadrup et al. 2018; Mathur et al. 2018; Zhang et al. 2014).

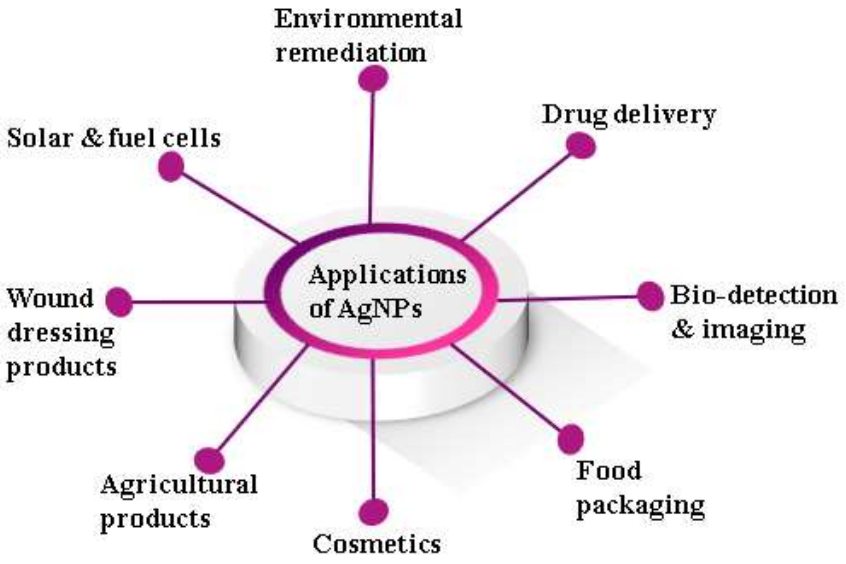

Figure 2.1.2: Applications of silver nanoparticles

2.1.3 Titanium dioxide nanoparticles

The TiO_2 NPs possess outstanding characteristics that enable them to be utilized in a vast array of industries, as indicated in Figure 2.1.3. They have distinctive thermal, electrical, optical and magnetic properties (Arun et al. 2023; Gopinath et al. 2020; Haider et al. 2019; Irshad et al. 2021; Waghmode et al. 2019). TiO_2 NPs are highly stable and insoluble in water under normal conditions, and have a high reflective index, allowing them to filter, scatter and absorb ultraviolet light (Taboada-López

et al. 2021; Yan et al. 2019). As such, they are used in the food industry as additives and nutritional supplements to improve texture, colour, flavour, and nutrient availability (Sohal et al. 2018; Waghmode et al. 2019; Wang et al. 2020). A wide variety of food products contain such as sweets, salad dressings, cheese products, chewing gums, nutritious ices, and non-dairy creamers contain them as well (aru et al. 2023; Chen et al. 2020; Taboada-López et al. 2021; Wang et al. 2022). TiO_2 NPs have been used as a pigment in paints, ink, food colouring agents, toothpaste, cosmetics (sunscreen), coatings, plastic, paper, and other products due to their ability to be bright, opacifying strength and prevent corrosion (Anupong et al., 2023; Chen et al. 2020; Irshad et al. 2021; Mercier-Bonin et al. 2018; Musial et al. 2020; Yan et al. 2019). When dispersed in water and exposed to ultraviolet light, TiO_2 nanoparticles demonstrate photoactivity leading to the production of reactive oxygen species (ROS) that can cause cell death (Kang et al. 2019; Musial et al. 2020). (Behnam et al. 2018; Ziental et al. 2020). Due to their ability to generate ROS, these particles are then used in photodynamic therapy to treat cancer cells (Behnam et al. 2018; Haider et al. 2019; Ziental et al. 2020). TiO_2 NPs possess antimicrobial properties with reports indicating their ability to photodynamically kill antibiotic-resistant bacteria (Behnam et al. 2018; Ziental et al. 2020). They are also used in the removal of environmental pollutants whereby they get incorporated in membranes used for water purification (Kang et al. 2019).

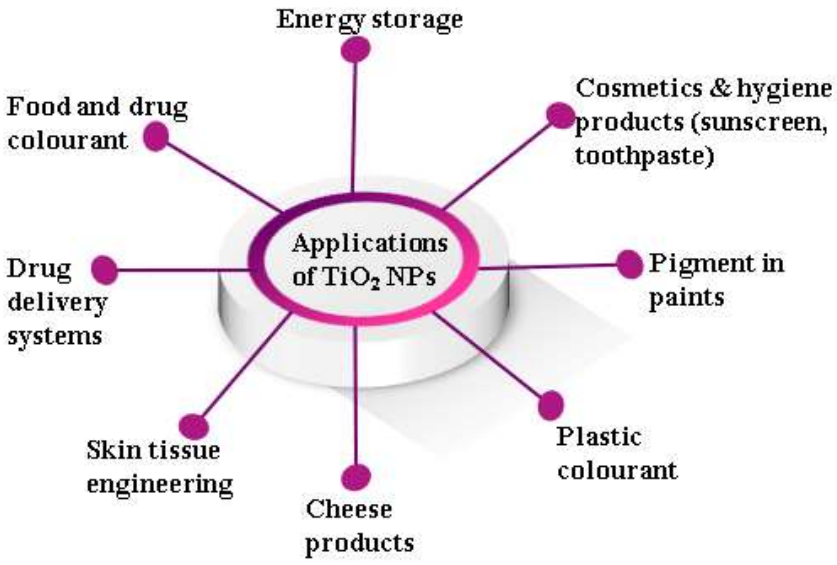

Figure 2.1.3: Applications of titanium dioxide nanoparticles

2.2 Dissolution in the context of nanoparticle safety

The previous sections have demonstrated the advantages and benefits of the applications of NPs. To realize this potential, however, necessitates a responsible and organized approach to address potential problems that may arise as a result of NPs concurrently with the advancement and application of nanotechnology. The risk assessment methodologies utilized to evaluate the toxicity of chemicals may not be suitable for NPs. Even though several investigations have been conducted on assessing the toxicity of NPs, the issues of biodurability and persistence are under addressed (OECD, 2018; Utembe et al. 2015). As such, when evaluating nanoparticle safety and their effects on biological systems and environmental surroundings, parameters such as dissolution, biodurability, and persistence become significant.

The term dissolution can be elucidated as the movement of materials' soluble ions, components and other species from a nanoparticle surface into the bulk fluid surrounding the particle to form a homogeneous mixture with the components of the bulk media (Borm et al. 2006; Innes et al. 2021; Misra et al. 2012). For this to occur, the nanoparticle must possess a certain level of solubility in the bulk fluid. The process of dissolution is driven by diffusion via a concentration gradient wherein particles' constituent molecules migrate from the region of high concentration (particles surface) to the bulk solution through a diffusion layer (Innes et al. 2021; Misra et al. 2012). Particle dissolution and the rate of dissolution are influenced by factors such as the particles' surface & physicochemical properties, size, agglomeration state and are further impacted by the surrounding biological and environmental media (Innes et al. 2021; Misra et al. 2012).

Dissolution is a parameter used to measure the biodurability and persistence of NPs (Borm et al. 2006). Biodurability is a measure of a particle resistance to clearance, whereby insoluble particles that resist enzymatic degradation, physical and

chemical clearance present a high chance of causing long-term health effects (Innes et al. 2021). Biodurability is used as a parameter to elucidate the behaviour of NPs in biological surroundings. Persistence describes a particle's capacity to remain unchanged in its surroundings for an extended period (OECD, 2018; Sohal et al. 2018). Dissolution as a measure of biodurability provides information about particle behaviour in biological and environmental surroundings. It allows for the categorization of particles between those that amenable to dissolution and those that are resistant which are more likely to accumulate in the body and cause long-term health effects (OECD, 2018; Utembe et al. 2015). Biodurability and persistence including how they are measured are further discussed in the subsequent sections.

The physical characteristics of the bulk fluid, including ionic strength, pH and temperature affect the solubility of NPs. As a result, dissolution may vary depending on the area of the body that is exposed to the specific biological environment (Borm et al. 2006). For this reason, the dissolution of nanoparticulate materials in different biological surroundings should be taken into account as it has a major impact on the persistence of nanoparticles *in vivo*, especially when interpreting biological responses to NPs exposures (Borm et al. 2006). Additionally, the physicochemical variables of NPs such as particle size, morphology, aggregation state, functional group, adsorbed species on the particle surface and surface charge may also influence their dissolution (Innes et al. 2021). For example, dissolution is size dependent whereby smaller particles tend to dissolve faster than larger particles (Borm et al. 2006). Therefore, dissolution, kinetics, biodurability and persistence of particles are the most important parameters that should be considered when evaluating the safety of NPs on biological systems and environmental surroundings (Sohal et al. 2018).

2.2.1 Biodurability

The biodurability of materials is described as the materials' tendency to resist chemical, physical and other physiological clearance mechanisms in biological media thereby causing accumulation and long-term health effects (Innes et al. 2021;

Madl & O'Neill, 2023; OECD, 2018; Utembe et al. 2015). The assessment of biodurability may therefore be an important component in the risk assessment of NPs (Madl & O'Neill, 2023; Wiecinski et al. 2009). Resistance to disintegration and clearance from the body is influence by the physical and chemical properties of NPs and by their interaction with the surrounding biological system (Innes et al. 2021; Sohal et al. 2018). For example, if particles release ions at a slow rate when exposed to simulated fluids *in vitro*, they are more likely to exhibit the same behaviour under similar biological conditions in real-life situations (Utembe et al. 2015; Wiecinski et al. 2009). Alternatively, if ions from the NP surface are released at a faster speed , the short-term effects of the particles will be similar and comparable to those of the liberated ions (Innes et al. 2021; Utembe et al. 2015). At present it is unclear if gold, silver, and titanium dioxide nanoparticles are entirely released from the body, and what detrimental effects they may cause if they remain in the body over extended periods of time. Comprehensive assessment of gold, silver and titanium dioxide nanoparticles dissolution and dissolution kinetics in simulated biological and synthetic environmental fluids is essential to understanding their effects on biological systems and environmental surroundings. Therefore, to ensure safer nanomaterials, their toxic effects should be thoroughly investigated including their dissolution, which ultimately provide insight into their biodurability and persistence.

2.2.2 Persistence

The term environmental persistence is used to describe a particle's capacity to remain unchanged in its surroundings for an extended period (Innes et al. 2021; OECD, 2018; Utembe et al. 2015). Dissolution and degradation have a major effect on this process. The process of degradation involves the breakdown of a substance by microbial and/or physical and chemical processes and is related to persistence (Innes et al. 2021; OECD, 2018; Utembe et al. 2015). As a result, it is essential to evaluate the persistence of particles by investigating their dissolution rates. If a particle is persistent in the environment, this means it is resistant to processes such as oxidation, hydrolysis, and decomposition (Gunsolus et al. 2015; OECD, 2018).

A nanoparticle with a higher level of environmental persistency is more likely to accumulate in the environment, potentially causing toxicity (Liu & Hurt, 2010).

There are several factors which influence the environmental persistency of particles including the media ionic strength, dissolved organic matter, particle morphology and aggregation state, solubility characteristics, particle size and functional group (Furtado et al. 2016; Liu & Hurt, 2010). The pH of the surrounding media has also been identified as one of the factors that influence dissolution and leaching of specific elements (Sauer et al. 2021).

2.3 Biodurability of nanoparticles in biological and environmental media

2.3.1 Studies in biological media

2.3.1.1 Gold nanoparticles

Studies assessing the toxicity of AuNPs have been conducted extensively and have been largely dedicated to examining their biodistribution, translocation, and accumulation *in vivo*. Research scientists have sought to decipher the behaviour of AuNPs under physiological conditions seeing the rise of their incorporation in consumer products. Carlander et al. (2019) evaluated the influence of particle size on dissolution in different models, including cell medium and cell medium with macrophages, to determine the fate of these particles in the human body. Small particles with a diameter of less than 1 nm were found to dissolve more readily than bigger particles with a size of 50 nm (diameter). Another investigation examined the biodistribution and pharmacokinetics of AuNPs and discovered that they were quickly eliminated from the bloodstream. However, the particles accumulated in the liver and spleen, where they were prone to cause long-term health consequences (Bailly et al. 2019). Another study investigated the toxicity of AuNPs by uptake and toxicity towards leukaemia cell lines (Connor et al. 2005). The rate at which particles released Au ions was negligible, and particles did not hinder cellular function. Several other models have been used to study the uptake and toxicity of AuNPs. For instance, a study conducted by Fede et al. (2015) used a model which

incorporated advection and shear stress to mimic continuous flow conditions usually found *in vivo* to determine the uptake and toxicity of AuNPs towards endothelial cells. It was observed that the particles deposited onto the cell surface formed larger aggregates making it difficult for intracellular uptake, as a result AuNPs exhibited lower toxicity (Fede et al. 2015). Another study investigated the stability and biodistribution of citrate stabilized and pentapeptide CALNN-coated AuNPs in rats to understand the effect of functionalization on particle toxicity (Fraga et al. 2014). It was observed that the biodistribution pattern was similar regardless of the functional groups with most accumulation found in the liver. The red blood cells and haemoglobin levels of rats injected with CALNN-coated AuNPs were significantly low, therefore it was concluded that CALNN-coated AuNPs were more toxic in rats compared to citrate coated AuNPs (Fraga et al. 2014). The effect of functionalization was further explored by England et al. (2015). Their study investigated the release kinetics of cisplatin (hydrophilic) and paclitaxel (hydrophobic) drugs from hexadecanethiol and phosphotidylcholine functionalized AuNPs. The hydrophilic drug released its components at a rapid rate compared to the hydrophobic one. Therefore, it was concluded that to achieve optimum drug release levels, the NP surface should have a combination of hexadecanethiol and phosphotidylcholine functionalization in order to regulate the release of both hydrophilic and hydrophobic drug components (England et al. 2015). The factor of nanoparticle surface charge was further explored and it was observed that positively charged particles were more toxic compared to negatively charged particles (Goodman et al. 2004). Similar to surface charge, size is another factor which influences particle toxicity. A study by Han et al. (2015) assessed how the variable of size (13 nm and 105 nm in diameter) influences the biodistribution of AuNPs in Sprague-Dawley rats via inhalation exposure. Both sizes of AuNPs were mainly deposited in rat lungs, however, the 13 nm sized particles were significantly translocated to secondary organs such as the liver, spleen, blood and brain. The larger particles were characterized by longer elimination half-time from the lungs unlike smaller particles which had shorter elimination half-time (Han et al. 2015; Hirn et al. 2011). Therefore, the effect of size of AuNPs is a critical factor in determining their toxicity. It influences how well AuNPs are taken up by cells,

where they are located, and where they accumulate when in a living organism. Therefore, when conducting a risk assessment of AuNPs it is critical to consider the effect of size on dissolution (De Jong et al. 2008; Jia et al. 2017; Kreyling et al. 2014).

Dissolution kinetics in relevant biological systems remains limited for most NPs. Of the few studies that have been conducted on the dissolution of AuNPs, Breitner et al. (2015) investigated the dissolution of AuNPs in A549 lung epithelial cells kept in a reaction vessel with a dynamic flow to mimic a complex physiological system. Under these conditions, AuNPs tended to form agglomerates, resulting in disruption of the localized surface plasmon resonance characteristics and low dissolution. Cherevko et al. (2014) observed that dissolution was heavily dependent on solution pH with higher dissolution observed in the alkaline media. These observation were made after studying the dissolution of AuNPs in perchloric and sulphuric acid solutions representing acidic medium and in sodium hydroxide solution representing alkaline media (Cherevko et al. 2014).

2.3.1.2 Silver nanoparticles

Several research studies have been conducted on the dissolution of silver nanoparticles in biological media (Ho et al. 2010; Kittler et al. 2010; Li et al. 2010; Loza et al. 2014). Kittler et al. (2010) investigated the dissolution of AgNPs in water for 125 days at various temperatures and found that the dissolution occurred instantly after exposure to water, even though the AgNPs did not completely dissolve. Nanoparticle surface functionalization was observed to greatly impact the rate and degree of dissolution of AgNPs (Kittler et al. 2010). For example, a study conducted by Martin et al. (2014) found that there was no observable release of silver ions when AgNPs surface was coated with bovine serum albumin protein. These observations were corroborated by those obtained by Tejamaya et al. (2012). The presence of hydrogen peroxide in media is another factor that promotes the release of silver ions (Ho et al. 2010; Loza et al. 2014). When organic compounds such as glucose interact with AgNPs, complexation between the particles and

compounds occurs and that has the potential to promotes dissolution (Loza et al. 2014). Another study by Yang et al. (2012) investigated factors influencing the toxicity of AgNPs and whether toxicity is induced by the particles themselves or the released Ag ions in *C. elegans.* It was discovered that dissolved silver ions were more toxic to the growth of *C. elegans*.

2.3.1.3 Titanium dioxide nanoparticles

TiO_2 NPs are known to be insoluble, thus limiting the research conducted to gain insight into their dissolution behaviour in biological and environmental settings (Anupong et al. 2023; Musial et al. 2020; Nam et al. 2012; Shinohara et al. 2017). In most cases, the toxicity of TiO_2 NPs is evaluated by examining their biodistribution, accumulation and genotoxicity in *in vivo* models. Most studies cited on this literature review focused on the effects of TiO_2 NPs on the respiratory system, particularly due to inhalation being the main method of exposure in occupational settings. Additionally, studies on translocation in the systemic circulation, dietary exposure resulting from food items containing TiO_2 NPs and studies from inhalation exposure, both *in vivo* and *in vitro* have also been included. Gastrointestinal tract is likely a major source of uptake for TiO_2 NPs, since they can be found in drug delivery systems, food, water and other liquids (Shi et al. 2013). Bettencourt et al. (2020) assessed the toxicity of TiO_2 NPs using the standardized static INFOGEST 2.0 *in vitro* digestion protocol, which combined gastrointestinal tract cells (Caco-2 and HT29-MTX-E12) to simulate the human digestive system. Upon exposure to HT29-MTX-E12 intestinal cells, it was observed that the digested form of anatase was more toxic than the other undigested crystal forms of TiO_2 NPs. Consequently, it was concluded that the inclusion of digestion simulation is necessary when assessing the safety of ingested nanoparticles (Bettencourt et al. 2020). Researchers have hypothesized that the toxicity of TiO_2 NPs is influenced by the crystal form in which they exist, such as anatase, rutile, and brookite (Musial et al. 2020). To assess this, De Matteis et al. (2016) studied the toxicity of anatase and rutile nanoparticles in two cell lines at pH values of 4.5 and 5.5, representing the lysosomal and physiological skin compartments, respectively. Anatase was

more prone to degradation and released ions at a faster rate in acidic conditions compared to rutile. It was concluded that pH and crystalline form have a significant effect on the toxicity of TiO_2 NPs (De Matteis et al. 2016; Shkol'nikov, 2016). A multitude of studies have used inhalation as the means of exposure to determine the genotoxicity of TiO_2 NPs. The deposition kinetics of aerosolized particles of TiO_2 NPs in male Sprague-dawley rats was investigated over a period of 14 days. Accumulation in blood, tissues, and excreta were determined and it became apparent that the highest accumulation was observed in the lungs after 48 hours. These results suggest that the particles display a certain level of biodurability upon entering biological compartments (Pujalté et al. 2017).

Of the few studies conducted to understand the solubility chemistry of TiO_2 NPs, a study assessed the dissolution of TiO_2 NPs in artificial physiological fluids and to gain insight into their potential adverse effects. The findings indicated a rapid aggregation immediately after particles were immersed in artificial body fluids, with the ionic strength of the fluid driving the process (Korábková et al. 2021; Nia et al. 2015). The influence of particle aggregation/ agglomeration on toxicity was explored by Murugadoss et al. (2020). Larger particles of TiO_2 NPs agglomerates were more toxic towards colon cell lines and caused more DNA damage in gavage mice compared to small agglomerates (Murugadoss et al. 2020). Schmidt & Vogelsberger, (2006, 2009) investigated how TiO_2 NPs dissolve in a liquid solution of NaCl. This was done to determine the effect that ionic strength, particle size, media pH, and temperature have on the dissolution. The solubility of TiO_2 was observed to be strongly impacted by the pH of the liquid medium, with a higher solubility in acidic environments. Smaller particles had a higher saturation concentration than larger particles, causing their dissolution to be driven by the kinetic size effect (Schmidt & Vogelsberger, 2006, 2009; Vogelsberger et al. 2008). Another study found that TiO_2 NPs remained unchanged and preserved their nanoscale size when dispersed in biological media (Taurozzi et al. 2013). Therefore, it was concluded that the particles would accumulate in the body and cause long-term health effects.

2.3.2 Studies in environmental media

The use of nanoparticles to synthesize membranes for water filtration extend the potential for their entry into the environment (Adams et al. 2017). When NPs enter the environment, there a is greater possibility that they interact with components of environmental surroundings and undergo dynamic transformation processes (Abbas et al. 2020; Angel et al. 2013; Kerin et al. 2023). Furthermore, they may remain persistent in the environment, accumulate, and reach levels that might be harmful to aquatic organisms and consumers (Angel et al. 2013; Kerin et al. 2023). Therefore, it is crucial to study the behaviour and fate of NPs in environmental compartments. Environmental factors such as aggregation, oxidation, reduction and adsorption influence the fate of NPs in the environment (Abbas et al. 2020; Adams et al. 2017). These processes are influenced by the acidity/alkalinity of the media, chemical composition, organic and inorganic colloids present in the environment (Abbas et al. 2020; Kerin et al. 2023).

2.3.2.1 Gold nanoparticles

A number of studies have been conducted to investigate the fate of AuNPs in aquatic environments. Avellan et al. (2018) investigated the effects of biogeochemical processes and seasonality in freshwater wetlands on the transformation of nanoparticles, concluding that oxidation of Au^0 to Au^+ or Au^{3+} was thermodynamically unfavourable. Further research has been conducted to elucidate transport and fate of AuNPs in aquatic systems (Kerin et al. 2023; Singh et al. 2023). Donovan et al. (2016) studied the capacity of six different conventional drinking water treatment models for the removal of AuNPs from drinking water and observed that the particles were completely removed after the limestone softening and addition of activated carbon. The addition of organic matter in simulated freshwater and seawater was found to promote coagulation of particles, encouraging them to settle in sediments, increasing the risks of ingestion by aquatic organisms (Blasco et al. 2015; Bour et al. 2015; Gallego-Urrea et al. 2016).

The intake of these particles by aquatic organisms poses a risk to the aquatic food chain. In order to assess the toxicity of AuNPs in the environment, a variety of methods have been employed. One study used phytoremediation to investigate the bioavailability of AuNPs to plants (Judy et al. 2011). Results indicated that smaller-sized AuNPs were more readily absorbed by tobacco plants, while no uptake of AuNPs was observed in wheat. These findings suggest that plants are able to absorb nanoparticles of varying sizes and compositions, thereby providing insight into how cell wall pores can affect AuNP uptake and how the plant species itself can influence nanoparticle accumulation.

2.3.2.2 Silver nanoparticles

Various models have been utilized to investigate the effects of AgNPs in the environment. For example, Fabrega et al. (2009) conducted an experiment in which *Pseudomonas flourescens* was exposed to AgNPs for 24 hours. This study was done to determine how pH, organic matter, and concentration affected the bacterial growth in the presence of these nanoparticles. Results showed that AgNPs had a toxic effect and inhibited bacterial growth, whereas organic matter promoted particle disaggregation (González-Pedroza et al. 2023). Meaning natural organic matter rich in sulphur and nitrogen content promoted strong interactions with AgNPs thereby leading to formation of stable colloids (Gunsolus et al. 2015). These results were confirmed by Pokhrel et al. (2014) who studied the effect of natural water chemistry on the fate, toxicity and dissolution of AgNPs. These researchers confirmed that the dissolved organic carbon tended to bind strongly to AgNPs surface forming larger aggregates thereby resulting in low release of Ag ions which prevented the toxicity of these particles towards *E. coli* (Pokhrel et al. 2014). Other researchers have used migration test to investigate the release of AgNPs from three commercial food containers and found low silver migration values below the permissible limits (Echegoyen & Nerín, 2013). Furthermore, AgNPs were immobilized on a glass substrate to monitor their dissolution in phosphate buffer solution with varying concentration of NaCl to predict their behaviour in natural waters (Kent & Vikesland, 2012). The immobilization on a glass substrate was to

inhibit formation of AgNPs aggregates. It was observed that on the first day of exposure to the buffer, the AgNPs changed morphology from triangular to spherical shape and their diameter decreased. It was concluded that NaCl accelerated the dissolution of AgNPs and is a variable that should be taken into consideration when evaluating the safety of AgNPs in aquatic environments (Kent & Vikesland, 2012).

A plethora of researchers have identified factors that influence silver nanoparticle solubility (Nikolić et al. 2023; Watanabe et al. 2023; Yang et al. 2023; Zhang & Wang, 2023). Among the identified factors, particle size and pH have been observed to either hinder or promote dissolution (González-Pedroza et al. 2023). In acidic environments Ag ions were released from the particle surface and formed complexes with chloride ions thereby forming a precipitate. This encourages particle growth and inhibit dissolution (Axson et al. 2015; González-Pedroza et al. 2023). The promotion of AgNPs dissolution in aquatic environments by the effect of chloride ions was observed by other researchers as well (Li et al. 2018). A study conducted by Lodeiro et al. (2016) investigated dissolution and aggregation kinetics of AgNPs in freshwater and seawater represented by varying concentration of sodium chloride found that, alginate coating was a weaker stabilizing agent compared to gum arabic and therefore, lead to greater dissolution of AgNPs. Since the release of silver ions induces toxicity, stronger stabilizing agents should be used to attenuate the toxicity of AgNPs in aquatic environments (Li et al. 2012; Lodeiro et al. 2016). Furthermore, surface functionalization and the presence of divalent cations were observed to also affect dissolution, whereby divalent cations promoted particles aggregation (Jin et al. 2010; Li et al. 2010; Metreveli et al. 2016). Non-functionalized silver nanoparticles formed clusters under conditions characterized by high ionic strength (Badawy et al. 2010). The effect of shape on the dissolution and toxicity of AgNPs to human mesenchymal stem cells was also studied, and it was discovered that all the particles tested were cytotoxic to the cells (Helmlinger et al. 2016). Additionally, there were no statistically significant difference in the toxicity regardless of the particle morphology. In this case the investigated particle morphology included particles that were spheres, rods, platelets and cubes (Helmlinger et al. 2016). Another study investigated the effect of size on the solubility of organic coated AgNPs in the environmental water represented by

$NaHCO_3$ and observed that smaller particles were more soluble compared to the large ones (Ma et al. 2012). However, the effect of coating agents was negligible Another study investigated the ecotoxicity of AgNPs in a wastewater treatment plant using wastewater biota *Nitrosomonas europaea* (Radniecki et al. 2011). It was observed that *N. europaea* was extremely sensitive to Ag ions with smaller particles (20 nm) releasing the highest amount of silver ions in comparison to larger particles (80 nm). These observations were attributed to the kinetic size effect whereby smaller particles exhibited higher dissolution rates because of a greater surface-area-to-volume-ratio compared to larger particles (Radniecki et al. 2011). These results were in agreement with those observed by Peretyazhko et al. (2014) and Silva et al. (2014).

2.3.2.3 Titanium dioxide nanoparticles

Brunelli et al. (2013) assessed the fate of TiO_2 NPs in aquatic environments over a period of two days, using synthetic and natural freshwater as well as seawater solutions of environmentally relevant concentrations. It was observed that the particles formed stable aggregates as soon as they were dispersed in seawater, with more pronounced aggregation observed in natural seawater compared to synthetic seawater. This suggested that particle aggregation and sedimentation should be considered when evaluating the ecotoxicological fate of TiO_2 NPs in the environment. It is essential to note, however, that there are other variables that can determine the impact of nanoparticles in the environment Cupi et al. (2016) investigated conditions which would maintain the stability of TiO_2 NPs in aquatic environments by elucidating the impact of pH, ionic strength, and water hardness on the immobilization of *Daphnia magna*. It was observed that when TiO_2 NPs were present in a medium with high ionic strength and alkaline pH, the particles tended to cluster, forming large aggregates (Cupi et al. 2016; Qi, et al. 2013). Interestingly, smaller particles were found to be toxic to *D. magna*, whereas no toxicity was observed in the highly agglomerated particles (Cupi et al. 2016). This is because generally, particles smaller in size tend to produce more acute toxicity, while larger agglomerates and filter feeders, such as daphnia, may encounter

secondary effects that can ultimately lead to mortality. These changes may include decreased reproduction, changes in swimming behaviour and feeding, and altered energy allocation. Another study investigated the persistence of TiO_2 NPs in a mesocosm that mimicked a freshwater wetland, and the particles were found to remain unchanged in the water column but were taken up by aquatic organisms (Espinasse et al. 2018). Factors influencing the toxicity of TiO_2 NPs in aquatic environments have been identified to include particle size & shape, surface coating agent, aggregation state, rate of dissolution and the ionic strength of the media (Baranowska-Wójcik et al. 2020; Oskam et al. 2003; Raza et al. 2016; Schmidt & Vogelsberger, 2006, 2009). Additional study explored how salinity and dissolved organic carbon in seawater influence the stability and clustering of TiO_2 NPs (Wang et al. 2014). The hydrodynamic diameters and zeta potentials were used to measure these effects. When the seawater had a low salinity, the dissolved organic carbon stabilized the TiO_2 NPs. However, when the salinity became higher, it decreased the stabilizing effect. Results demonstrated that salinity was the most influential factor on the aggregation of the TiO_2 NPs, with dissolved organic carbon coming in second. Subsequently, when TiO_2 NPs are released in an aquatic environment, they will aggregate in the water column, settle, and accumulate in sediments (Wang et al. 2014).

2.4 Factors influencing dissolution

There are several factors that influence the dissolution of NPs in biological and environmental media including the pH & ionic strength of the media, concentration of the species, the kinetic facility of electron transfers, and the redox conditions of the media where nanoparticles are found (Avellan et al. 2018; Avramescu et al. 2017; Bachler et al. 2015; Breitner et al. 2015; Cherevko et al. 2014; Donovan et al. 2016). The ionic strength and pH of biological fluids can influence the surface chemistry of nanoparticles by effecting their aggregation status (Axson et al. 2015; Fernando & Zhou, 2019; Pallavicini et al. 2020; Peretyazhko et al. 2014). Nanoparticle dissolution is governed by the solubility of the metal in a particular environment and is also influenced by the concentrations gradient existing between

the nanoparticle and the bulk fluid (Borm et al. 2006; Innes et al. 2021). The influence of the factors on nanoparticle dissolution are further described below.

.

2.4.1 Size effect

It is well known that the size and the surface area of nanoparticles will affect the dissolution (Watanabe et al. 2023; Yang et al. 2023; Zhang & Wang, 2023). Nanoparticles are more prone to oxidation and dissolution compared to the bulk sample, since nanoparticles exhibit a higher surface-to-volume ratio (Abbasi et al. 2023; Misra et al. 2012; Nia et al. 2015; Pareek et al. 2018). When considering the same volume of micro- and nanoparticles, the nanoparticles will exhibit for surface which will increase the surface area (Figure 2.4.1).

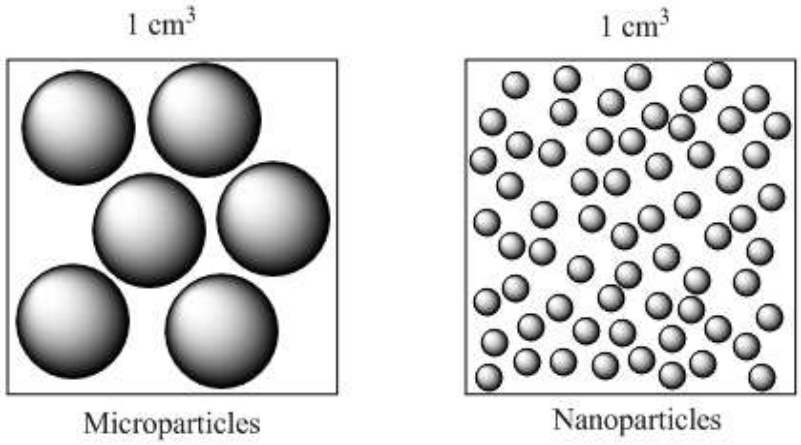

Figure 2.4.1: Surface to volume ratio compared between micro- and nanoparticles using a volume of 1 cm^3. The image was obtained from Atkins & de Paula, (2006).

Not only will the surface area of nanoparticles be larger, but they also exhibit a greater fraction of atoms at the edges and corners compared to larger particles which have planar terraces (Abbasi et al. 2023). This makes it easier for ions and small cluster to break away from the surface of the nanoparticle (Bian et al. 2011). There are numerous models and equations that describe the dissolution rates of nanoparticles due to size and surface area since the dissolution will be dependent

on different parameters (Keller et al. 2020; Koltermann-Jülly et al. 2018; Utembe et al. 2015; Wang et al. 2016).

2.4.2 Agglomeration and aggregation

Nanoparticles have the tendency to agglomerate or aggregate when they encounter environmental or biological fluid. Aggregation and/or agglomeration are terms used to define secondary particles formed as a result of primary nanoparticle adhesion (Abbasi et al. 2023; Borm et al. 2006). This occurs when the ionic strength of a solution increase, due to the ions that decreases the electrostatic repulsion that exists between particles (Bozich et al. 2014; Li et al. 2013). The aggregation or agglomeration state of the nanoparticles will largely influence the dissolution kinetics. The dissolution rates of numerous nanoparticles decreases and the nanoparticles aggregation in an exposure media (Badawy et al. 2010; Sperling & Parak, 2010). This is due to that aggregations will decrease the movement of particles in the solution. The dissolution kinetics will be hindered due to reduced average equilibrium solubility (Borm et al. 2006). Particle aggregation also reduces the sites available which are prone to oxidation and dissolution (Bian et al. 2011; De Matteis et al. 2016; Wang et al. 2014; Zhong et al. 2017).

2.4.3 Interfering ions or molecules

Although ions may cause aggregation and decrease the dissolution rates, some ions or molecules (sulphides, cysteine and methionines) (Behra et al. 2013) may increase the dissolution rates by the formation of more soluble species (Borm et al. 2006). A study found that the dissolution rate increased with an increasing chloride concentration since more soluble silver complexes were formed. These soluble complexes included $AgCl_2^-$ and $AgCl_3^{2-}$ (He et al. 2013). However, contradictory results have also been found by other researchers where it was found that chloride has a potential to significantly decreased the dissolution rates of AgNPs (Guerrini et al. 2018; Levard et al. 2013).

2.4.4 Surface modification: Ligands

Nanoparticle functionalization is done to enhance biocompatibility, increase binding interactions between the nanoparticles and target biomolecules and also to increase aqueous solubility (Gunsolu et al. 2015). Various functional groups can be used in the surface modification of NPs and some of these control properties such as NP stability (Gunsolus et al., 2015; Pokhrel et al. 2014). Surface ligands also determine how NPs interact with biological and environmental fluids. Ligands can influence dissolution processes in two ways; they can either assume a protective role thus reducing dissolution of nanomaterials or enhance dissolution through a ligand promoted process (Chambers et al. 2014; Peretyazhko et al. 2014; Rak et al. 2014; Taurozzi et al. 2013; Zhong et al. 2017). The extent of dissolution will depend on the strength of ligand binding, composition, density and on their biodurability in environmental and biological surroundings (Jia et al. 2017; Joo & Zhao, 2017; Pareek et al. 2018; Turan et al. 2019). Gunsolus et al. (2015) stated that in some instances the attachment of some surface ligands enhances the biocompatibility and hydrophilicity of some NPs. In this study, different ligands were used to modify NP surface chemistry to probe the interactions of NPs with biological and environmental fluids. In the present research study, a range of different ligands were utilized to modify the NP surface composition to investigate their interactions with physiological fluids and environmental media. The purpose of doing this was to synthesize NPs with precise bulk and surface chemistries in order to evaluate how the chemical structure and surface functional groups may affect their biodurability, dissolution rate and ultimately their toxicity. These factors have been summarized in Figure 2.4.4 below.

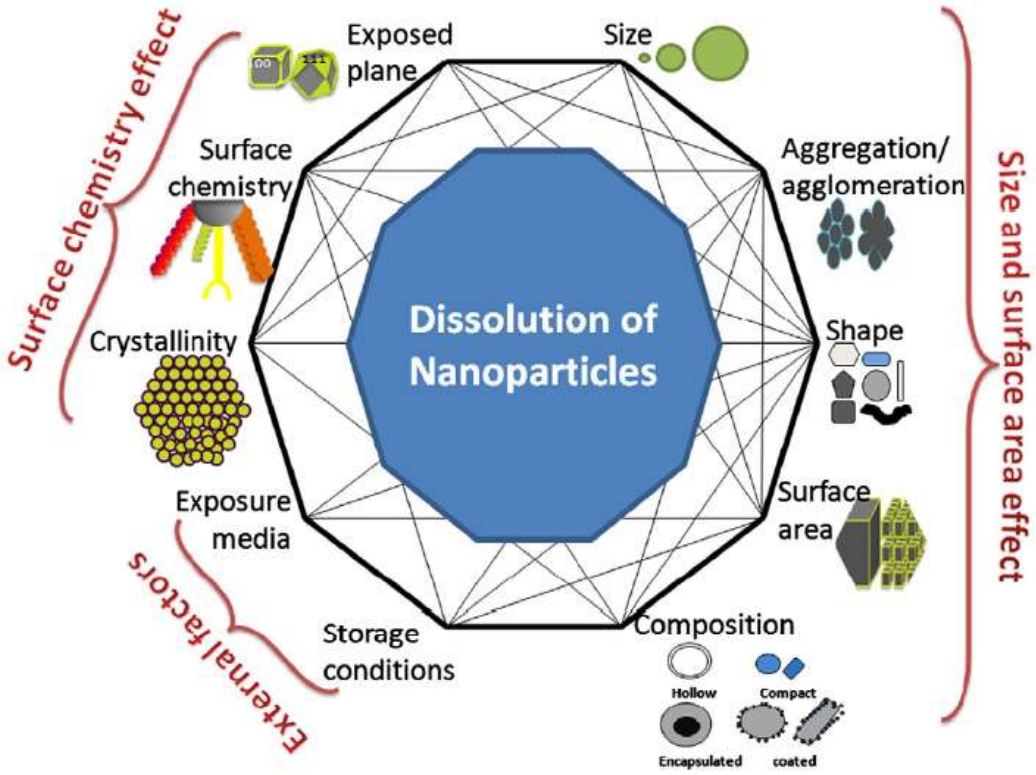

Figure 2.4.4: A graphical summary of factors influencing dissolution. This image was obtained from (Misra et al. 2012).

2.5 Parameters required for risk assessment

The determination of dissolution rates, biodurability and persistence will give an indication on how nanoparticles may interact with biological and environmental surroundings (Innes et al. 2021). The faster the rate at which molecules and/or ions are released from nanoparticle surface, the more identical their behaviour will be to the dissolved ions (Utembe et al. 2015). Contrary, those nanoparticles that release ions at a slow rate are associated with greater toxicity and observed long-term adverse effects (Avramescu et al. 2017; Utembe et al. 2015). The aforementioned parameters are of great importance when it comes to the risk assessment of the behaviour of engineered nanoparticles in biological and environmental media.

2.5.1 Dissolution kinetics

Biodurability can be monitored and determined through studying the dissolution rate of nanoparticles. Generally, different chemical reactions will have different reaction kinetics. There are many parameters that affect the dissolution of nanoparticle, for example the physicochemical properties of the nanoparticle as well as the exposure environment (Borm et al. 2006; Misra et al. 2012; Turan et al. 2019). The physicochemical properties of nanoparticles include size, shape, surface area, aggregation and agglomeration state together with the composition of the particles (Borm et al. 2006; Joo & Zhao, 2017; Misra et al. 2012; Pareek et al. 2018; Peng et al. 2017). Other characteristics of the surface to consider include the surface chemistry (surface modification), crystallinity and exposure plane of the particles (Avramescu et al. 2019; Shkol'nikov, 2016). Properties of the exposure media (extrinsic properties) include the pH, composition and temperature (Misra et al. 2012).

When a substance dissolves the rate law can be expressed as shown in Equation 1:

$$Rate = -\frac{dM}{dt} = k[reactants]^n \qquad (1)$$

The rate law in equation 1 gives the change in the mass of a substance M, over a time period t, and the rate constant is expressed as k with the order given as n (0, 1, 2 or 3). When the dissolution follows a zero-order reaction, it means that the rate at which the reaction is occurring does not depend on the concentration(s) of the reactant(s) (Table 2.5.1), compared to first-and second-order, where the speed of the reaction will be determined by the concentration of at least one of its reactants. A second-order reaction will depend on the concentration of two or more reactants or when one reactant is in excess (Atkins & de Paula, 2006). When the rate of the dissolution is determined, it can be used to calculate the halftime of the reaction which predicts the biodurability.

Table 2.5.1: Rate laws and halftime for zero-, first- and second-order kinetic reactions.

Order	Zero-	First-	Second-
Rate law	$-dM/dt = k$	$-dM/dt = kM$	$-dM/dt = k[M]^2$
Integrated	$[M]_t = -kt + [M]_0$	$\ln [M]_t = -kt + \ln [M]_0$	$1/[M]_t = kt + 1/[M]_0$
Units of k	$mol.s^{-2}.L^{-1}$	s^{-2}	$mol^{-1}.L.s^{-2}$
Halftime	$t_{1/2} = [M]_0/2k$	$t_{1/2} = \ln 2/k$	$t_{1/2} = 1/[M]_0 k$
Lifetime	$\tau = (e-1)[M]_0/ek$	$\tau = 1/k$	$\tau = (e-1)/k$

Note that e is the number $e \approx 2.718$

As mentioned earlier, the surface area of nanoparticles plays a major role in its reaction with the surrounding. The specific surface area of nanoparticles may affect the dissolution kinetics, and hence should be considered when calculating the kinetics (Keller et al. 2020; Koltermann-Jülly et al. 2018). Therefore, the rate law should be expressed in terms of mass dissolved and specific surface area as shown in equation 2. The rate law of nanoparticles releasing ions by first-order kinetic is expressed as shown in Equation 2:

$$\frac{dM}{dt} = -k_{dis}AM \qquad (2)$$

Where dM/dt is the rate of dissolution for a given mass *M*, k_{dis} is the rate constant and *A* is the specific surface area. The rate constant is normalised against the specific surface area. The same will apply to zero-, and second-order reactions, where the surface area should be incorporated into the rate law. The dissolution rate increases with increasing surface area. Smaller nanoparticles will exhibit a larger surface-area-to-volume ratio and subsequently become more reactive (Keller et al. 2020; Koltermann-Jülly et al. 2018; Wang et al. 2016). This implies that smaller nanoparticles will be more prone to reaction when exposed to the environment and may dissolve at a greater rate.

Generally the dissolution of nanoparticles occurs via the first-order reaction kinetics (Ho et al. 2010; Keller et al. 2020; Kittler et al. 2010; Koltermann-Jülly et al. 2018; Liu & Hurt, 2010; Schmidt & Vogelsberger, 2006, 2009). Hence it is hypothesised that the NPs under investigation will also follow first-order dissolution kinetics. The half-time of particles can be determined by using the rate constant as shown in the following Equation 3:

:

$$t_{1/2} = \frac{\ln (2)}{k_{dis}} \qquad (3)$$

Using the half-time, the biodurability and persistence of the nanoparticles can be determined.

2.6 Implications of dissolution

2.6.1 Particles with high dissolution

When silver nanoparticles encounter biological and environmental surroundings they quickly dissolve and release Ag ions (Valsami-Jones & Lynch, 2015). From a safety standpoint, soluble nanoparticles offer the best-case situation because their short-term toxic effects will be evident and similar to those of the released ions (Utembe et al., 2015; Valsami-Jones & Lynch, 2015). Moreover, since nanoparticles are small in size and only small amounts are used in application, it is unlikely that the dissolved ions will result in a major environmental threat (Valsami-Jones & Lynch, 2015). However, humans or organisms being directly exposed had still been of concern, especially if nanoparticles were taken up by cells as particles, only to release and deliver toxic ions inside the cells (Valsami-Jones & Lynch, 2015). Several studies have been conducted which had contributed to the assessment of the impact of AgNPs on physiological systems and aquatic environments (Huang et al. 2023; Nie et al. 2023; Suthar et al. 2023). Research conducted *in vivo* and *in vitro* suggested that exposure to AgNPs could possibly lead to genetic damage and build-up of silver ions in the spleen, liver, and testes (Prasath & Palaniappan, 2019; Pulit-Prociak & Banach, 2016; Sharifi et al. 2012).

Additionally, when AgNPs entered the body through inhalation, ingestion, or dermal exposure, they spread throughout the body, accumulated in organs and tissues, and even showed up in the blood (Prasath & Palaniappan, 2019). Braydich-Stolle et al. (2014) investigated the *in vitro* toxicity of AgNP on a mouse spermatogonial stem cell line and found that with an increase in the concentration of AgNP, there was an associated rise in cytotoxicity of the mitochondrial function and membrane leakage. It was also observed that AgNPs reduced ATP content in the cells (Fabian et al. 2008). An analysis of the silver levels in the organs of rats exposed to silver nanoparticles revealed a strong correlation between the concentration of Ag ions in the suspension and the silver levels. This suggests that the majority of Ag ions, with only a minor amount of silver nanoparticles, were transported to the intestines (Fabian et al. 2008; Sahu et al. 2012). Beer et al. (2012) conducted a study to elucidate the degree to which Ag ions from AgNPs might be toxic towards A549 lung epithelial cells. It was determined that when the amount of Ag ions was higher it solely contributed to the toxicity of A549 lung cells. However, this contribution to toxicity was negligible when the concentration of Ag ions was low. Therefore, it was concluded that silver ions present in AgNP preparations had a significant impact on the toxicity of AgNP suspensions (Beer et al. 2012).

In the environment, water is the fastest way of dispersing contamination over a wide area. When AgNPs are released into the environment they can accumulate in reservoirs, there is the potential for them to spread to a wide area, creating a hazard for not just aquatic life, but also for the creatures that live near the shore (Pulit-Prociak & Banach, 2016). Pulit-Prociak & Banach, (2016) stated that mud and sewage may bind AgNPs, which could potentially spread to agricultural fields in the future and result in bioaccumulation and toxicological danger. Researchers have observed that exposure to AgNPs for some aquatic organisms lead to oxygen deprivation or decreased resistance to hypoxia (Pulit-Prociak & Banach, 2016).

2.6.2 Particles with low dissolution

Despite numerous research studies conducted *in vivo*, there is a scarcity of research conducted *in vitro* to elucidate the implications of the dissolution of AuNPs. However, *in vivo* models offer more information and are preferred for toxicologic evaluation of nanoparticles, they are beneficial in providing clarity regarding the toxicity of AuNPs (Jia et al. 2017; Sani et al. 2021). Researchers showed that if AuNPs were not excreted from organisms they would accumulate in the liver and spleen and eventually lead to apoptosis and inflammation of tissues (Balasubramanian et al. 2010; De Jong et al. 2008; Hirn et al. 2011; Sani et al. 2021; Simpson et al. 2013). Since particle size played a major role in determining the toxicity of AuNPs, other research showed that smaller particles were able to cross the blood brain barrier leading to damage of the central nervous system (Gnach et al. 2015; Han et al. 2015; Lasagna-Reeves et al. 2010). Moreover, smaller-sized AuNPs had the capability to produce reactive oxygen species thereby inducing cytotoxicity and cell damage (Shukla et al. 2005). A study conducted by Pompa et al. (2011) found that when *Drosophila melanogaster* was exposed to 15 nm citrate stabilized AuNPs, it caused a decline in fertility and life span as well as over-expression of stress protein. The *in vitro* studies conducted on cell lines treated with AuNPs had shown that these particles had the propensity to cause long term toxic effects on cells, DNA damage and genotoxicity (Fraga et al. 2014; Rosi et al. 2006; Schaeublin et al. 2011).

TiO_2 NPs are also an example of nano sized particles that are biodurable and have low dissolution rates in biological and environmental media (Avramescu et al. 2017; Bove et al. 2017; Brunelli et al. 2013). Despite the lack of solid evidence of their potential systemic toxicity, it is recommended that their effects after prolonged-exposure assessment be investigated further in light of the possibility of them accumulating in systemic organs (da Silva et al. 2020; Gualtieri et al. 2018; Larue et al. 2011; Murugadoss et al. 2020). If nanoparticles can accumulate in the body without being excreted that might induce undesirable genetic alteration in living organisms (Albrecht et al. 2006). Fabian et al. (2008) intravenously administered TiO_2 NPs in rats to study their tissue distribution and observed that

most accumulation was found in the liver after a 28-day period. Researchers have observed that when insoluble particles such as TiO_2 NPs were inhaled by rats, they were also likely to cause inflammation in the lungs as the time of exposure was prolonged (Albrecht et al. 2006; Pujalté et al. 2017). Of the many factors which influence the toxicity of particles, it has been determined that the toxicity of TiO_2 NPs also depended on the crystallographic form. For example, it had been stated that TiO_2 NPs in anatase form measuring 10 nm and 20 nm in diameter could cause oxidative stress in human bronchial epithelial cells (Albrecht et al. 2006; Czajka et al. 2015; De Matteis et al. 2016). Oxidative stress was thought to play a role in aging, atherosclerosis, carcinogenesis and inflammatory conditions (Albrecht et al. 2006; Czajka et al. 2015; De Matteis et al. 2016). Another researcher has shown that when TiO_2 NPs entered the human body via inhalation, they had the potential to accumulate in the brain and cross the blood brain barrier (Czajka et al. 2015). Marques et al. (2011) studied the toxicity of TiO_2 NPs in human cells u373 and rat C6 glial cells and found that the particles induced alterations in cell morphology which then triggered apoptosis. Additionally, these particles were also able to enter the human body through ingestion of products identified to have a high titanium content, such as sweets, chewing gums, powdered sugar toppings, and white icing (Musial et al. 2020). However, in some cases there has been contradictory evidence presented which indicated that most of the titanium content that entered the human body through ingestion becomes excreted in faeces, and therefore was unlikely to cause cytotoxicity *in vivo* (Musial et al. 2020).

According to research, as the use of nanoparticles expands in terms of quantity and product range, it will lead to a wider variety of pollutants being released into the environment (Bundschuh et al. 2018). TiO_2 NPs, for example, accumulate in sewage sludge during wastewater treatment and may thus be introduced into aquatic and terrestrial environments (Bundschuh et al. 2018). TiO_2 NPs may undergo various transformation processes in the environment, including dissolution, disaggregation, aggregation, sedimentation, and chemical transformation (Bundschuh et al. 2018). In aquatic environments, AuNPs will most likely aggregate and form stable complexes with natural organic matter, increasing their stability (Stankus et al. 2011). Aggregates are less mobile than individual particles,

these complexes will react with their surroundings and form toxic complexes in the long run (Walters et al. 2013). Furthermore, they may be consumed by aquatic organisms, enter the food chain, and be transferred to higher order consumers (Unrine et al. 2012). Although aggregated particles are less prone to dissolution, filter feeders and creatures living at the bottom of the aquatic environment can still absorb them, potentially leading to biomagnification in the food chain (Walters et al. 2013).

CHAPTER 3

3. Aims and objectives of the study

3.1 Aims

The purpose of this research was to evaluate how AuNPs, AgNPs and TiO_2 NPs behave when immersed in artificial physiological fluids and synthetic environmental media. It also aimed to examine the dissolution kinetics of three nanoparticle types. Lastly, the study sought to explore the effects of the particles' physicochemical properties on dissolution, with a special focus on particle size, shape, agglomeration state, crystal phase, chemical composition, surface area and charge. The static and flow through systems were employed to conduct these dissolution experiments.

3.2 Objectives

The above aims were accomplished by addressing the following specific objectives:

- To assess the dissolution behaviour of nanoparticles in artificial physiological fluids and environmental media.
- To investigate if the size, shape, or surface area of NPs changed when exposed to different artificial media.
- To determine whether functional groups disintegrated from the NP surface during dissolution to clarify the impact of functional groups on nanoparticle dissolution.
- To calculate the dissolution kinetics of nanoparticles.
- To predict the biodurability and persistence of nanoparticles.

3.3 Hypothesis and Questions

3.3.1 Hypothesis

Since nanoparticles are used in a broad range of consumer products, there is concern about potential exposure to them. If these nanoparticles are released into the ecosystem, they may pose a threat to environmental safety as well as living organisms. When exposed to simulated acidic fluids, it is assumed that the nanoparticles would release ions, whereas in neutral simulated fluid the nanoparticles would be stable. Short-term toxicity effects could be attributed to either the particles themselves or the ions released from them. However, nanoparticles with longer half-times will cause more severe long-term effects.

3.3.2 Questions

The research was conducted to answer the following questions:

- Are AuNPs, AgNPs and TiO_2 NPs biodurable under simulated physiological conditions and persistent in environmental surroundings?
- Will they release ions to such an extent that the entire particles disintegrate?
- Does surface functionalization promote or hinder dissolution?
- What are the particles' physicochemical properties which influence nanoparticle dissolution?
- What are the implications of the dissolution kinetics of nanoparticles with low or high dissolution rates?

REFERENCES

Abbas, Q., Yousaf, B., Ali, M. U., Munir, M. A. M., El-Naggar, A., Rinklebe, J., & Naushad, M. (2020). Transformation pathways and fate of engineered nanoparticles (ENPs) in distinct interactive environmental compartments: A review. *Environment International*, *138*, 105646.

Abbasi, R., Shineh, G., Mobaraki, M., Doughty, S., & Tayebi, L. (2023). Structural parameters of nanoparticles affecting their toxicity for biomedical applications: a review. *Journal of Nanoparticle Research*, *25*(3),43.

Abdelghany, T. M., Al-Rajhi, A. M. H., Al Abboud, M. A., Alawlaqi, M. M., Ganash Magdah, A., Helmy, E. A. M., & Mabrouk, A. S. (2018). Recent Advances in Green Synthesis of Silver Nanoparticles and Their Applications: About Future Directions. A Review. *BioNanoScience*, *8*, 5–16.

Adams, J., Wright, M., Wagner, H., Valiente, J., Britt, D., & Anderson, A. (2017). Cu from dissolution of CuO nanoparticles signals changes in root morphology. *Plant Physiology and Biochemistry*, *110*, 108–117.

Agrawal, S., Bhatt, M., Rai, S. K., Bhatt, A., Dangwal, P., & Agrawal, P. K. (2018). Silver nanoparticles and its potential applications: A review. *Journal of Pharmacognosy and Phytochemistry*, *7*(2), 930–937.

Albrecht, M. A., Evans, C. W., & Raston, C. L. (2006). Green chemistry and the health implications of nanoparticles. *Green Chemistry*, *8*(5), 417–432.

Angel, B. M., Batley, G. E., Jarolimek, C. V., & Rogers, N. J. (2013). The impact of size on the fate and toxicity of nanoparticulate silver in aquatic systems. *Chemosphere*, *93*(2), 359–365.

Anupong, W., On-uma, R., Jutamas, K., Salmen, S. H., Alharbi, S. A., Joshi, D., & Jhanani, G. K. (2023). Antibacterial, antifungal, antidiabetic, and antioxidant activities potential of Coleus aromaticus synthesized titanium dioxide nanoparticles. *Environmental Research*, *216*, 114714.

Atkins, P., & de Paula, J. (2006). *Atkins' Physical chemistry*. *Oxford University*

Press, 8, 789.

Avellan, A., Simonin, M., McGivney, E., Bossa, N., Spielman-Sun, E., Rocca, J. D., Bernhardt, E.S., Geitner, N. K., Unrine, J. M., Weisner, M. R & Lowry, G. V. (2018). Gold nanoparticle biodissolution by a freshwater macrophyte and its associated microbiome. *Nature Nanotechnology*, *13*(11), 1072-1077.

Avramescu, M. L., Chénier, M., Gardner, H. D., & Rasmussen, P. E. (2019). Solubility of metal oxide nanomaterials: Cautionary notes on sample preparation. *Journal of Physics: Conference Series*, *1323*(1), p012001. IOP Publishing.

Avramescu, M. L., Rasmussen, P. E., Chénier, M., & Gardner, H. D. (2017). Influence of pH, particle size and crystal form on dissolution behaviour of engineered nanomaterials. *Environmental Science and Pollution Research, 24*, 1553–1564.

Axson, J. L., Stark, D. I., Bondy, A. L., Capracotta, S. S., Maynard, A. D., Philbert, M. A., Bergin, I. L., & Ault, A. P. (2015). Rapid Kinetics of Size and pH-Dependent Dissolution and Aggregation of Silver Nanoparticles in Simulated Gastric Fluid. *Journal of Physical Chemistry C*, *119*(35), 20632–20641.

Bachler, G., Losert, S., Umehara, Y., von Goetz, N., Rodriguez-Lorenzo, L., Petri-Fink, A., & Rothen-Rutishauser, B Hungerbuehler, K. (2015). Translocation of gold nanoparticles across the lung epithelial tissue barrier: Combining in vitro and in silico methods to substitute in vivo experiments. *Particle and Fibre Toxicology*, *12*(1), 1–18.

Badawy, A. M. ., Luxton, T. P., Silva, R. G., Scheckel, K. G., Suidan, M. T., & Tolaymat, T. M. (2010). Impact of environmental conditions (pH, ionic strength, and electrolyte type) on the surface charge and aggregation of silver nanoparticles suspensions. *Environmental Science and Technology*, *44*(4), 1260–1266.

Bailly, A. L., Correard, F., Popov, A., Tselikov, G., Chaspoul, F., Appay, R., Esteve, M. A. (2019). In vivo evaluation of safety, biodistribution and pharmacokinetics of laser-synthesized gold nanoparticles. *Scientific Reports*,

9(1), 12890.

Balasubramanian, S. K., Jittiwat, J., Manikandan, J., Ong, C. N., Liya, E. Y., & Ong, W. Y. (2010). Biodistribution of gold nanoparticles and gene expression changes in the liver and spleen after intravenous administration in rats. *Biomaterials*, *31*(8), 2034–2042.

Baranowska-Wójcik, E., Szwajgier, D., Oleszczuk, P., & Winiarska-mieczan, A. (2020). Effects of Titanium Dioxide Nanoparticles Exposure on Human Health-a Review. *Biological Trace Element Research, 193*, 118–129.

Beer, C., Foldbjerg, R., Hayashi, Y., Sutherland, D. S., & Autrup, H. (2012). Toxicity of silver nanoparticles-Nanoparticle or silver ion? *Toxicology Letters*, *208*(3), 286–292.

Behnam, M. A., Emami, F., Sobhani, Z., & Dehghanian, A. R. (2018). The application of titanium dioxide (TiO2) nanoparticles in the photo-thermal therapy of melanoma cancer model. *Iranian Journal of Basic Medical Sciences*, *21(11)*, 1133.

Behra, R., Sigg, L., Clift, M. J. D., Herzog, F., Minghetti, M., Johnston, B., Rothen-Rutishauser, B. (2013). Bioavailability of silver nanoparticles and ions: From a chemical and biochemical perspective. *Journal of the Royal Society Interface*, *10(87)*, 20130396.

Bettencourt, A., Gonçalves, L. M., Gramacho, A. C., Vieira, A., Rolo, D., Martins, C., … Louro, H. (2020). Analysis of the characteristics and cytotoxicity of titanium dioxide nanomaterials following simulated in vitro digestion. *Nanomaterials*, *10*(8), 1516.

Bian, S. W., Mudunkotuwa, I. A., Rupasinghe, T., & Grassian, V. H. (2011). Aggregation and dissolution of 4 nm ZnO nanoparticles in aqueous environments: Influence of pH, ionic strength, size, and adsorption of humic acid. *Langmuir*, *27*(10), 6059–6068.

Blasco, J., Corsi, I., & Matranga, V. (2015). Particles in the oceans: Implication for a safe marine environment. *Marine Environmental Research*, *111*, 1–4.

Borm, P., Klaessig, F. C., Landry, T. D., Moudgil, B., Pauluhn, J., Thomas, K., Wood, S. (2006). Research strategies for safety evaluation of nanomaterials, Part V: Role of dissolution in biological fate and effects of nanoscale particles. *Toxicological Sciences, 90(1),* 23–32.

Bour, A., Mouchet, F., Silvestre, J., Gauthier, L., & Pinelli, E. (2015). Environmentally relevant approaches to assess nanoparticles ecotoxicity: A review. *Journal of Hazardous Materials*, *283,* 764–777.

Bove, P., Malvindi, M. A., Kote, S. S., Bertorelli, R., Summa, M., & Sabella, S. (2017). Dissolution test for risk assessment of nanoparticles: A pilot study. *Nanoscale*, *9(19),* 6315–6326.

Bozich, J. S., Lohse, S. E., Torelli, M. D., Murphy, C. J., Hamers, R. J., & Klaper, R. D. (2014). Surface chemistry, charge and ligand type impact the toxicity of gold nanoparticles to Daphnia magna. *Environmental Science: Nano, 1(3),* 260–270.

Braydich-Stolle, L. K., Breitner, E. K., Comfort, K. K., Schlager, J. J., & Hussain, S. M. (2014). Dynamic characteristics of silver nanoparticles in physiological fluids: Toxicological implications. *Langmuir*, *30(50),* 15309–15316.

Breitner, E. K., Hussain, S. M., & Comfort, K. K. (2015). The role of biological fluid and dynamic flow in the behavior and cellular interactions of gold nanoparticles. *Journal of Nanobiotechnology*, *13(1),* 1–10.

Brunelli, A., Pojana, G., Callegaro, S., & Marcomini, A. (2013). Agglomeration and sedimentation of titanium dioxide nanoparticles (n-TiO2) in synthetic and real waters. *Journal of Nanoparticle Research, 15*, 1–10.

Bundschuh, M., Filser, J., Lüderwald, S., McKee, M. S., Metreveli, G., Schaumann, G. E., Wagner, S. (2018). Nanoparticles in the environment: where do we come from, where do we go to? *Environmental Sciences Europe*, *30(1),* 1–17.

Carabineiro, S. A. C. (2017). Applications of gold nanoparticles in nanomedicine: Recent advances in vaccines. *Molecules*, *22(5),* 857.

Carlander, U, Midander, K., Hedberg, Y. S., Johanson, G., Bottai, M., & Karlsson,

H. L. (2019). Macrophage-Assisted Dissolution of Gold Nanoparticles. *ACS Applied Bio Materials*, *2(3)*, 1006–1016.

Carlander, Ulrika, Midander, K., Hedberg, Y. S., Johanson, G., Bottai, M., & Karlsson, H. L. (2019). Macrophage-Assisted Dissolution of Gold Nanoparticles. *ACS Applied Bio Materials*, *2(3)*, 1006–1016.

Chambers, B. A., Afrooz, A. N., Bae, S., Aich, N., Katz, L., Saleh, N. B., & Kirisits, M. J. (2014). Effects of chloride and ionic strength on physical morphology, dissolution, and bacterial toxicity of silver nanoparticles. *Environmental Science and Technology*, *48(1)*, 761–769.

Chen, Z., Han, S., Zhou, S., Feng, H., Liu, Y., & Jia, G. (2020). Review of health safety aspects of titanium dioxide nanoparticles in food application. *NanoImpact*, *18*, 100224.

Cherevko, S., Zeradjanin, A., Keeley, G. P., & Mayrhofer, K. (2014). A comparative study on gold and platinum dissolution in acidic and alkaline media. *Journal of the Electrochemical Society*, *161(12)*, H822.

Connor, E. E., Mwamuka, J., Gole, A., Murphy, C. J., & Wyatt, M. D. (2005). Gold nanoparticles are taken up by human cells but do not cause acute cytotoxicity. *Small*, *1(3)*, 325–327.

Cupi, D., Hartmann, N. B., & Baun, A. (2016). Influence of pH and media composition on suspension stability of silver, zinc oxide, and titanium dioxide nanoparticles and immobilization of Daphnia magna under guideline testing conditions. *Ecotoxicology and Environmental Safety*, *127*, 144–152.

Czajka, M., Sawicki, K., Sikorska, K., Popek, S., Kruszewski, M., & Kapka-Skrzypczak, L. (2015). Toxicity of titanium dioxide nanoparticles in central nervous system. *Toxicology in Vitro*, *29(5)*, 1042–1052.

da Silva, A. B., Miniter, M., Thom, W., Hewitt, R. E., Wills, J., Jugdaohsingh, R., & Powell, J. J. (2020). Gastrointestinal absorption and toxicity of nanoparticles and microparticles: Myth, reality and pitfalls explored through titanium dioxide. *Current Opinion in Toxicology*, *19*, 112–120.

De Jong, W. H., Hagens, W. I., Krystek, P., Burger, M. C., Sips, A. J. A. M., & Geertsma, R. E. (2008). Particle size-dependent organ distribution of gold nanoparticles after intravenous administration. *Biomaterials*, *29(12)*, 1912–1919.

De Matteis, V., Cascione, M., Brunetti, V., Toma, C. C., & Rinaldi, R. (2016). Toxicity assessment of anatase and rutile titanium dioxide nanoparticles: The role of degradation in different pH conditions and light exposure. *Toxicology in Vitro*, *37*, 201–210.

Deshmukh, S. P., Patil, S. M., Mullani, S. B., & Delekar, S. D. (2019). Silver nanoparticles as an effective disinfectant: A review. *Materials Science and Engineering C*, *97*, 954–965.

Donovan, A. R., Adams, C. D., Ma, Y., Stephan, C., Eichholz, T., & Shi, H. (2016). Single particle ICP-MS characterization of titanium dioxide, silver, and gold nanoparticles during drinking water treatment. *Chemosphere*, *144*, 148–153.

Echegoyen, Y., & Nerín, C. (2013). Nanoparticle release from nano-silver antimicrobial food containers. *Food and Chemical Toxicology*, *62*, 16–22.

Elahi, N., Kamali, M., & Baghersad, M. H. (2018). Recent biomedical applications of gold nanoparticles: A review. *Talanta*, *184*, 537–556.

England, C. G., Miller, M. C., Kuttan, A., Trent, J. O., & Frieboes, H. B. (2015). Release kinetics of paclitaxel and cisplatin from two and three layered gold nanoparticles. *European Journal of Pharmaceutics and Biopharmaceutics*, *92*, 120–129.

Espinasse, B. P., Geitner, N. K., Schierz, A., Therezien, M., Richardson, C. J., Lowry, G. V., … Wiesner, M. R. (2018). Comparative Persistence of Engineered Nanoparticles in a Complex Aquatic Ecosystem. *Environmental Science and Technology*, *52*(7), 4072–4078.

Fabian, E., Landsiedel, R., Ma-Hock, L., Wiench, K., Wohlleben, W., & Van Ravenzwaay, B. (2008). Tissue distribution and toxicity of intravenously administered titanium dioxide nanoparticles in rats. *Archives of Toxicology*,

82(3), 151–157.

Fabrega, J., Fawcett, S. R., Renshaw, J. C., & Lead, J. R. (2009). Silver nanoparticle impact on bacterial growth: Effect of pH, concentration, and organic matter. *Environmental Science and Technology*, *43*(19), 7285–7290.

Fede, C., Fortunati, I., Weber, V., Rossetto, N., Bertasi, F., Petrelli, L., … Ferrante, C. (2015). Evaluation of gold nanoparticles toxicity towards human endothelial cells under static and flow conditions. *Microvascular Research*, *97*, 147–155.

Fernando, I., & Zhou, Y. (2019). Impact of pH on the stability, dissolution and aggregation kinetics of silver nanoparticles. *Chemosphere*, *216*, 297–305.

Foldbjerg, R., Jiang, X., Miclăuş, T., Chen, C., Autrup, H., & Beer, C. (2015). Silver nanoparticles - Wolves in sheep's clothing? *Toxicology Research*, *4*(3), 563–575.

Fraga, S., Brandão, A., Soares, M. E., Morais, T., Duarte, J. A., Pereira, L., … Carmo, H. (2014). Short- and long-term distribution and toxicity of gold nanoparticles in the rat after a single-dose intravenous administration. *Nanomedicine: Nanotechnology, Biology, and Medicine*, *10*(8), 1757–1766.

Fratoddi, I, Venditti, I., Cametti, C., & Russo, M. V. (2015). How toxic are gold nanoparticles? The state-of-the-art. *Nano Research*, *8*(6), 1771–1799.

Fratoddi, Ilaria, Venditti, I., Cametti, C., & Russo, M. V. (2015). How toxic are gold nanoparticles? The state-of-the-art. *Nano Research*, *8*(6), 1771–1799.

Freyre-Fonseca, V., Téllez-Medina, D. I., Medina-Reyes, E. I., Cornejo-Mazón, M., López-Villegas, E. O., Alamilla-Beltrán, L., … Gutiérrez-López, G. F. (2016). Morphological and Physicochemical Characterization of Agglomerates of Titanium Dioxide Nanoparticles in Cell Culture Media. *Journal of Nanomaterials*, *2016*, 1–19.

Furtado, L. M., Bundschuh, M., & Metcalfe, C. D. (2016). Monitoring the Fate and Transformation of Silver Nanoparticles in Natural Waters. *Bulletin of Environmental Contamination and Toxicology*, *97*(4), 449–455.

Gallego-Urrea, J. A., Hammes, J., Cornelis, G., & Hassellöv, M. (2016). Coagulation and sedimentation of gold nanoparticles and illite in model natural waters: Influence of initial particle concentration. *NanoImpact, 3*, 67–74.

Ganasan, E., Mohd Yusoff, H., Azmi, A. A., Chia, P. W., Lam, S. S., Kan, S. Y., Teo, C. K. (2023). Food additives for the synthesis of metal nanoparticles: a review. *Environmental Chemistry Letters*, *21*(1), 525–538.

Gnach, A., Lipinski, T., Bednarkiewicz, A., Rybka, J., & Capobianco, J. A. (2015). Upconverting nanoparticles: Assessing the toxicity. *Chemical Society Reviews*, *44*(6), 1561–1584.

González-Pedroza, M. G., Benítez, A. R. T., Navarro-Marchal, S. A., Martínez-Martínez, E., Marchal, J. A., Boulaiz, H., & Morales-Luckie, R. A. (2023). Biogeneration of silver nanoparticles from Cuphea procumbens for biomedical and environmental applications. *Scientific Reports*, *13*(1), 790.

Goodman, C. M., McCusker, C. D., Yilmaz, T., & Rotello, V. M. (2004). Toxicity of gold nanoparticles functionalized with cationic and anionic side chains. *Bioconjugate Chemistry*, *15*(4), 897–900.

Gopinath, K. P., Madhav, N. V., Krishnan, A., Malolan, R., & Rangarajan, G. (2020). Present applications of titanium dioxide for the photocatalytic removal of pollutants from water: A review. *Journal of Environmental Management*, *270*, 110906.

Gottardo, S., Mech, A., Drbohlavová, J., Małyska, A., Bøwadt, S., Riego Sintes, J., & Rauscher, H. (2021). Towards safe and sustainable innovation in nanotechnology: State-of-play for smart nanomaterials. *NanoImpact*, *21*, 100297.

Gualtieri, A. F., Pollastri, S., Bursi Gandolfi, N., & Gualtieri, M. L. (2018). In vitro acellular dissolution of mineral fibres: A comparative study. *Scientific Reports*, *8*(1), 7071.

Guerrini, L., Alvarez-Puebla, R. A., & Pazos-Perez, N. (2018). Surface

modifications of nanoparticles for stability in biological fluids. *Materials*, *11*(7), 1145.

Gulumian, M., & Cassee, F. R. (2021). Safe by design (SbD) and nanotechnology: a much-discussed topic with a prudence? *Particle and Fibre Toxicology*, *18*(1), 1–4.

Gunsolus, I. L., Mousavi, M. P. S., Hussein, K., Bühlmann, P., & Haynes, C. L. (2015a). Effects of Humic and Fulvic Acids on Silver Nanoparticle Stability, Dissolution, and Toxicity. *Environmental Science and Technology*, *49*(13), 8078–8086.

Gunsolus, I. L., Mousavi, M. P. S., Hussein, K., Bühlmann, P., & Haynes, C. L. (2015b). Effects of Humic and Fulvic Acids on Silver Nanoparticle Stability, Dissolution, and Toxicity. *Environmental Science and Technology*, *49*(13), 8078–8086.

Hadrup, N., Sharma, A. K., & Loeschner, K. (2018). Toxicity of silver ions, metallic silver, and silver nanoparticle materials after in vivo dermal and mucosal surface exposure: A review. *Regulatory Toxicology and Pharmacology*, *98*, 257–267.

Haider, A. J., Jameel, Z. N., & Al-Hussaini, I. H. M. (2019). Review on: Titanium dioxide applications. *Energy Procedia*, *157*, 17–29.

Han, S. G., Lee, J. S., Ahn, K., Kim, Y. S., Kim, J. K., Lee, J. H., … Yu, I. J. (2015). Size-dependent clearance of gold nanoparticles from lungs of Sprague–Dawley rats after short-term inhalation exposure. *Archives of Toxicology*, *89*(7), 1083–1094.

He, D., Bligh, M. W., & Waite, T. D. (2013). Effects of aggregate structure on the dissolution kinetics of citrate-stabilized silver nanoparticles. *Environmental Science and Technology*, *47*(16), 9148–9156.

Helmlinger, J., Sengstock, C., Groß-Heitfeld, C., Mayer, C., Schildhauer, T. A., Köller, M., & Epple, M. (2016). Silver nanoparticles with different size and shape: Equal cytotoxicity, but different antibacterial effects. *RSC Advances*,

6(22), 18490–18501.

Hieu, D. M. (2017). Silver and Gold Nanoparticles : a Toxicological Aspect Silver and Gold Nanoparticles : a Toxicological Aspect. *Journal of Science & Technology*, *118*, 020–025.

Hirn, S., Semmler-Behnke, M., Schleh, C., Wenk, A., Lipka, J., Schäffler, M., … Kreyling, W. G. (2011). Particle size-dependent and surface charge-dependent biodistribution of gold nanoparticles after intravenous administration. *European Journal of Pharmaceutics and Biopharmaceutics*, *77*(3), 407–416.

Ho, C. M., Yau, S. K. W., Lok, C. N., So, M. H., & Che, C. M. (2010). Oxidative dissolution of silver nanoparticles by biologically relevant oxidants: A kinetic and mechanistic study. *Chemistry - An Asian Journal*, *5*(2), 285–293.

Innes, E., Yiu, H. H. P., McLean, P., Brown, W., & Boyles, M. (2021). Simulated biological fluids–a systematic review of their biological relevance and use in relation to inhalation toxicology of particles and fibres. *Critical Reviews in Toxicology*, *51*(3), 217–248.

Irshad, M. A., Nawaz, R., Rehman, M. Z. ur, Adrees, M., Rizwan, M., Ali, S., … Tasleem, S. (2021). Synthesis, characterization and advanced sustainable applications of titanium dioxide nanoparticles: A review. *Ecotoxicology and Environmental Safety*, *212*, 111978.

Jia, Y. P., Ma, B. Y., Wei, X. W., & Qian, Z. Y. (2017). The in vitro and in vivo toxicity of gold nanoparticles. *Chinese Chemical Letters*, *28*(4), 691–702.

Jin, X., Li, M., Wang, J., Marambio-Jones, C., Peng, F., Huang, X., … Hoek, E. M. V. (2010). High-throughput screening of silver nanoparticle stability and bacterial inactivation in aquatic media: Influence of specific ions. *Environmental Science and Technology*, *44*(19), 7321–7328.

Joo, S. H., & Zhao, D. (2017). Environmental dynamics of metal oxide nanoparticles in heterogeneous systems: A review. *Journal of Hazardous Materials*, *322*, 29–47.

Joseph, T. M., Kar Mahapatra, D., Esmaeili, A., Piszczyk, Ł., Hasanin, M. S.,

Kattali, M., … Thomas, S. (2023). Nanoparticles: Taking a Unique Position in Medicine. *Nanomaterials*, *13*(3), 574.

Kang, X., Liu, S., Dai, Z., He, Y., Song, X., & Tan, Z. (2019). Titanium dioxide: From engineering to applications. *Catalysts 9*(2), 191.

Kao, J. Y., & Cheng, W. T. (2020). Study on Dispersion of TiO2 Nanopowder in Aqueous Solution via near Supercritical Fluids. *ACS Omega*, *5*(4), 1832–1839.

Keller, J. G., Graham, U. M., Koltermann-Jülly, J., Gelein, R., Ma-Hock, L., Landsiedel, R., Wohlleben, W. (2020). Predicting dissolution and transformation of inhaled nanoparticles in the lung using abiotic flow cells: The case of barium sulfate. *Scientific Reports*, *10*(1), 1–15.

Kent, R. D., & Vikesland, P. J. (2012). Controlled evaluation of silver nanoparticle dissolution using atomic force microscopy. *Environmental Science and Technology*, *46*(13), 6977–6984.

Kerin, H., Nagaraj, K., & Kamalesu, S. (2023). Review on aquatic toxicity of metal oxide nanoparticles. *Materials Today: Proceedings*.

Kittler, S., Greulich, C., Diendorf, J., Koller, M., & Epple, M. (2010). Toxicity of silver nanoparticles increases during storage because of slow dissolution under release of silver ions. *Chemistry of Materials*, *22*(16), 4548–4554.

Klaessig, F. C. (2018). Dissolution as a paradigm in regulating nanomaterials. *Environmental Science: Nano*, *5*(5), 1070–1077.

Koltermann-Jülly, J., Keller, J. G., Vennemann, A., Werle, K., Müller, P., Ma-Hock, L., Wohlleben, W. (2018). Abiotic dissolution rates of 24 (nano)forms of 6 substances compared to macrophage-assisted dissolution and in vivo pulmonary clearance: Grouping by biodissolution and transformation. *NanoImpact*, *12*, 29–41.

Korábková, E., Kašpárková, V., Jasenská, D., Moricová, D., Daďová, E., Truong, T. H., Humpolíček, P. (2021). Behaviour of titanium dioxide particles in artificial body fluids and human blood plasma. *International Journal of Molecular Sciences*, *22*(19), 10614.

Kraegeloh, A., Suarez-Merino, B., Sluijters, T., & Micheletti, C. (2018). Implementation of safe-by-design for nanomaterial development and safe innovation: Why we need a comprehensive approach. *Nanomaterials*, *8*(4), 239.

Kreyling, W. G., Fertsch-Gapp, S., Schäffler, M., Johnston, B. D., Haberl, N., Pfeiffer, C., … Epple, M. (2014). In vitro and in vivo interactions of selected nanoparticles with rodent serum proteins and their consequences in biokinetics. *Beilstein Journal of Nanotechnology*, *5*(1), 1699–1711.

Larue, C., Khodja, H., Herlin-Boime, N., Brisset, F., Flank, A. M., Fayard, B., … Carrière, M. (2011). Investigation of titanium dioxide nanoparticles toxicity and uptake by plants. *Journal of Physics: Conference Series*, *304*(1), 012057.

Lasagna-Reeves, C., Gonzalez-Romero, D., Barria, M. A., Olmedo, I., Clos, A., Sadagopa Ramanujam, V. M., … Soto, C. (2010). Bioaccumulation and toxicity of gold nanoparticles after repeated administration in mice. *Biochemical and Biophysical Research Communications*, *393*(4), 649–655.

Laux, P., Riebeling, C., Booth, A. M., Brain, J. D., Brunner, J., Cerrillo, C., … Jungnickel, H. (2017). NanoImpact Biokinetics of nanomaterials : The role of biopersistence. *NanoImpact*, *6*, 69–80.

León-Silva, S., Fernández-Luqueño, F., & López-Valdez, F. (2016). Silver Nanoparticles (AgNP) in the Environment: a Review of Potential Risks on Human and Environmental Health. *Water, Air, and Soil Pollution*, *227*(9), 306.

Levard, C., Mitra, S., Yang, T., Jew, A. D., Badireddy, A. R., Lowry, G. V., & Brown, G. E. (2013). Effect of chloride on the dissolution rate of silver nanoparticles and toxicity to E. coli. *Environmental Science and Technology*, *47*(11), 5738–5745.

Li, X., Lenhart, J. J., & Walker, H. W. (2010). Dissolution-accompanied aggregation kinetics of silver nanoparticles. *Langmuir*, *26*(22), 16690–16698.

Li, X., Lenhart, J. J., & Walker, H. W. (2012). Aggregation kinetics and dissolution of coated silver nanoparticles. *Langmuir*, *28*(2), 1095–1104.

Li, Y., Zhang, W., Niu, J., & Chen, Y. (2013). Surface-coating-dependent dissolution, aggregation, and reactive oxygen species (ROS) generation of silver nanoparticles under different irradiation conditions. *Environmental Science and Technology*, *47*(18), 10293–10301.

Li, Y., Zhao, J., Shang, E., Xia, X., Niu, J., & Crittenden, J. (2018). Effects of Chloride Ions on Dissolution, ROS Generation, and Toxicity of Silver Nanoparticles under UV Irradiation. *Environmental Science and Technology*, *52*(8), 4842–4849.

Lin, Z., Monteiro-Riviere, N. A., Kannan, R., & Riviere, J. E. (2016). A computational framework for interspecies pharmacokinetics, exposure and toxicity assessment of gold nanoparticles. *Nanomedicine*, *11*(2), 107–119.

Liu, J., & Hurt, R. H. (2010). Ion release kinetics and particle persistence in aqueous nano-silver colloids. *Environmental Science and Technology*, *44*(6), 2169–2175.

Lodeiro, P., Achterberg, E. P., Pampín, J., Affatati, A., & El-Shahawi, M. S. (2016). Silver nanoparticles coated with natural polysaccharides as models to study AgNP aggregation kinetics using UV-Visible spectrophotometry upon discharge in complex environments. *Science of the Total Environment*, *539*, 7–16.

Loza, K., Diendorf, J., Sengstock, C., Ruiz-Gonzalez, L., Gonzalez-Calbet, J. M., Vallet-Regi, M., Epple, M. (2014). The dissolution and biological effects of silver nanoparticles in biological media. *Journal of Materials Chemistry B*, *2*(12), 1634–1643.

Ma, R., Levard, C., Marinakos, S. M., Cheng, Y., Liu, J., Michel, F. M., … Lowry, G. V. (2012). Size-controlled dissolution of organic-coated silver nanoparticles. *Environmental Science and Technology*, *46*(2), 752–759.

Marques, M. R., Loebenberg, R., & Almukainzi, M. (2011). Simulated biological fluids with possible application in dissolution testing. *Dissolution Technologies*, *18*(3), 15–28.

Martin, M. N., Allen, A. J., Maccuspie, R. I., & Hackley, V. A. (2014). Dissolution, agglomerate morphology, and stability limits of protein-coated silver nanoparticles. *Langmuir*, *30*(38), 11442–11452.

Mathur, P., Jha, S., Ramteke, S., & Jain, N. K. (2018). Pharmaceutical aspects of silver nanoparticles. *Artificial Cells, Nanomedicine and Biotechnology*, *46(sup1)*, 115–126.

Mercier-Bonin, M., Despax, B., Raynaud, P., Houdeau, E., & Thomas, M. (2018). Mucus and microbiota as emerging players in gut nanotoxicology: The example of dietary silver and titanium dioxide nanoparticles. *Critical Reviews in Food Science and Nutrition*, *58*(6), 1023–1032.

Metreveli, G., Frombold, B., Seitz, F., Grün, A., Philippe, A., Rosenfeldt, R. R., … Schaumann, G. E. (2016). Impact of chemical composition of ecotoxicological test media on the stability and aggregation status of silver nanoparticles. *Environmental Science: Nano*, *3*(2), 418–433.

Misra, S. K., Dybowska, A., Berhanu, D., Luoma, S. N., & Valsami-Jones, E. (2012). The complexity of nanoparticle dissolution and its importance in nanotoxicological studies. *Science of the Total Environment*, *438*, 225–232.

Murugadoss, S., Brassinne, F., Sebaihi, N., Petry, J., Cokic, S. M., Van Landuyt, K. L., Van Den Brule, S. (2020). Agglomeration of titanium dioxide nanoparticles increases toxicological responses in vitro and in vivo. *Particle and Fibre Toxicology*, *17*(1), 1–14.

Musial, J., Krakowiak, R., Mlynarczyk, D. T., Goslinski, T., & Stanisz, B. J. (2020). Titanium dioxide nanoparticles in food and personal care products—what do we know about their safety? *Nanomaterials*, *10*(6), 1110.

Nam, S. H., Kim, S. W., & An, Y. J. (2012). No evidence of the genotoxic potential of gold, silver, zinc oxide and titanium dioxide nanoparticles in the SOS chromotest. *Journal of Applied Toxicology*, *33*(10), 1061–1069.

Nia, H. M., Rezaei-Tavirani, M., Nikoofar, A. R., Masoumi, H., Nasr, R., Hasanzadeh, H., Shadnush, M. (2015). Stabilizing and dispersing methods of

TiO 2 nanoparticles in biological studies. *Journal of Paramedical Sciences (JPS)*, *6*(2), 96–105.

Nikolić, N., Spasojević, J., Radosavljević, A., Milošević, M., Barudžija, T., Rakočević, L., & Kačarević-Popović, Z. (2023). Influence of poly(vinyl alcohol)/poly(N-vinyl-2-pyrrolidone) polymer matrix composition on the bonding environment and characteristics of Ag nanoparticles produced by gamma irradiation. *Radiation Physics and Chemistry*, *202*, 110564.

OECD. (2018). Assessment of Biodurability of Nanomaterials and their Surface ligands Series on the Safety of Manufactured Nanomaterials No. 86, *ENV/JM/MON*(86), 1–90.

Oh, N., & Park, J. H. (2014). Endocytosis and exocytosis of nanoparticles in mammalian cells. *International Journal of Nanomedicine*, *9*(Suppl 1), 51–63.

Oskam, G., Nellore, A., Penn, R. L., & Searson, P. C. (2003). The growth kinetics of TiO2 nanoparticles from titanium(IV) alkoxide at high water/titanium ratio. *Journal of Physical Chemistry B*, *107*(8), 1734–1738.

Pallavicini, P., Preti, L., Vita, L. De, Dacarro, G., Diaz Fernandez, Y. A., Merli, D., … Vigani, B. (2020). Fast dissolution of silver nanoparticles at physiological pH. *Journal of Colloid and Interface Science*, *563*, 177–188.

Pareek, V., Gupta, R., & Panwar, J. (2018). Do physico-chemical properties of silver nanoparticles decide their interaction with biological media and bactericidal action? A review. *Materials Science and Engineering C*, *90*(April), 739–749.

Peng, C., Zhang, W., Gao, H., Li, Y., Tong, X., Li, K., … Chen, Y. (2017). Behavior and potential impacts of metal-based engineered nanoparticles in aquatic environments. *Nanomaterials*, *7*(1), 21.

Peretyazhko, T. S., Zhang, Q., & Colvin, V. L. (2014). Size-controlled dissolution of silver nanoparticles at neutral and acidic pH conditions: Kinetics and size changes. *Environmental Science and Technology*, *48*(20), 11954–11961.

Pokhrel, L. R., Dubey, B., & Scheuerman, P. R. (2014). Natural water chemistry

(dissolved organic carbon, pH, and hardness) modulates colloidal stability, dissolution, and antimicrobial activity of citrate functionalized silver nanoparticles. *Environmental Science: Nano*, *1*(1), 45–54.

Pompa, P. P., Vecchio, G., Galeone, A., Brunetti, V., Sabella, S., Maiorano, G., … Cingolani, R. (2011). In Vivo toxicity assessment of gold nanoparticles in Drosophila melanogaster. *Nano Research*, *4*(4), 405–413.

Prasath, S., & Palaniappan, K. (2019). Is using nanosilver mattresses/pillows safe? A review of potential health implications of silver nanoparticles on human health. *Environmental Geochemistry and Health*, *41*(5), 2295–2313.

Pujalté, I., Dieme, D., Haddad, S., Serventi, A. M., & Bouchard, M. (2017). Toxicokinetics of titanium dioxide (TiO2) nanoparticles after inhalation in rats. *Toxicology Letters*, *265*, 77–85.

Pulit-Prociak, J., & Banach, M. (2016). Silver nanoparticles - A material of the future...? *Open Chemistry*, *14*(1), 76–91.

Qi, J., Ye, Y. Y., Wu, J. J., Wang, H. T., & Li, F. T. (2013). Dispersion and stability of titanium dioxide nanoparticles in aqueous suspension: Effects of ultrasonication and concentration. *Water Science and Technology*, *67*(1), 147–151.

Radniecki, T. S., Stankus, D. P., Neigh, A., Nason, J. A., & Semprini, L. (2011). Influence of liberated silver from silver nanoparticles on nitrification inhibition of Nitrosomonas europaea. *Chemosphere*, *85*(1), 43–49.

Rak, M. J., Saadé, N. K., Friščić, T., & Moores, A. (2014). Mechanosynthesis of ultra-small monodisperse amine-stabilized gold nanoparticles with controllable size. *Green Chemistry*, *16*(1), 86–89.

Raza, G., Amjad, M., Kaur, I., & Wen, D. (2016). Stability and Aggregation Kinetics of Titania Nanomaterials under Environmentally Realistic Conditions. *Environmental Science and Technology*, *50*(16), 8462–8472.

Rosi, N. L., Giljohann, D. A., Thaxton, C. S., Lytton-Jean, A. K. R., Han, M. S., & Mirkin, C. A. (2006). Oligonucleotide-modified gold nanoparticles for

infracellular gene regulation. *Science*, *312*(5776), 1027–1030.

Sani, A., Cao, C., & Cui, D. (2021). Toxicity of gold nanoparticles (AuNPs): A review. *Biochemistry and Biophysics Reports*, *26*, 100991.

Sauer, U. G., Werle, K., Waindok, H., Hirth, S., Hachmöller, O., & Wohlleben, W. (2021). Critical Choices in Predicting Stone Wool Biodurability: Lysosomal Fluid Compositions and Binder Effects. *Chemical Research in Toxicology*, *34*(3), 780–792.

Schaeublin, N. M., Braydich-Stolle, L. K., Schrand, A. M., Miller, J. M., Hutchison, J., Schlager, J. J., & Hussain, S. M. (2011). Surface charge of gold nanoparticles mediates mechanism of toxicity. *Nanoscale*, *3*(2), 410–420.

Schmidt, J., & Vogelsberger, W. (2006). Dissolution kinetics of titanium dioxide nanoparticles: The observation of an unusual kinetic size effect. *Journal of Physical Chemistry B*, *110*(9), 3955–3963.

Schmidt, J., & Vogelsberger, W. (2009). Aqueous long-term solubility of titania nanoparticles and titanium(IV) hydrolysis in a sodium chloride system studied by adsorptive stripping voltammetry. *Journal of Solution Chemistry*, *38*(10), 1267–1282.

Sharifi, S., Behzadi, S., Laurent, S., Forrest, M. L., Stroeve, P., & Mahmoudi, M. (2012). Toxicity of nanomaterials. *Chemical Society Reviews*, *41*(6), 2323–2343.

Sharma, V. K., Siskova, K. M., Zboril, R., & Gardea-Torresdey, J. L. (2014). Organic-coated silver nanoparticles in biological and environmental conditions: Fate, stability and toxicity. *Advances in Colloid and Interface Science*, *204*, 15–34.

Shi, H., Magaye, R., Castranova, V., & Zhao, J. (2013). Titanium dioxide nanoparticles: a review of current toxicological data. *Particle and Fibre Toxicology*, *10*(1), 1–33.

Shinohara, N., Zhang, G., Oshima, Y., Kobayashi, T., Imatanaka, N., Nakai, M., Gamo, M. (2017). Kinetics and dissolution of intratracheally administered

nickel oxide nanomaterials in rats. *Particle and Fibre Toxicology*, *14*(1), 1–14.

Shkol'nikov, E. V. (2016). Thermodynamics of the dissolution of amorphous and polymorphic TiO2 modifications in acid and alkaline media. *Russian Journal of Physical Chemistry A*, *90*(3), 567–571.

Shukla, R., Bansal, V., Chaudhary, M., Basu, A., Bhonde, R. R., & Sastry, M. (2005). Biocompatibility of gold nanoparticles and their endocytotic fate inside the cellular compartment: A microscopic overview. *Langmuir*, *21*(23), 10644–10654.

Silva, T., Pokhrel, L. R., Dubey, B., Tolaymat, T. M., Maier, K. J., & Liu, X. (2014). Particle size, surface charge and concentration dependent ecotoxicity of three organo-coated silver nanoparticles: Comparison between general linear model-predicted and observed toxicity. *Science of the Total Environment*, *468*, 968–976.

Simpson, C. A., Salleng, K. J., Cliffel, D. E., & Feldheim, D. L. (2013). In vivo toxicity, biodistribution, and clearance of glutathione-coated gold nanoparticles. *Nanomedicine: Nanotechnology, Biology, and Medicine*, *9*(2), 257–263.

Sohal, I. S., Cho, Y. K., O'Fallon, K. S., Gaines, P., Demokritou, P., & Bello, D. (2018a). Dissolution behavior and biodurability of ingested engineered nanomaterials in the gastrointestinal environment. *ACS Nano*, *12*(8), 8115–8128. https://doi.org/10.1021/acsnano.8b02978

Sohal, I. S., Cho, Y. K., O'Fallon, K. S., Gaines, P., Demokritou, P., & Bello, D. (2018b). Dissolution behavior and biodurability of ingested engineered nanomaterials in the gastrointestinal environment. *ACS Nano*, *12*(8), 8115–8128.

Sperling, R. A., & Parak, W. J. (2010). Surface modification, functionalization and bioconjugation of colloidal Inorganic nanoparticles. *Philosophical Transactions of the Royal Society A: Mathematical, Physical and Engineering Sciences*, *368*(1915), 1333–1383.

Stankus, D. P., Lohse, S. E., Hutchison, J. E., & Nason, J. A. (2011). Interactions between natural organic matter and gold nanoparticles stabilized with different organic capping agents. *Environmental Science and Technology*, *45*(8), 3238–3244.

Taboada-López, M. V., Vázquez-Expósito, G., Domínguez-González, R., Herbello-Hermelo, P., Bermejo-Barrera, P., & Moreda-Piñeiro, A. (2021). Biopersistence rate of metallic nanoparticles in the gastro-intestinal human tract (stage 0 of the EFSA guidance for nanomaterials risk assessment). *Food Chemistry*, *360*, 130002.

Taurozzi, J. S., Hackley, V. A., & Wiesner, M. R. (2013). A standardised approach for the dispersion of titanium dioxide nanoparticles in biological media. *Nanotoxicology*, *7*(4), 389–401.

Tejamaya, M., Römer, I., Merrifield, R. C., & Lead, J. R. (2012). Stability of citrate, PVP, and PEG coated silver nanoparticles in ecotoxicology media. *Environmental Science and Technology*, *46*(13), 7011–7017.

Tiwari, P. M., Vig, K., Dennis, V. A., & Singh, S. R. (2011). Functionalized Gold Nanoparticles and Their Biomedical Applications. *Nanomaterials*, *1*(1), 31–63.

Turan, N. B., Erkan, H. S., Engin, G. O., & Bilgili, M. S. (2019). Nanoparticles in the aquatic environment: Usage, properties, transformation and toxicity—A review. *Process Safety and Environmental Protection*, *130*, 238–249.

Unrine, J. M., Shoults-Wilson, W. A., Zhurbich, O., Bertsch, P. M., & Tsyusko, O. V. (2012). Trophic transfer of Au nanoparticles from soil along a simulated terrestrial food chain. *Environmental Science and Technology*, *46*(17), 9753–9760.

Utembe, W., Potgieter, K., Stefaniak, A. B., & Gulumian, M. (2015). Dissolution and biodurability: Important parameters needed for risk assessment of nanomaterials. *Particle and Fibre Toxicology*, *12*(1), 1–12.

Vogelsberger, W., Schmidt, J., & Roelofs, F. (2008). Dissolution kinetics of oxidic

nanoparticles: The observation of an unusual behaviour. *Colloids and Surfaces A: Physicochemical and Engineering Aspects*, *324*(1–3), 51–57.

Waghmode, M. S., Gunjal, A. B., Mulla, J. A., Patil, N. N., & Nawani, N. N. (2019). Studies on the titanium dioxide nanoparticles: biosynthesis, applications and remediation. *SN Applied Sciences*, *1*(4), 310.

Walters, C., Pool, E., & Somerset, V. (2013). Aggregation and dissolution of silver nanoparticles in a laboratory-based freshwater microcosm under simulated environmental conditions. *Toxicological and Environmental Chemistry*, *95*(10), 1690–1701.

Wang, H., Burgess, R. M., Cantwell, M. G., Portis, L. M., Perron, M. M., Wu, F., & Ho, K. T. (2014). Stability and aggregation of silver and titanium dioxide nanoparticles in seawater: Role of salinity and dissolved organic carbon. *Environmental Toxicology and Chemistry*, *33*(5), 1023–1029.

Wang, J., Wang, Z., Wang, W., Wang, Y., Hu, X., Liu, J., … Tang, J. (2022). Synthesis, modification and application of titanium dioxide nanoparticles: a review. *Nanoscale*, 6709–6734.

Wang, N., Tong, T., Xie, M., & Gaillard, J. F. (2016). Lifetime and dissolution kinetics of zinc oxide nanoparticles in aqueous media. *Nanotechnology*, *27*(32), 324001.

Wang, S., Li, D., Zhang, M., Chen, M., Xu, N., Yang, L., & Chen, J. (2020). Competition between fulvic acid and phosphate-mediated surface properties and transport of titanium dioxide nanoparticles in sand porous media. *Journal of Soils and Sediments*, *20*(10), 3681–3687.

Watanabe, C. H., Domingos, R. F., Benedetti, M. F., & Rosa, A. H. (2023). Dissolution and fate of silver nanoparticles in the presence of natural aquatic organic matter. *Journal of Environmental Exposure Assessment*, *2*(1), 1–17.

Yan, L., Zhao, F., Wang, J., Zu, Y., Gu, Z., & Zhao, Y. (2019). A Safe-by-Design Strategy towards Safer Nanomaterials in Nanomedicines. *Advanced Materials*, *31*(45), 1–33.

Yang, S., Wei, P., Wang, J., Tan, Y., & Qu, X. (2023). Impacts of dissolved organic matter on the aggregation and photo-dissolution of cadmium pigment nanoparticles in aquatic systems. *Science of the Total Environment*, *865*, 161313.

Yang, X., Gondikas, A. P., Marinakos, S. M., Auffan, M., Liu, J., Hsu-Kim, H., & Meyer, J. N. (2012). Mechanism of silver nanoparticle toxicity is dependent on dissolved silver and surface coating in caenorhabditis elegans. *Environmental Science and Technology*, *46*(2), 1119–1127.

Yaqoob, A. A., Umar, K., & Ibrahim, M. N. M. (2020). Silver nanoparticles: various methods of synthesis, size affecting factors and their potential applications–a review. *Applied Nanoscience (Switzerland)*, *10*(5), 1369–1378.

Yu, Q., Wang, H., Peng, Q., Li, Y., Liu, Z., & Li, M. (2017). Different toxicity of anatase and rutile TiO2 nanoparticles on macrophages: Involvement of difference in affinity to proteins and phospholipids. *Journal of Hazardous Materials*, *335*, 125–134.

Zeng, S., Yong, K. T., Roy, I., Dinh, X. Q., Yu, X., & Luan, F. (2011). A Review on Functionalized Gold Nanoparticles for Biosensing Applications. *Plasmonics*, *6*(3), 491–506.

Zhang, L., & Wang, W. X. (2023). Silver nanoparticle toxicity to the larvae of oyster Crassostrea angulata: Contribution of in vivo dissolution. *Science of the Total Environment*, *858*, 159965.

Zhang, T., Wang, L., Chen, Q., & Chen, C. (2014). Cytotoxic potential of silver nanoparticles. *Yonsei Medical Journal*, *55*(2), 283–291. https://doi.org/10.3349/ymj.2014.55.2.283

Zhang, W., Ke, S., Sun, C., Xu, X., Chen, J., & Yao, L. (2019). Fate and toxicity of silver nanoparticles in freshwater from laboratory to realistic environments: a review. *Environmental Science and Pollution Research*, *26*(8), 7390–7404.

Zhong, L., Yu, Y., Lian, H. zhen, Hu, X., Fu, H., & Chen, Y. jun. (2017). Solubility of nano-sized metal oxides evaluated by using in vitro simulated lung and

gastrointestinal fluids: implication for health risks. *Journal of Nanoparticle Research*, *19*(11), 1–10.

Ziental, D., Czarczynska-Goslinska, B., Mlynarczyk, D. T., Glowacka-Sobotta, A., Stanisz, B., Goslinski, T., & Sobotta, L. (2020). Titanium dioxide nanoparticles: Prospects and applications in medicine. *Nanomaterials*, *10*(2), 387.

CHAPTER 4

4 Publications and manuscript

This section contains all the published research articles and a submitted manuscript that should be considered when evaluating this thesis. All the articles and manuscript have their own referencing style that was formatted according to the requirements of the various journals where the articles were submitted and published. The figures and tables have been placed in the text in appropriate potions near each citation with a caption.

4.1 Paper 1

This first article entitled “Dissolution of citrate stabilized, polyethylene glycol coated carboxyl and amine functionalized gold nanoparticles in simulated biological fluids and environmental media” has been published in the Journal of Nanoparticle Research. The article compared the dissolution kinetics of gold nanoparticles exposed to various simulated biological fluids and environmental media to predict their behaviour in real-life situations. The effect of functional groups on dissolution was also elucidated.

Journal of Nanoparticle Research (2021)
https://doi.org/10.1007/s11051-020-05132-x

Odwa Mbanga- Principal author

Ewa Cukrowska- Supervisor

Mary Gulumian- Supervisor

J Nanopart Res (2021) 23: 29
https://doi.org/10.1007/s11051-020-05132-x

RESEARCH PAPER

Dissolution of citrate-stabilized, polyethylene glycol–coated carboxyl and amine-functionalized gold nanoparticles in simulated biological fluids and environmental media

Odwa Mbanga · Ewa Cukrowska · Mary Gulumian

Received: 12 May 2020 / Accepted: 22 December 2020 / Published online: 7 January 2021

Abstract Dissolution is an important property utilized to elucidate both short- and long-term effects of nanoparticles for their potential to cause harm to humans and the environment. Nanoparticles may therefore be classified based on their (bio)durability between those that are amenable and those that are resistant to dissolution, biodegradation and/or disintegration. The dissolution kinetics of uncoated citrate-stabilized, polyethylene glycol–coated (PEGylated) gold nanoparticles functionalized with carboxyl and amine functional groups in simulated biological and environmental fluids at physiological and room temperature, respectively, were studied using the static dialysis protocol to predict their (bio)durability. Citrate-stabilized gold nanoparticles showed high degrees of resistance to dissolution in the simulated media unlike those which were coated with polyethylene glycol and functionalized with carboxyl and amine functional groups. Generally, the extent of AuNP dissolution in acidic media (phagolysosomal fluid and gastric fluid) was greater than that in neutral or alkaline media such as Gamble's fluid, blood plasma and intestinal fluids, freshwater and seawater. However, in all these experimental conditions, the particles did not completely dissolve. In the case of amine-functionalized AuNPs, the nanoparticles released a maximum of only 15% of their original concentration whereas carboxyl-functionalized and citrate-stabilized gold nanoparticles released 9% and 8.5% of gold ions, respectively. The rate and degree of dissolution depended on the surface functionalization, pH, ionic strength of the simulated fluid and particle aggregation. Therefore, the results indicate that gold nanoparticles with low dissolution rates are expected to be (bio)durable in biological and environmental surroundings; thus, they might impose long-term effects on humans and the environment. In contrast, those with high dissolution rate are not (bio)durable and hence may cause short-term effects.

Keywords Dissolution · (bio)durability · Gold nanoparticles · In vitro acellular · Dissolution kinetics · Health and environmental effects

O. Mbanga · E. Cukrowska
Molecular Sciences Institute, School of Chemistry, University of the Witwatersrand, Private Bag X3, Johannesburg 2050, South Africa

O. Mbanga
e-mail: odwa.mbanga@students.wits.ac.za

E. Cukrowska
e-mail: ewa.cukrowska@wits.ac.za

O. Mbanga · M. Gulumian
Toxicology and Biochemistry Department, National Institute for Occupational Health, Johannesburg, Gauteng 2000, South Africa

M. Gulumian (✉)
Water Research Group, Unit for Environmental Sciences and Management, North-West University, Private Bag X6001, Potchefstroom 2520, South Africa
e-mail: MaryG@nioh.ac.za

Introduction

There has been a growing interest in gold nanoparticle (AuNPs) due to their unique physicochemical properties

(Arnida et al. 2011; Auffan et al. 2009). Their high biocompatibility and ease of manipulation in the size and shape have seen them being utilized in the field of biotechnology and biomedicine including catalysis, biosensors and nanophotonics (Tiwari et al. 2011; Zeng et al. 2011). Furthermore, the application of AuNPs also extends to their use as drug delivery agents and in diagnostic and photothermal therapeutic applications (Bachler et al. 2015; Baker et al. 2014; Kreyling et al. 2014).

Despite the promise of AuNPs and other nanoparticles (NPs), there are occupational, consumer and environmental safety concerns raised regarding their effects on human health and the environment (Fratoddi et al. 2015; Lin et al. 2016; Oh and Park 2014). One parameter that can be used to determine the effects of NPs is dissolution, which affects their (bio)durability and biopersistence. Dissolution can be defined as the movement of species from the NP surface into the bulk fluid forming a homogenous mixture (Laux et al. 2017; Utembe et al. 2015). (Bio)durability is the ability to resist chemical/biochemical alteration (Laux et al. 2017; Utembe et al. 2015), whilst biopersistence is the propensity to which NPs can resist chemical clearance in the body through dissolution, enzymatic degradation and other physiological clearance mechanisms (Oyabu et al. 2017). Investigating the dissolution behaviour of NPs helps to provide insight into how they may interact with their biological and environmental surroundings (Utembe et al. 2015). Furthermore, it allows for their classification between those that are amenable and those that are resistant to dissolution. For example, if the rate at which NPs release species is fast, their short-term effects will be similar to those of the dissolved ions. Conversely, if the release occurs at a slow rate, chances are that those particles are (bio)durable and may cause long-term effects in humans (Utembe et al. 2015). For these reasons, the dissolution rate is an important property for the assessment of the effects of NPs. Research studies have been conducted that focused on the in vitro and in vivo toxicity and biodistribution of AuNPs (Arnida et al. 2011; Balasubramanian et al. 2010; Alkilany and Murphy 2010; Vetten et al. 2013; Simpson et al. 2013). Moreover, there are several studies that have investigated the fate of AuNPs in aquatic environments. Hull et al. (Hull et al. 2011) assessed the capacity of *Corbicula fluminea* to uptake AuNPs and found that this aquatic organism retained the smaller sized particles within the digestive tract and excreted the larger particle sizes in faeces. Aiken et al. (Aiken et al. 2011) investigated the impact of amine-functionalized gold nanoparticles on freshwater organisms, namely *Scenedesmus subspicatus* (algae) and *Corbicula fluminea* (benthic bivalve), and observed the bioaccumulation of AuNPs on the walls of algae whilst the benthic bivalve showed the particles to be bioaccumulated and penetrate the gills and digestive epithelium.

Most research studies conducted so far focused on the biodistribution and accumulation of AuNPs in several cell lines and murine models and the factors identified to influence their toxicity have been correlated to surface charge and functionalization, size and shape of AuNPs (Arnida et al. 2011; Bachler et al. 2015; Balasubramanian et al. 2010; Simpson et al. 2013; Bozich et al. 2014; Cohen et al. 2014; Hornos Carneiro and Barbosa Jr 2016; Libralato et al. 2017). Dissolution of AuNPs has to a certain degree been tested in several model solutions such as artificial alveolar fluid, weak hydrochloric acid (HCl) to simulate gastric conditions, ammonium acetate solution to simulate the neutral lung fluids, freshwater wetland mesocosms, estuarine mesocosms, pure water and Suwannee River fulvic acid (Ferry et al. 2009; Breitner et al. 2015; Avramescu et al. 2017; Avellan et al. 2018; Hitchman et al. 2013). In simulated systems, the dissolution behaviour of AuNPs has been shown to depend on characteristics of the simulated model including its pH and ionic strength as well as the chemical and physical properties of the particles (Bachler et al. 2015; Breitner et al. 2015; Avramescu et al. 2017; Avellan et al. 2018; Cherevko et al. 2014; Donovan et al. 2016). These studies however did not investigate the effects of ligands or their functional groups affecting dissolution. Hence, the contribution of the present work which we think will advance the field and have implications in a number of applications including nanomedicine.

It is therefore of great relevance to study the dissolution behaviour of AuNPs in simulated biological and environmental fluids with a wide variety of pH values and chemical compositions to mimic their behaviour in real-life situations. It is also important to investigate the effect of different surface ligands on the dissolution of AuNPs in these simulated biological and environmental media. Contrary to most research conducted so far, the present study also elucidates the dissolution kinetics; namely, the dissolution rates, rate constants, order of reaction and half-times of uncoated citrate-stabilized

AuNPs (cit-AuNPs), polyethylene glycol (PEG)–coated AuNPs functionalized with carboxylic acid (COOH-AuNPs) and amine (NH_2-AuNPs) functional groups were therefore investigated in biological and environmental simulated fluids. The former simulated fluids have included the Gamble's fluid (GF) and phagolysosomal fluid (PSF) representative of fluids found deep within the lungs and in lysosomes, gastrointestinal fluids represented by gastric fluid (GIF) and intestinal fluid (IF) and lastly blood plasma (BP). Finally, simulated environmental fluids include freshwater (FW) and seawater (SW).

Materials and methods

Synthesis and characterization of gold nanoparticles

The 14-nm-diameter AuNPs in a 1% citrate solution, PEGylated COOH and NH_2 stock solutions were provided by MINTEK (Randburg, South Africa). All the nanoparticle suspensions were prepared from the stock solutions under sterile conditions with the concentration varying from 3.8, 4.0 and 3.0 nM for citrate-stabilized AuNPs, PEGylated COOH and NH_2 stock solutions, respectively. A transmission electron microscope (TEM) (JEOL Ltd., JEM-2100) (Lireweg, The Netherlands) was used to characterize and monitor the morphology and agglomeration state of nanoparticles before and after exposure to different simulated biological and environmental fluids. Nanoparticle suspensions were deposited onto TEM grid (200 mesh size Cu grid) coated with a lacey carbon film. The images of the nanoparticles were verified using a digital charge-coupled device (CCD) camera connected to the TEM. A Bruker Tensor 27 Fourier transform infrared (FTIR) spectroscopy (Billerica, MA, USA) was used to investigate changes in the functional groups on the surface of nanoparticles. The Varian Ultraviolet-Visible (UV-Vis) 50 Conc. spectrophotometer was utilized to monitor changes at the surface of AuNPs by observing alterations in the intensity of the surface plasmon resonance absorbance peak at 520 nm before and after dissolution in biological fluids. The concentration of dissolved gold ions in simulated fluids was determined using an inductively coupled plasma mass spectrometer (ICP-MS) (Agilent Technologies, 7700 series ICP-MS, Santa Clara, CA, USA).

Experimental procedure

Preparation of biological fluids and environmental media

In vitro acellular tests were used to assess the dissolution of AuNPs in simulated biological fluids and environmental media. The dissolution experiments were determined using the static dialysis membrane protocol in the presence of the simulated biological fluids and environmental media (Avramescu et al. 2017; Chen and Jafvert 2018; Kittler et al. 2010; Probst et al. 2017). This methodology uses the principle of diffusion and the implication is that the rate at which released ions diffuse from the dialysis membrane occurs faster than the release of ions from the nanoparticle surface (Kittler et al. 2010). Therefore, it can be assumed that through measuring the concentration of released ions that passed the dialysis membrane in the bulk fluid by ICP-MS, dissolution kinetics of AuNPs could be predicted.

Dissolution studies were conducted in different simulated biological fluids and synthetic environmental media with different pH and chemical compositions (Table 1). The biological fluids were Gamble's fluid (GF) found deep within the lungs and phagolysosomal fluid (PSF) in cellular lysosomes at pH 7.4 and pH 4.5, respectively. The other fluids were GIF at pH 2.0 and IF at pH 7.5 representing the stomach and intestinal fluids, respectively, and lastly, blood plasma (BP) at pH 7.2 which is a fluid that carries blood components throughout the body. These simulated body fluids were prepared according to the procedures described in literature (Marques et al. 2011) using the reagents listed in Table 1. In the case of environmental media for FW and SW, the composition followed was as recommended by the United States (U.S.) Environmental Protection Agency (EPA) (Weber 2002). These reagents were added to 700 mL of d-H_2O in the order given in Table 1, and after the addition of each reagent, the pH was adjusted with either 1 M hydrochloric acid to make solutions acidic or 1 M sodium hydroxide to increase the pH values. The final volume was then adjusted to 1 L with d-H_2O. A 13.7-mM concentration of alkylbenzyldimethylammonium chloride (ABDC) (51 μL), an anti-fungal agent, was added to each beaker to preserve the simulated fluids.

Dissolution tests

A 5 mL of 3.8 nM citrate-stabilized AuNPs, 4.0 nM COOH-AuNPs and 3.0 nM NH_2-AuNPs stock solutions were transferred to centrifuge tubes and were centrifuged at 13,000×*g* for 30 min. The supernatant was discarded, and the pellet was re-suspended into centrifuge tubes containing 5 mL of simulated biological and environmental fluids. This was sonicated for 15 min to redisperse the particles. The NP suspension was transferred into dialysis bags (SnakeSkin Dialysis tubing, 3.5 K MWCO, 22 mm-dry diameter). A dialysis membrane with a significantly smaller pore size was chosen such that gold in the particle form typically will be fully retained in the sample, and species such as charged ions from the nanoparticle surface and salts smaller in size will dialyze out of the tubing. The dialysis bags were rinsed with de-ionized water to eliminate any possible contaminants. Meanwhile, the water bath was maintained at 37 °C to mimic physiological temperature whilst synthetic environmental media were kept at 25 °C.

The NP suspensions were transferred into a dialysis membrane then immersed in 500 mL of each simulated biological or environmental fluids in a beaker placed in a water bath. Experiments were conducted in the dark. Samples from the simulated fluids outside the dialysis membrane were collected every 30 min for the first day for 4 h and twice a day for the subsequent 10 days. The pH levels of the simulated biological fluid were monitored before, during and after each experiment using a Jenway 3510 pH meter. Samples were digested with microwave-assisted extraction for 1 h with 65% HNO_3 to ensure that the particles are converted to ionic phase then diluted with 20 μg L^{-1} rhenium and indium standards and analysed on an ICP-MS. The purpose of using rhenium and indium as internal standards was to improve and ensure accuracy and precision of the results where volume errors are difficult to predict and control. In addition, it was also to correct for the loss of the analyte during sample preparation and sample inlet.

Kinetic model for dissolution process

The current research study employed the use of a static dissolution method which involves the exposure of known concentrations of AuNPs inside a dialysis membrane to a fixed volume of simulated fluids. Over time, a concentration gradient develops between the nanoparticle suspension fluid inside the dialysis membrane and the particle free bulk fluid in the beaker. Therefore, the Noyes-Whitney equation provides practical information relevant to the dissolution process. And it states that the rate of change in concentration of dissolved material with time is directly proportional to the concentration difference between the ionic concentration of particles on the NP surface and the concentration of ions in the bulk fluid.

Therefore, a kinetic model in the form of the Noyes-Whitney Eq. (1) was modified and used to calculate the dissolution rate and half-time of AuNPs to elucidate their dissolution behaviour in various simulated fluids (Kittler et al. 2010; Wang et al. 2016).

$$\frac{d[\mathrm{AuNPs}]}{dt} = -D\frac{A}{d}\left([\mathrm{Au}]_T - [\mathrm{Au}]_{\mathrm{dis}}\right) \tag{1}$$

where [AuNPs], $[\mathrm{Au}]_T$ and $[\mathrm{Au}]_{\mathrm{dis}}$ represent the concentration of AuNPs in the stock solution, the concentration of gold ions on the nanoparticle surface during the dissolution process and ultimately the dissolved concentration of gold ions, respectively. *A* is the surface area of AuNPs, *D* is the diffusion coefficient of gold ions and *d* is the diffusion layer thickness.

The mass balance for Au in the system is presented by Eq. 2.

$$[\mathrm{Au}]_T = [\mathrm{AuNPs}] + [\mathrm{Au}]_{\mathrm{dis}} \tag{2}$$

where $[\mathrm{Au}]_T$ is the total amount of gold nanoparticles added before dissolution process. The [AuNPs] is then substituted by Eq. 3 in the formula:

$$[\mathrm{AuNPs}] = [\mathrm{Au}]_T - [\mathrm{Au}]_{\mathrm{dis}} \tag{3}$$

However, $[\mathrm{Au}]_T - [\mathrm{Au}]_{\mathrm{dis}}$ can also be written in the following form presented by Eq. 4:

$$[\mathrm{Au}]_T - [\mathrm{Au}]_{\mathrm{dis}} = [\mathrm{Au}]_T\left(1 - \frac{[\mathrm{Au}]_{\mathrm{dis}}}{[\mathrm{Au}]_T}\right) \tag{4}$$

such that

$$[\mathrm{AuNPs}] = [\mathrm{Au}]_T\left(1 - \frac{[\mathrm{Au}]_{\mathrm{dis}}}{[\mathrm{Au}]_T}\right) \tag{5}$$

Equation 5 is then substituted into Eq. 1 to obtain the following Eq. (6):

Table 1 Chemical composition and pH of simulated biological fluids and synthetic environmental media (Marques et al. 2011)

Simulated fluid	Ionic strength (mol L^{-1})	pH	Chemical composition (g L^{-1})
BP[a]	0.15	7.2	Sodium chloride (NaCl) (8.035), sodium hydrogen carbonate ($NaHCO_3$) (0.355), potassium chloride (KCl) (0.225), potassium phosphate dibasic trihydrate ($K_2HPO_4{\cdot}3H_2O$) (0.231), magnesium chloride hexahydrate ($MgCl_2{\cdot}6H_2O$) (0.331), 1 M HCl (39 mL), calcium chloride ($CaCl_2$) (0.292), sodium sulphate (Na_2SO_4) (0.072), Tris(hydroxymethyl)aminomethane ($NH_2C(CH_2OH)_3$) (6.118)
GF[b]	0.17	7.4	Magnesium chloride ($MgCl_2$) (0.203), sodium chloride (NaCl) (6.019), potassium chloride (KCl) (0.298), sodium hydrogen phosphate (Na_2HPO_4) (0.142), sodium sulphate anhydrous (Na_2SO_4) (0.017), calcium chloride dihydrate ($CaCl_2{\cdot}2H_2O$) (0.368), sodium acetate (CH_3COONa) (0.953), sodium hydrogen carbonate ($NaHCO_3$) (2.604), trisodium citrate dihydrate ($C_6H_9Na_3O_9$) (0.097)
GIF[c]	0.16	2.0	Sodium chloride (NaCl) (2.922), potassium chloride (KCl) (7.007), potassium hydrogen phthalate ($C_8H_5O_4K$) (0.243), pepsin (1 mL mL^{-1}), mucin (3 mg mL^{-1})
IF[d]	0.16	6.8	Potassium chloride (KCl) (0.298), calcium chloride ($CaCl_2$) (0.499), magnesium chloride ($MgCl_2$) (0.190), urea (0.300), bile salts (9 mL mL^{-1}), pancreatin (9 mg mL^{-1})
PSF[e]	0.34	4.5	Sodium hydrogen phosphate (Na_2HPO_4) (0.142), sodium chloride (NaCl) (6.650), sodium sulphate (Na_2SO_4) (0.072), calcium chloride dihydrate ($CaCl_2{\cdot}2H_2O$) (0.029), glycine (0.450), potassium hydrogen phthalate ($C_8H_5O_4K$) (4.086)
FW[f]	0.05	6.8	Sodium hydrogen carbonate ($NaHCO_3$) (0.012), calcium sulphate anhydrous ($CaSO_4$) (0.075), magnesium sulphate anhydrous ($MgSO_4$) (0.0075), potassium chloride (KCl) (0.0005)
SW[g]	3.5	8.0	Sodium chloride (NaCl) (21.03), sodium sulphate (Na_2SO_4) (3.52), potassium chloride (KCl) (0.61), potassium bromide (KBr) (0.088), borax (0.034), magnesium chloride ($MgCl_2$) (9.50), calcium chloride anhydrous ($CaCl_2$) (1.320), strontium chloride ($SrCl_2$) (0.02), sodium hydrogen carbonate ($NaHCO_3$) (0.17)

[a] BF simulated biological fluid for blood plasma, [b] GF simulated biological fluid for Gamble's fluid, [c] GIF simulated biological fluid for gastric fluid, [d] IF simulated biological fluid for intestinal fluid, [e] PSF simulated biological fluid for phagolysosomal fluid, [f] FW synthetic environmental media for freshwater, [g] SW synthetic environmental media for seawater

$$[\mathrm{Au}]_T \frac{d\left(1-\frac{[\mathrm{Au}]_{\mathrm{dis}}}{[\mathrm{Au}]_T}\right)}{dt} = -D\frac{A}{d}[\mathrm{Au}]_T\left(1-\frac{[\mathrm{Au}]_{\mathrm{dis}}}{[\mathrm{Au}]_T}\right) \quad (6)$$

Upon dividing by $[\mathrm{Au}]_T$ on both sides of the equation, Eq. 6 is transformed into Eq. 7:

$$\frac{d\left(1-\frac{[\mathrm{Au}]_{\mathrm{dis}}}{[\mathrm{Au}]_T}\right)}{dt} = -D\frac{A}{d}\left(1-\frac{[\mathrm{Au}]_{\mathrm{dis}}}{[\mathrm{Au}]_T}\right) \quad (7)$$

If we let $\left(1-\frac{[\mathrm{Au}]_{\mathrm{dis}}}{[\mathrm{Au}]_T}\right) = x$

Equation 7 can be presented as:

$$\frac{dx}{dt} = -D\frac{A}{d}x \quad (8)$$

In order to bring x to the left-hand side of the equation and dt to the right-hand side of the equation, the above equation is divided by x and multiplied by dt on both sides of the equation:

$$\frac{dx}{x} = -D\frac{A}{d}dt \quad (9)$$

Upon integration, the above equation becomes:

$$\ln x = c - D\frac{A}{d}t \quad (10)$$

where $k = -D\frac{A}{d}$ and c is a constant, and therefore k is the slope representative of the dissolution rate constant.

Ultimately, the integration of Eq. 7 yields Eq. 11

$$\ln\left(1-\frac{[\mathrm{Au}]_{\mathrm{dis}}}{[Au]_T}\right) = c - kt \quad (11)$$

The plot of $\ln\left(1-\frac{[\mathrm{Au}]_{\mathrm{dis}}}{[\mathrm{Au}]_T}\right)$ versus time during the dissolution process allows for the prediction of dissolution kinetics. This is a straight-line graph with slope k, which represents the dissolution rate of AuNPs subjected to simulated biological fluids and environmental media. Furthermore, dissolution predicted by this kinetic model follows the first-order reaction kinetics and half-time of a first-

order reaction can be obtained by the following Eqs. 12.

$$t_{1/2} = \frac{\ln 2}{k} \quad (12)$$

Results

Characterization

TEM

The AuNPs were characterized before and after 10 days of exposure to biological fluids and environmental media. TEM, UV-Vis and FTIR were used to characterize, identify and monitor changes of AuNPs during these experiments in order to link these changes in their physicochemical properties to their dissolution behaviour. TEM images of cit-AuNPs, PEGylated COOH-AuNPs and NH_2-AuNPs in simulated biological fluids and environmental media before and after dissolution are presented in Fig. 1a, b and c, respectively. The average diameters for cit-stabilized AuNPs, COOH-AuNPs and NH_2-AuNPs before dissolution experiments in simulated biological and environmental fluids were 14 ± 3 nm, 14 ± 0.5 nm and 14 ± 0.4 nm, respectively, and had no statistically significant difference $p < 0.05$. All the functionalized and non-functionalized nanoparticles were spherical in morphology as seen in the TEM images (Fig. 1a–c). However, the citrate-stabilized nanoparticles were highly agglomerated before and after dissolution (Fig. 1a).

UV-Vis

AuNPs were further characterized with UV-Vis to monitor the aggregation state by observing changes in the intensity of the localized surface plasmon resonance (LSPR) absorbance peak. UV-Vis spectra of cit-AuNPs, PEGylated COOH-AuNPs and NH_2-AuNPs in simulated biological fluids before and after dissolution are presented in Fig. 2a, b and c, respectively. A well-defined localized surface plasmon resonance peak centred at 520 nm was observed for cit-AuNPs, COOH-AuNPs and NH_2-AuNPs in all the biological fluids and environmental media before the dissolution tests. As the period of exposure to simulated media increased, there was an observable decrease in peak intensity after the dissolution experiments accompanied by a slight shift in peak position to longer wavelengths. However, this shift was particle specific but more pronounced for particles exposed to acidic media after dissolution experiments. The cit-AuNPs shifted from 520 to 549 nm, whereas COOH-AuNPs and NH_2-AuNPs both shifted to 547 nm and 540 nm, respectively. In the case of particles exposed to simulated phagolysosomal fluid, the wavelength shift was in the order of 549 > 547 > 540 nm for cit-AuNPs, COOH-AuNPs and NH_2-AuNPs, respectively.

Also, worth noting is the drastic decrease in the stability of all the particles after dissolution in simulated seawater. For example, Rouhana et al. (Rouhana et al. 2007) studied how the effect of increasing the ionic strength of electrolytes impacts the stability of gold nanoparticles and found that solutions of higher ionic strength encourage formation of nanoparticle aggregates.

Generally, peak shift in wavelength to longer wavelength was observed in the UV-Vis spectra. Surprisingly, the shift in wavelength was almost the same for all the particles but was dependent on the particle used where the shift was more pronounced for cit-AuNPs and therefore supports the argument that these particles had the highest aggregation followed by COOH-AuNPs and lastly by NH_2-AuNPs. This correlated with the TEM images presented in Fig. 1. Citrate-stabilized gold nanoparticles in this current research study had exhibited the least form of stability. Similar observations have been made by Sun et al. (Sun et al. 2005) who studied the stability of gold nanoparticles in various buffer solutions where the stability of citrate-stabilized gold nanoparticles was influenced by various pH values from acidic to neutral. These results were also corroborated by other investigators (Wang et al. 2014; Chen et al. 2006; Islam et al. 2019).

FTIR

FTIR spectra recorded between 500 and 4000 cm^{-1} were used to monitor the behaviour of functional groups during the in vitro acellular tests. The citrate-stabilized (a), PEGylated carboxyl (b) and amine-functionalized (c) gold nanoparticle FTIR spectra are shown in Fig. 3. This shows the FTIR spectra of gold nanoparticle suspension inside the dialysis bag (labelled "before" and "after") and bulk fluid outside the dialysis membrane. The general observation was that functional groups used

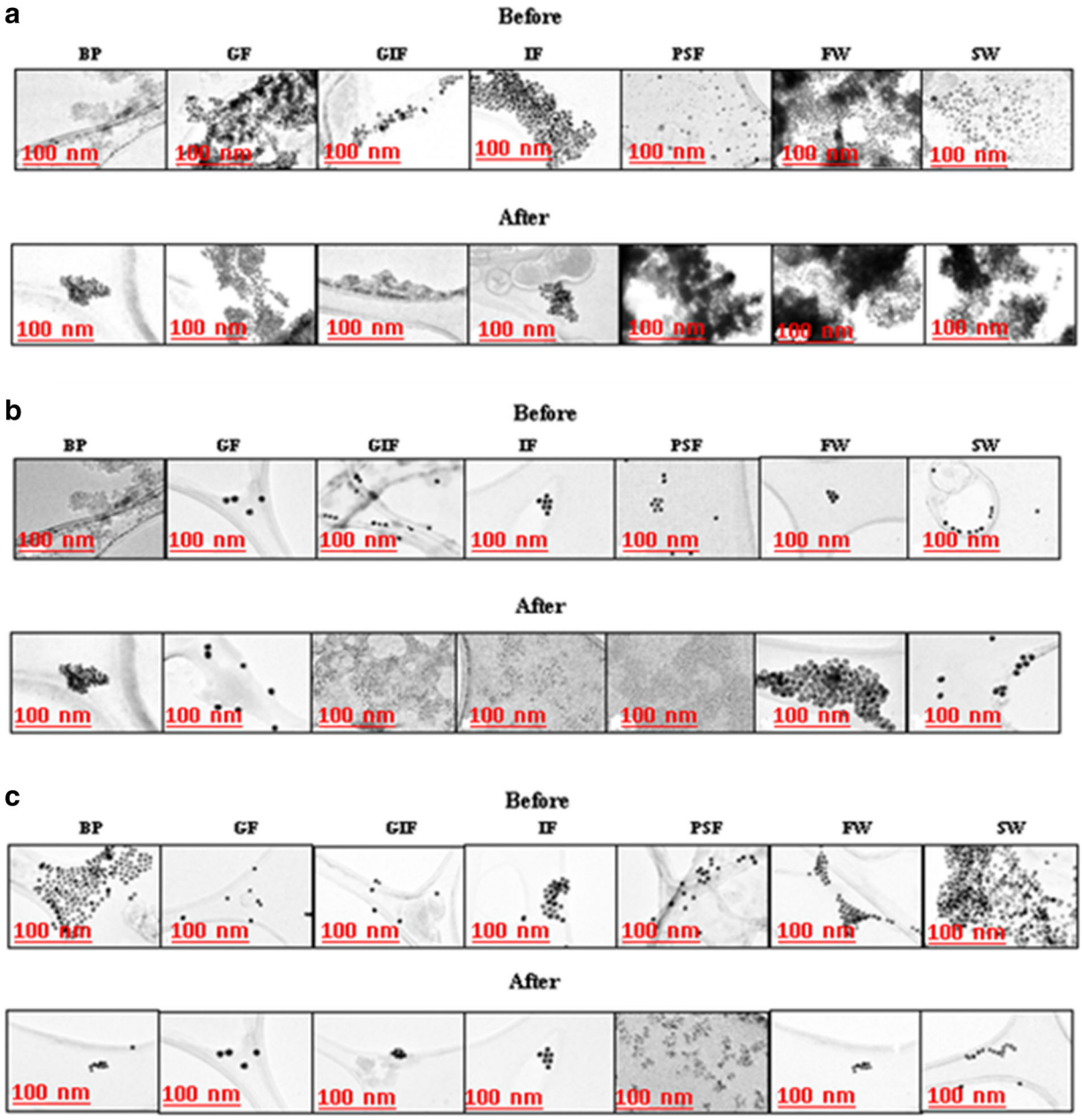

Fig. 1 TEM images of cit-stabilized AuNPs (**a**); COOH-AuNPs (**b**); and NH_2-AuNPs (**c**) in simulated biological and environmental fluids before and after dissolution tests. BP, GF, GIF, IF and PSF are simulated biological fluids for blood plasma, Gamble's fluid, gastric fluid, intestinal fluid and phagolysosomal fluid, respectively. FW and SW are synthetic environmental fluids for freshwater and seawater, respectively

for the surface modification of the AuNPs were detected by FTIR in the nanoparticle suspension before dissolution. There were no noticeable differences between the FTIR spectra of gold nanoparticles inside the dialysis membrane after dissolution experiments. The asymmetric stretching and symmetric stretching of the components of citrate stabilizing agents are observed in Fig. 3a. The various bands at 1432 cm^{-1}, 1619 cm^{-1}, 1716 cm^{-1} and 3451 cm^{-1} correspond to C–O stretch, O–H stretch, C=O stretch and O–H stretch, respectively. Figure 3b shows the FTIR spectra of the carboxylic acid functional group. The absorption bands

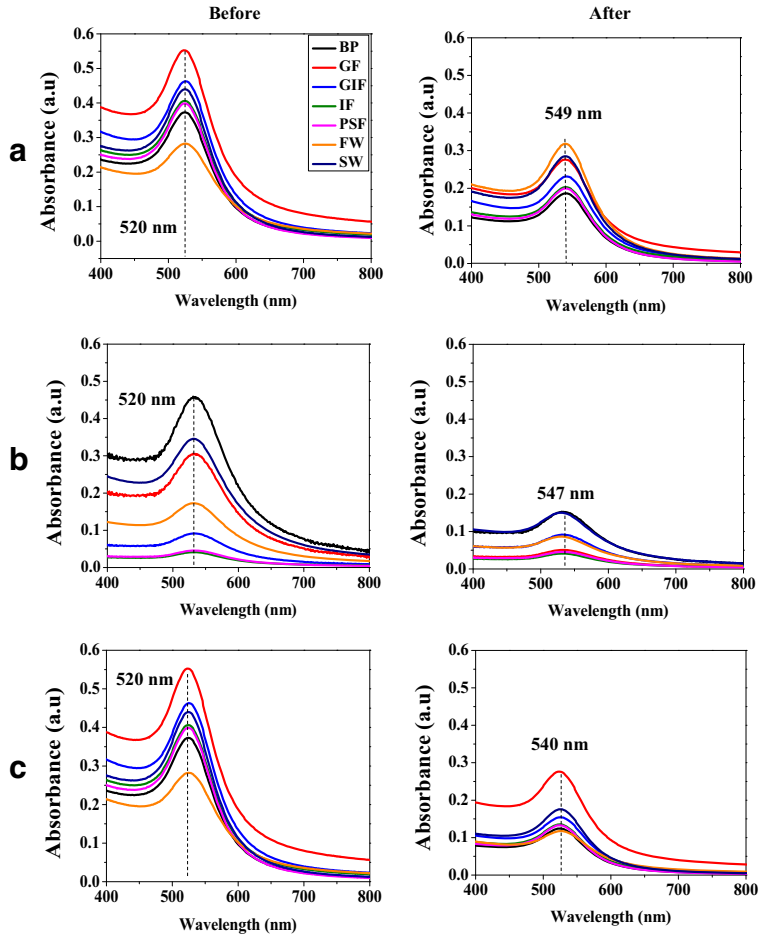

Fig. 2 UV-Vis absorption spectra of cit-stabilized AuNPs (**a**); COOH-AuNPs (**b**); and NH_2-AuNPs (**c**) in simulated biological fluids and environmental media before and after dissolution tests. BP, GF, GIF, IF and PSF are simulated biological fluids for blood plasma, Gamble's fluid, gastric fluid, intestinal fluid and phagolysosomal fluid, respectively. FW and SW are synthetic environmental media for FW and SW, respectively

observed at 1296 cm^{-1}, 1511 cm^{-1} and 1712 cm^{-1} and the broad band at 3000 cm^{-1} correspond to C–O stretch, O–H stretch, C=O stretch and O–H stretch, respectively. The FTIR spectra of the amine functional group are presented in Fig. 3c. The bands around the region of 1000 cm^{-1} correspond to the interactions of the N–H bonds. The very broad band of NH_2^+ stretch was observed in the 3000–3500 cm^{-1} range.

However, there were noticeable changes in the FTIR spectra of all the simulated fluids outside the dialysis membrane. At the end of the dissolution experiment, no functional groups could be found in the bulk fluid, meaning they remain inside the dialysis membrane, and only the water molecules used in the synthesis of biological fluids and environmental media were detected by the FTIR. As a result, the absorbance maximum of the O–H stretch was observed at band 3450 cm^{-1}, followed by water bending band between the 1600 and 2000 cm^{-1} region. The absence of the absorption bands in the FTIR spectra of all the biological and environmental fluids indicates the possibility that the functional groups remained on the nanoparticle surface inside the dialysis membrane. These results were corroborated in (Aryal et al. 2006; Marchewka and Pietraszko 2003).

Dissolution behaviour in biological fluids and environmental media

The dissolution of AuNPs was expressed in terms of concentration (μg L^{-1}) versus time (h) as in the presentation adopted from literature (Chen and Jafvert 2018; Kittler et al. 2010; Probst et al. 2017; Arts et al. 2015). Figure 4 a, b and c show dissolution curves of gold nanoparticles in simulated biological and environmental fluids over a period of 10 days for cit-AuNPs, COOH-AuNPs and NH_2-AuNPs, respectively. In all cases, no complete dissolution of gold nanoparticles was observed. This was confirmed by the analyses of the NP

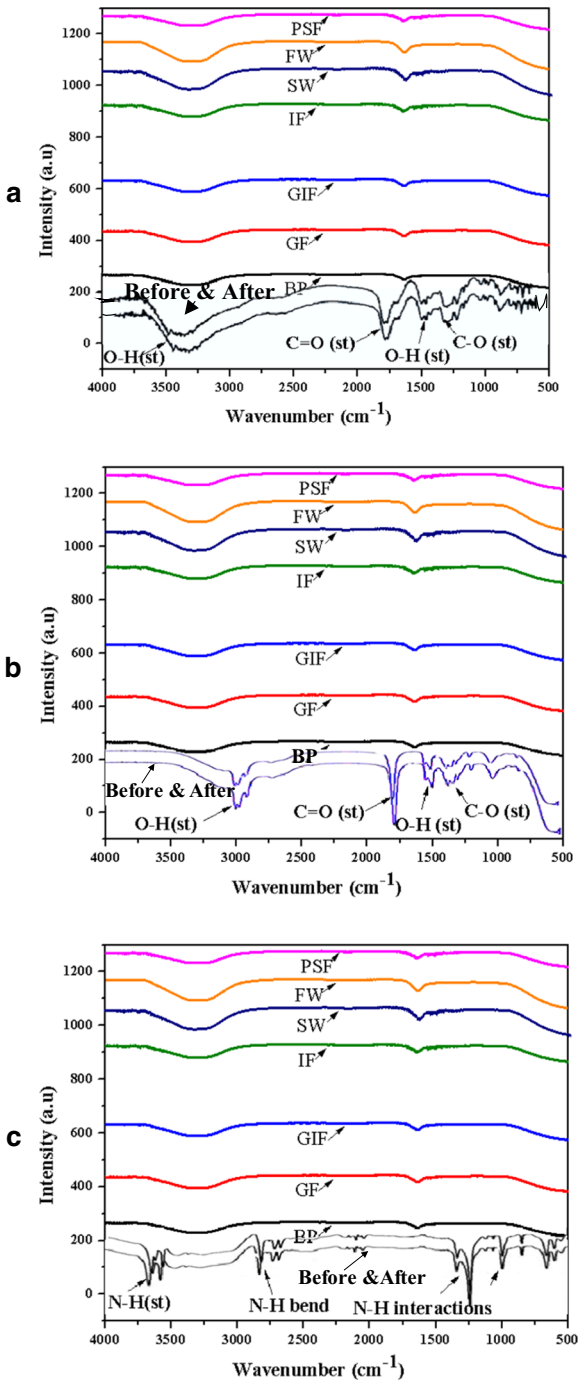

Fig. 3 FTIR spectra of the citrate-stabilized (**a**), PEGylated carboxyl (**b**) and amine-functionalized (**c**) gold nanoparticle in the dialysis membrane before and after dissolution and in the bulk fluid after the dissolution process. BP, GF, GIF, IF and PSF are simulated biological fluids for blood plasma, Gamble's fluid, gastric fluid, intestinal fluid and phagolysosomal fluid, respectively. FW and SW are synthetic environmental media for freshwater and seawater, respectively

suspension inside the dialysis membrane after completion of the dissolution experiments, where AuNPs were observed under a TEM (Fig. 1). The concentration of dissolved gold was generally low and significantly different ($p < 0.05$) between the three types of nanoparticles. The corresponding percentage of maximum dissolved gold ions from the total amount of gold nanoparticles added was 8.52, 9.15 and 14.03% for cit-AuNPs, COOH-AuNPs and NH_2-AuNPs, respectively (Fig. 4). Accordingly, maximum dissolved gold ions of up to 0.063 ± 0.256 μg L^{-1} in gastric fluid were observed for cit-AuNPs, followed by COOH-AuNPs (0.72 ± 0.73 μg L^{-1}) in phagolysosomal fluid, whilst NH_2-AuNPs had the highest concentration of dissolved gold ions at 8.30 ± 0.22 μg L^{-1} in gastric fluid. For all the three types of AuNPs, dissolution started from 24 h, gradually increased then reached a plateau from 72 h towards 216 h. Generally, higher dissolution of AuNPs was observed in acidic simulated stomach and phagolysosomal fluids, namely gastric fluid at pH 2.0 for cit-AuNPs and NH_2-AuNPs, whereas for COOH-AuNPs, this occurred in phagolysosomal fluid at pH 4.5. Conversely, alkaline simulated fluids such as Gamble's fluid, intestinal fluid, blood plasma, freshwater and seawater showed low dissolution of gold nanoparticles. However, blood plasma showed higher dissolution for amine-functionalized gold nanoparticles.

Results presented in Fig. 4, the dissolution of the three AuNPs, can be seen to be as follows: For cit-AuNPs, the order was GIF > PSF > IF = GF > BP > FW = SW; for COOH-AuNPs, the order was PSF > GIF > GF > BP > SW = IF > FW; and for NH_2-AuNPs, the order was GIF > BP > GF > PSF > IF > FW > SW.

The high ionic strength of phagolysosomal fluid and seawater encouraged NP aggregation which was more pronounced for COOH-AuNPs as was observed from the UV-Vis results, leading to the reduction of the nanoparticle surface area, thus reducing chances of dissolution. However, it seems that in addition to the degree of aggregation, the higher dissolution of PEGylated COOH-AuNPs and NH_2-AuNPs compared to cit-AuNPs could be due to some ligand-promoted processes. Minimal dissolution of cit-AuNPs could be due to the high stability of these particles.

A statistical analysis tool was used to determine whether the dissolution of citrate-stabilized and PEGylated AuNPs was significantly different. The *p* values are presented in Table 2.

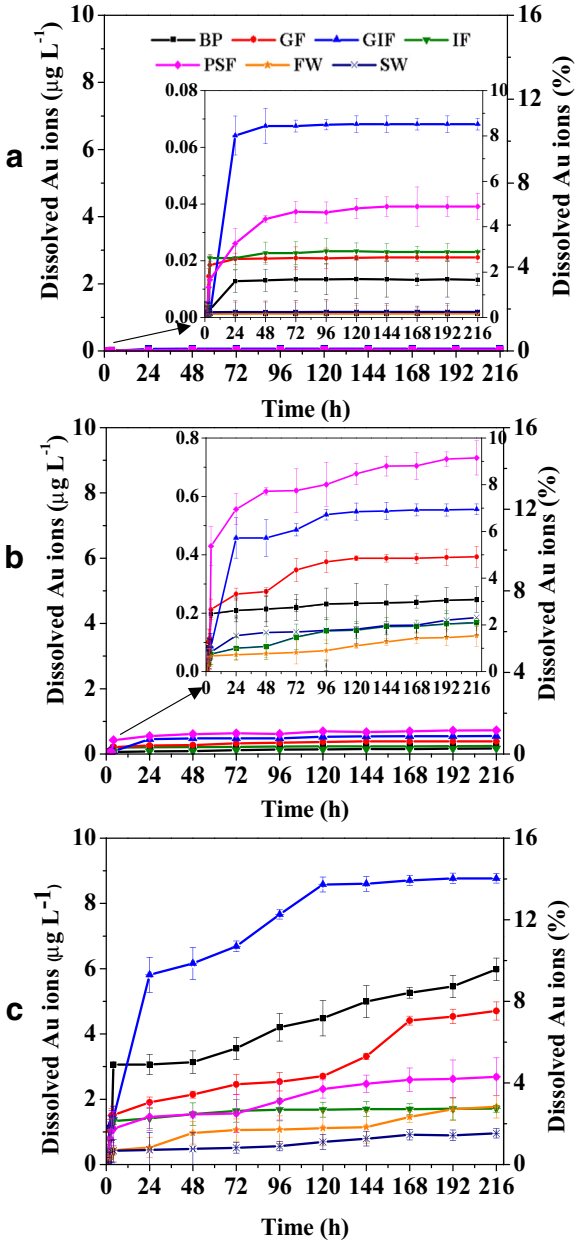

Fig. 4 Dissolution curves of gold ions released in simulated biological fluids over a period of 10 days for cit-AuNPs (**a**), COOH-AuNPs (**b**) and NH_2-AuNPs (**c**). BP, GF, GIF, IF and PSF are simulated biological fluids for blood plasma, Gamble's fluid, gastric fluid, intestinal fluid and phagolysosomal fluid, respectively. FW and SW are synthetic environmental media for freshwater and seawater. Dissolved Au ions in % was calculated as $[\mathrm{Au}(I)]t/[\mathrm{AuNPs}]T \times 100\%$

According to the multiple variable ANOVA statistical analysis performed in RStudio version 1.2 software where $p < 0.05$, there was a statistically significant difference in the dissolution of citrate-stabilized, PEGylated COOH-AuNPs and NH_2-AuNPs. However, even though the dissolution of NH_2-AuNPs in simulated gastric fluid was greater in magnitude compared to that of NH_2-AuNPs in intestinal fluid and cit-AuNPs exposed to freshwater, the dissolution of AuNPs in these fluids was not statistically significant.

Dissolution kinetics

The dissolution kinetics of AuNPs in this study were explained by the first-order reaction kinetics model. This model was used to predict the dissolution rate and half-time of AuNPs. The dissolution kinetics were calculated according to the parameters described in literature (Kittler et al. 2010; Wang et al. 2016; Atkins and de Paula 2006). Therefore, Fig. 5a, b and c show the dissolution rates of citrate-stabilized AuNPs, PEGylated COOH-AuNPs and NH_2-AuNPs, respectively. The results of dissolution rates k (h^{-1}) and the calculated corresponding half-times $t_{1/2}$ (days) are presented in Table 3.

The dissolution rates of NH_2-AuNPs were faster followed by COOH-AuNPs then citrate-stabilized gold nanoparticles. This was more pronounced in acidic media such as the simulated gastric fluid whereby the half-times of NH_2-AuNPs and COOH-AuNPs were significantly ($p < 0.05$) shorter than that of cit-AuNPs at 11, 128 and 259 days, respectively. In phagolysosomal fluid, the half-times were 53, 63 and 307 days long for NH_2-AuNPs, COOH-AuNPs and sit-AuNPs, respectively (Table 3). The half-times of AuNPs in alkaline media such as Gamble's fluid, blood plasma and intestinal fluid were generally longer, ranging between 400, 409 and 400 days respectively for cit-AuNPs; 172, 280 and 563 days, respectively, for COOH-AuNPs; and in the case of NH_2-AuNPs, those particles suspended in simulated alkaline intestinal fluid had the highest half-time of 137 days. This observation was also made for cit-AuNPs, COOH-AuNPs and NH_2-AuNPs suspended in synthetic environmental fluids which were generally characterized by longer half-times. Dissolution rates and half-time results calculated from the kinetic model show the same trend (Fig. 5). Generally, the slope of the linearized model was significantly steeper for NH_2-AuNPs followed by COOH-AuNPs in simulated media compared to cit-AuNPs. Furthermore, the slopes of citrate-stabilized and amine-functionalized gold nanoparticles in gastric fluid were much steeper and in the case of carboxyl-functionalized nanoparticles, this was

Table 2 Multiple variable ANOVA of the dissolution of citrate-stabilized and PEGylated gold nanoparticles in simulated biological fluids and synthetic environmental media

Functional group	Biological fluid	DF 14	SS	*F*-value	*p* value
Citrate-AuNPs	BP	1	45,581	91,162.447	0.0021
Citrate-AuNPs	GF	1	45,581	26.5984	0.0008
Citrate-AuNPs	GIF	1	967	1933.366	0.0144
Citrate-AuNPs	IF	1	75	149.119	0.0420
Citrate-AuNPs	PSF	1	378	755.048	0.0231
Citrate-AuNPs	FW	1	88	149.119	0.0520
Citrate-AuNPs	SW	1	78	755.048	0.0231
COOH-AuNPs	BP	1	6439	12,877.596	0.0056
COOH-AuNPs	GF	1	13,017	25.9699	0.0009
COOH-AuNPs	GIF	1	17,811	35,622.940	0.0033
COOH-AuNPs	IF	1	11	21.753	0.0344
COOH-AuNPs	PSF	1	177	354.738	0.0337
COOH-AuNPs	FW	1	20	21.753	0.0344
COOH-AuNPs	SW	1	120	354.738	0.0237
NH_2-AuNPs	BP	1	7777	15,554.431	0.0051
NH_2-AuNPs	GF	1	5817	23.3089	0.0013
NH_2-AuNPs	GIF	1	47	93.716	0.0655
NH_2-AuNPs	IF	1	57	114.001	0.0594
NH_2-AuNPs	PSF	1	6	11.273	0.0142
NH_2-AuNPs	FW	1	44	114.001	0.0394
NH_2-AuNPs	SW	1	60	11.273	0.0042

DF degree of freedom, *SS* sum of squares

observed for those particles exposed to phagolysosomal fluid. This is indicative of a faster dissolution of AuNPs in these fluids. However, for the neutral simulated fluids such as intestinal fluids, blood plasma, freshwater and seawater, the slope was shallow indicating a slower dissolution process.

Discussion

Considering that the simulated biological fluids and environmental media were maintained at various pH and ionic strength, the difference in dissolution rates of citrate-stabilized gold nanoparticles, PEGylated COOH-AuNPs and NH_2-AuNPs within a particular dissolution medium was attributed to differences in surface functionalization of the nanoparticle and aggregation state, ionic strength and pH of the exposure media. The notable decrease in absorbance and peak broadening observed in the UV-Vis results might be indicative of particle aggregation over time. The reduction in absorption intensity was also observed by others (Aryal et al. 2006; Stebounova et al. 2011). Badawy et al. (Badawy et al. 2010) and Sperling et al. (Sperling and Parak 2010) have demonstrated that NPs exposed to biological fluids and environmental media are prone to aggregation because they are sensitive to changes in ionic strength and pH of the exposure media. Fluids of biological systems usually have high ionic strength and it encourages nanoparticle aggregation (Guerrini et al. 2018). The presence of biological salts can induce particle aggregation, and this can lead to altering the signal intensity of the LSPR peak. The results of this study were in support of those obtained by these and other investigators (Rouhana et al. 2007).

The biological salts and high ionic strength of phagolysosomal fluid and seawater can lead to the formation of nanoparticle aggregates via electrostatic interactions, thereby reducing the surface area of nanoparticles thus reducing chances of dissolution (Alkilany and

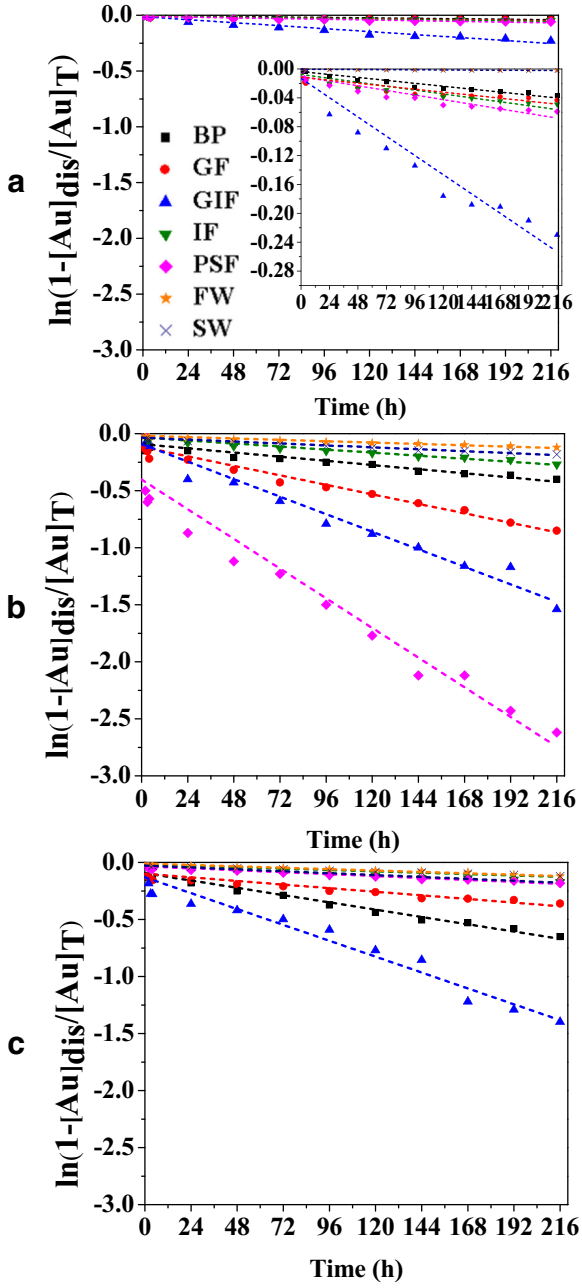

Fig. 5 Plot of $\ln(1\text{-}[Au(t)]_t/[AuNPs]_0)$ with the dissolution time in simulated biological and environmental fluids showing the dissolution rates of citrate-stabilized AuNPs (**a**), PEGylated COOH-AuNPs (**b**) and NH_2-AuNPs (**c**). BP, GF, GIF, IF and PSF are simulated biological fluids for blood plasma, Gamble's fluid, gastric fluid, intestinal fluid and phagolysosomal fluid, respectively. FW and SW are synthetic environmental media for freshwater and seawater

Murphy 2010). Particle aggregation reduces the surface area-to-volume ratio thus resulting in lower NP reactivity and NP dissolution (Bozich et al. 2014; Tejamaya et al. 2012; Li et al. 2013). In addition, it may reduce the surface area of the particles by minimizing their interaction with the biological ions in the surrounding media, therefore inhibiting nanoparticle dissolution. These factors explain low dissolution of citrate-stabilized gold nanoparticles.

Furthermore, low dissolution of citrate-stabilized gold nanoparticles was probably because citrate as a stabilizing agent weakly bound to the NPs can be easily displaced from the NP surface and this facilitates particle aggregation (Bozich et al. 2014; Tejamaya et al. 2012; Li et al. 2013). In addition, electrostatic interactions between citrate-stabilized AuNPs and counterions in the biological media neutralize the NP surface charge, thereby rendering the surface of the NP prone to aggregation. Therefore, these nanoparticles lose stability through the reduction of electrostatic repulsive forces between the nanoparticles causing them to form aggregates; thus, dissolution occurs to a very small extent. In literature, higher dissolution rates are correlated to smaller NP sizes. For example, Kittler et al. (Kittler

Table 3 Dissolution rates and half-time of AuNPs in simulated biological and environmental fluids

Functional group	Sample	k (h^{-1})	$t_{1/2}$ (days)
Citrate-AuNPs	BP	1.69E−03	409
Citrate-AuNPs	GF	1.73E−03	400
Citrate-AuNPs	GIF	2.67E−03	259
Citrate-AuNPs	IF	1.73E−03	400
Citrate-AuNPs	PSF	2.25E−03	307
Citrate-AuNPs	FW	8.12E−04	853
Citrate-AuNPs	SW	7.86E−04	881
COOH-AuNPs	BP	2.47E−03	280
COOH-AuNPs	GF	4.01E−03	172
COOH-AuNPs	GIF	5.40E−03	128
COOH-AuNPs	IF	1.23E−03	563
COOH-AuNPs	PSF	1.08E−02	63
COOH-AuNPs	FW	1.20E−03	577
COOH-AuNPs	SW	1.23E−03	562
NH_2-AuNPs	BP	3.66E−02	18
NH_2-AuNPs	GF	1.32E−02	52
NH_2-AuNPs	GIF	5.80E−02	11
NH_2-AuNPs	IF	5.05E−03	137
NH_2-AuNPs	PSF	1.29E−02	53
NH_2-AuNPs	FW	5.01E−03	138
NH_2-AuNPs	SW	1.90E−03	364

et al. 2010) observed that the dissolution rate of citrate-stabilized silver nanoparticles was lower than that of polyvinylpyrrolidone-stabilized particles due to particle agglomeration. Therefore, these authors concluded that the rate of dissolution depends on the type of functional group attached to the nanoparticle surface. Botha et al. (Botha et al. 2015) studied the dissolution effects of AuNPs in vivo and obtained similar results where no dissolution of AuNPs was observed for larger particle aggregates.

Amine- and carboxyl-functionalized gold nanoparticles displayed minimal inter-particle binding in simulated biological fluids and synthetic environmental media due to steric effect from PEG coating and repulsive forces that arise from the functional groups on the nanoparticle surface (Breitner et al. 2015; Hong et al. 2011). This action maintains the monodispersity of particles and PEG coating attenuates formation of aggregates. Smaller sized NPs have a greater surface area for the interactions with the surrounding media; therefore, this might explain the higher dissolution of COOH-AuNPs and NH_2-AuNPs compared to cit-AuNPs.

Furthermore, amine- and carboxyl-functionalized gold nanoparticles suspended in acidic media such as gastric fluid and phagolysosomal fluid respectively showed significantly higher dissolution compared to those in alkaline media including intestinal fluid, Gamble's fluid, blood plasma, freshwater and seawater. This is because acidic conditions demonstrated by low pH values that characterize gastric and phagolysosomal fluids are an enabling factor for the oxidation of gold nanoparticles into gold ions thereby increasing their solubility and hence greater chance of dissolution (Chambers et al. 2014). Thus gold NPs exposed to acidic media would be less stable and dissolve to a greater extent than in alkaline media (Bian et al. 2011). This could explain the faster dissolution rate of NH_2-AuNPs submerged in the very acidic simulated gastric fluid.

The calculated rate constants of COOH-AuNPs and NH_2-AuNPs were similar in that they were faster, but significantly different meaning that these ligands behave differently when exposed to biological fluids and environmental media. The differences observed between these functional groups on AuNP dissolution can be elucidated by some ligand-promoted process facilitated by protons in the simulated fluids. The carboxyl group is an acid; therefore, in solution, it is likely to donate a proton thereby becoming negatively charged species and interacts with positively charged ions in the fluid (Bozich et al. 2014). In addition, carboxylic acids act as both hydrogen bond acceptors, due to the carbonyl group, and hydrogen bond donors, due to the hydroxyl group (Lemmerer et al. 2015; Hosseini-Monfared et al. 2015). As a result, they often participate in hydrogen bonding. This tendency to hydrogen bond gives them increased solubility in aqueous solutions; hence, COOH-AuNPs have faster dissolution rates compared to citrate-stabilized particles.

Conversely, the amine group under acidic conditions is likely to get protonated and form a positively charged PEG ammonium compound. This proton transfer to the functional group on the ligand can hinder full attachment of the ligand to the nanoparticle surface thereby exposing it to dissolution (Rak et al. 2014). Secondly, this occurrence may weaken the nanoparticle-ligand bond at the surface, making the particles more susceptible to proton-promoted dissolution (Ludwig et al. 1996). Finally, amine is smaller in size compared to the carboxyl group; therefore, its proton transfer process is faster, and this might have a bigger effect on dissolution.

These results were similar to those obtained by (Arnida et al. 2011; Sakka et al. 2016). In general, the dissolution rate of AuNPs was faster in simulated freshwater than seawater for all the nanoparticles (Adeleye et al. 2014). The dissolution rate constants in Table 3 show that the dissolution rates of AuNPs increase in the order of NH_2 > COOH > citrate. The results showed a slow dissolution behaviour of citrate-stabilized AuNPs. Considering their low dissolution rates and propensity to form agglomerates, these gold nanoparticles would be (bio)durable and biopersistent in biological and aquatic environments and are expected to illicit long-term effects (Bardaxoglou et al. 2017). Conversely, functional groups encourage nanoparticle solubility; therefore, their effects would manifest in the short term. These observations are presently further confirmed in our laboratory by implementing a flow-through dissolution system recently described by other investigators (Oberdörster and Kuhlbusch 2018).

Conclusion

Dissolution of gold nanoparticles in simulated biological fluids and synthetic environmental media occurs to a small extent. Their dissolution rates are highly

dependent on the agglomeration/aggregation state and surface functionalization of the nanoparticles. Gold nanoparticles are prone to aggregation when stabilized by citrate and thus have a propensity to form aggregates under biological and environmental conditions. This effect reduces their surface area to volume ratio thus leading to low dissolution. PEGylated gold nanoparticles are less prone to aggregation; their higher dissolution compared to cit-AuNPs is due to some ligand-promoted processes. Therefore, citrate-stabilized particles may cause long-term health effects because they are more (bio)durable and show high biopersistence, meaning these nanoparticles might resist chemical or biochemical alteration in biological systems. Surface modification can considerably influence the dissolution of gold nanoparticles. The results demonstrate that dissolution of gold nanoparticles is a complex process and is influenced by various intrinsic and extrinsic factors. Therefore, by evaluating these factors, comprehensive research needs to be done to investigate the dissolution of several other NPs to understand their behaviour in different simulated biological fluids and environmental media in order to understand their effects on humans and the environment.

Funding This work was funded by the South African Department of Science and Technology (DST) and the National Institute for Occupational Health (NIOH).

Compliance with ethical standards

Conflict of interest The authors declare that they have no conflict of interest.

References

Adeleye AS, Conway JR, Perez T, Rutten P, Keller A (2014) Influence of extracellular polymeric substances on the long-term fate, dissolution, and speciation of copper-based nanoparticles. Environ Sci Technol 48(21):12561–12568

Aiken GR, Hsu-Kim H, Ryan JN (2011) Influence of dissolved organic matter on the environmental fate of metals, nanoparticles, and colloids. Environ Sci Technol 45:3196–3201

Alkilany AM, Murphy CJ (2010) Toxicity and cellular uptake of gold nanoparticles: what we have learned so far? J Nanopart Res 12(7):2313–2333

Arnida MM, Ray A, Peterson CM, Ghandehari H (2011) Geometry and surface characteristics of gold nanoparticles influence their biodistribution and uptake by macrophages. Eur J Pharm Biopharm 77(3):417–423

Arts JH, Hadi M, Irfan MA, Keene AM, Kreiling R, Lyon D et al (2015) A decision-making framework for the grouping and testing of nanomaterials (DF4nanoGrouping). Regul Toxicol Pharmacol 71(2):S1–S27

Aryal S, Remant BK, Dharmaraj N, Bhattarai N, Kim CH, Kim HY (2006) Spectroscopic identification of SAu interaction in cysteine capped gold nanoparticles. Spectrochim Acta Part A Mol Biomol Spectrosc 63(1):160–163

Atkins P, de Paula J. Atkins' physical chemistry. Oxford University Press. 2006. 8th Edition

Auffan M, Rose J, Wiesner MR, Bottero JY (2009) Chemical stability of metallic nanoparticles: a parameter controlling their potential cellular toxicity in vitro. Environ Pollut 157(4):1127–1133

Avellan A, Simonin M, McGivney E, Bossa N, Spielman-Sun E, Rocca JD, Bernhardt ES, Geitner NK, Unrine JM, Wiesner MR, Lowry GV (2018) Gold nanoparticle biodissolution by a freshwater macrophyte and its associated microbiome. Nat Nanotechnol 13(11):1072–1077

Avramescu ML, Rasmussen PE, Chénier M, Gardner HD (2017) Influence of pH, particle size and crystal form on dissolution behaviour of engineered nanomaterials. Environ Sci Pollut Res 24(2):1553–1564

Bachler G, Losert S, Umehara Y, von Goetz N, Rodriguez-Lorenzo L, Petri-Fink A, Rothen-Rutishauser B, Hungerbuehler K (2015) Translocation of gold nanoparticles across the lung epithelial tissue barrier: combining in vitro and in silico methods to substitute in vivo experiments. Part Fibre Toxicol 12(1):18

Badawy AM, Luxton TP, Silva RG, Scheckel KG, Suidan MT, Tolaymat TM (2010) Impact of environmental conditions (pH, ionic strength, and electrolyte type) on the surface charge and aggregation of silver nanoparticles suspensions. Environ Sci Technol 44(4):1260–1266

Baker TJ, Tyler CR, Galloway TS (2014) Impacts of metal and metal oxide nanoparticles on marine organisms. Environ Pollut 186:257–271

Balasubramanian SK, Jittiwat J, Manikandan J, Ong CN, Liya EY, Ong WY (2010) Biodistribution of gold nanoparticles and gene expression changes in the liver and spleen after intravenous administration in rats. Biomaterials. 31(8):2034–2042

Bardaxoglou G, Rouleau C, Pelletier E (2017) High stability and very slow dissolution of bare and polymer coated silver nanoparticles dispersed in river and coastal waters. J Aquat Pollut Toxicol 1(2):1–15

Bian SW, Mudunkotuwa IA, Rupasinghe T, Grassian VH (2011) Aggregation and dissolution of 4 nm ZnO nanoparticles in aqueous environments: influence of pH, ionic strength, size, and adsorption of humic acid. Langmuir. 27(10):6059–6068

Botha TL, James TE, Wepener V (2015) Comparative aquatic toxicity of gold nanoparticles and ionic gold using a species sensitivity distribution approach. J Nanomater 2015:1–16

Bozich JS, Lohse SE, Torelli MD, Murphy CJ, Hamers RJ, Klaper RD (2014) Surface chemistry, charge and ligand type impact the toxicity of gold nanoparticles to Daphnia magna. Environ Sci Nano 1(3):260–270

Breitner EK, Hussain SM, Comfort KK (2015) The role of biological fluid and dynamic flow in the behavior and cellular interactions of gold nanoparticles. J Nanobiotechnol 13(1):56

Chambers BA, Afrooz AN, Bae S, Aich N, Katz L, Saleh NB et al (2014) Effects of chloride and ionic strength on physical morphology, dissolution, and bacterial toxicity of silver nanoparticles. Environ Sci Technol 48(1):761–769

Chen M, Jafvert CT (2018) Anion recovery from water by cross-linked cationic surfactant nanoparticles across dialysis membranes. Environ Sci Nano 5(6):1350–1360

Chen H, Wang Y, Wang Y, Dong S, Wang E (2006) One-step preparation and characterization of PDDA-protected gold nanoparticles. Polymer (Guildf) 47(2):763–766

Cherevko S, Zeradjanin A, Keeley GP, Mayrhofer K (2014) A comparative study on gold and platinum dissolution in acidic and alkaline media. J Electrochem Soc 161(12):H822–H830

Cohen JM, Teeguarden JG, Demokritou P (2014) An integrated approach for the in vitro dosimetry of engineered nanomaterials. Part Fibre Toxicol 11(1):20

Donovan AR, Adams CD, Ma Y, Stephan C, Eichholz T, Shi H (2016) Single particle ICP-MS characterization of titanium dioxide, silver, and gold nanoparticles during drinking water treatment. Chemosphere. 144:148–153

Ferry JL, Craig P, Hexel C, Sisco P, Frey R, Pennington PL, Fulton MH, Scott IG, Decho AW, Kashiwada S, Murphy CJ, Shaw TJ (2009) Transfer of gold nanoparticles from the water column to the estuarine food web. Nat Nanotechnol 4(7):441–444

Fratoddi I, Venditti I, Cametti C, Russo MV (2015) How toxic are gold nanoparticles? The state-of-the-art. Nano Res 8(6): 1771–1799

Guerrini L, Alvarez-Puebla RA, Pazos-Perez N (2018) Surface modifications of nanoparticles for stability in biological fluids. Materials (Basel) 11(7):1145

Hitchman A, Sambrook Smith GH, Ju-Nam Y, Sterling M, Lead JR (2013) The effect of environmentally relevant conditions on PVP stabilised gold nanoparticles. Chemosphere. 90(2): 410–416

Hong SC, Lee JH, Lee J, Kim HY, Park JY, Cho J, Lee J, Han DW (2011) Subtle cytotoxicity and genotoxicity differences in superparamagnetic iron oxide nanoparticles coated with various functional groups. Int J Nanomedicine 6:3219–3231

Hornos Carneiro MF, Barbosa F Jr (2016) Gold nanoparticles: a critical review of therapeutic applications and toxicological aspects. J Toxicol Environ Heal - Part B Crit Rev 19(3–4): 129–148

Hosseini-Monfared H, Parchegani F, Alavi S (2015) Carboxylic acid effects on the size and catalytic activity of magnetite nanoparticles. J Colloid Interface Sci 437:1–9

Hull MS, Chaurand P, Rose J, Auffan M, Bottero JY, Jones JC, Schultz IR, Vikesland PJ (2011) Filter-feeding bivalves store and biodeposit colloidally stable gold nanoparticles. Environ Sci Technol 45(15):6592–6599

Islam NU, Jalil K, Shahid M, Rauf A, Muhammad N, Khan A, Shah MR, Khan MA (2019) Green synthesis and biological activities of gold nanoparticles functionalized with Salix alba. Arab J Chem 12(8):2914–2925

Kittler S, Greulich C, Diendorf J, Koller M, Epple M (2010) Toxicity of silver nanoparticles increases during storage because of slow dissolution under release of silver ions. Chem Mater 22(16):4548–4554

Kreyling WG, Fertsch-Gapp S, Schäffler M, Johnston BD, Haberl N, Pfeiffer C, Diendorf J, Schleh C, Hirn S, Semmler-Behnke M, Epple M, Parak WJ (2014) In vitro and in vivo interactions of selected nanoparticles with rodent serum proteins and their consequences in biokinetics. Beilstein J Nanotechnol 5(1):1699–1711

Laux P, Riebeling C, Booth AM, Brain JD, Brunner J, Cerrillo C, Creutzenberg O, Estrela-Lopis I, Gebel T, Johanson G, Jungnickel H, Kock H, Tentschert J, Tlili A, Schäffer A, Sips AJAM, Yokel RA, Luch A (2017) Nanoimpact biokinetics of nanomaterials : the role of biopersistence. NanoImpact. 6:69–80

Lemmerer A, Govindraju S, Johnston M, Motloung X, Savig KL (2015) Co-crystals and molecular salts of carboxylic acid/pyridine complexes: can calculated pKa's predict proton transfer? A case study of nine complexes. CrystEngComm. 17(19):3591–3595

Li Y, Zhang W, Niu J, Chen Y (2013) Surface-coating-dependent dissolution, aggregation, and reactive oxygen species (ROS) generation of silver nanoparticles under different irradiation conditions. Environ Sci Technol 47(18):10293–10301

Libralato G, Galdiero E, Falanga A, Carotenuto R, De Alteriis E, Guida M (2017) Toxicity effects of functionalized quantum dots, gold and polystyrene nanoparticles on target aquatic biological models: a review. Molecules. 22(9):1439

Lin Z, Monteiro-Riviere NA, Kannan R, Riviere JE (2016) A computational framework for interspecies pharmacokinetics, exposure and toxicity assessment of gold nanoparticles. Nanomedicine. 11(2):107–119

Ludwig C, Devidal JL, Casey WH (1996) The effect of different functional groups on the ligand-promoted dissolution of NiO and other oxide minerals. Geochim Cosmochim Acta 60(2): 213–224

Marchewka MK, Pietraszko A (2003) Structure and spectra of melaminium citrate. J Phys Chem Solids 64(11):2169–2181

Marques MR, Loebenberg R, Almukainzi M (2011) Simulated biological fluids with possible application in dissolution testing. Dissolution Technol 18(3):15–28

Oberdörster G, Kuhlbusch TAJ (2018) In vivo effects: methodologies and biokinetics of inhaled nanomaterials. NanoImpact. 10(April 2017):38–60

Oh N, Park JH (2014) Endocytosis and exocytosis of nanoparticles in mammalian cells. Int J Nanomedicine 9(Suppl 1):51

Oyabu T, Myojo T, Lee BW, Okada T, Izumi H, Yoshiura Y, Tomonaga T, Li YS, Kawai K, Shimada M, Kubo M, Yamamoto K, Kawaguchi K, Sasaki T, Morimoto Y (2017) Biopersistence of NiO and TiO_2 nanoparticles following intratracheal instillation and inhalation. Int J Mol Sci 18(12):2757

Probst M, Schmidt M, Tietz K, Klein S, Weitschies W, Seidlitz A (2017) In vitro dissolution testing of parenteral aqueous solutions and oily suspensions of paracetamol and prednisolone. Int J Pharm 532(1):519–527

Rak MJ, Saadé NK, Friščić T, Moores A (2014) Mechanosynthesis of ultra-small monodisperse amine-stabilized gold nanoparticles with controllable size. Green Chem 16(1):86–89

Rouhana LL, Jaber JA, Schlenoff JB (2007) Aggregation-resistant water-soluble gold nanoparticles. Langmuir. 23(26):12799–12801

Sakka Y, Skjolding LM, Mackevica A, Filser J, Baun A (2016) Behavior and chronic toxicity of two differently stabilized silver nanoparticles to Daphnia magna. Aquat Toxicol 177: 526–535

Simpson CA, Salleng KJ, Cliffel DE, Feldheim DL (2013) In vivo toxicity, biodistribution, and clearance of glutathione-coated gold nanoparticles. Nanomed Nanotechnol Biol Med 9(2): 257–263

Sperling RA, Parak WJ (2010) Surface modification, functionalization and bioconjugation of colloidal inorganic nanoparticles. Philos Trans R Soc A Math Phys Eng Sci 368(1915):1333–1383

Stebounova LV, Guio E, Grassian VH (2011) Silver nanoparticles in simulated biological media: a study of aggregation, sedimentation, and dissolution. J Nanopart Res 13(1):233–244

Sun X, Dong S, Wang E (2005) One-step preparation of highly concentrated well-stable gold colloids by direct mix of polyelectrolyte and HAuCl4 aqueous solutions at room temperature. J Colloid Interface Sci 288(1):301–303

Tejamaya M, Römer I, Merrifield RC, Lead JR (2012) Stability of citrate, PVP, and PEG coated silver nanoparticles in ecotoxicology media. Environ Sci Technol 46(13):7011–7017

Tiwari PM, Vig K, Dennis VA, Singh SR (2011) Functionalized gold nanoparticles and their biomedical applications. Nanomaterials 1(1):31–63

Utembe W, Potgieter K, Stefaniak AB, Gulumian M (2015) Dissolution and biodurability: important parameters needed for risk assessment of nanomaterials. Part Fibre Toxicol 12(1):11

Vetten MA, Tlotleng N, Rascher DT, Skepu A, Keter FK, Boodhia K et al (2013) Label-free in vitro toxicity and uptake assessment of citrate stabilised gold nanoparticles in three cell lines. Part Fibre Toxicol 10(1):50

Wang A, Ng HP, Xu Y, Li Y, Zheng Y, Yu J, Han F, Peng F, Fu L (2014) Gold nanoparticles: synthesis, stability test, and application for the rice growth. J Nanomater 2014:1–6

Wang N, Tong T, Xie M, Gaillard JF (2016) Lifetime and dissolution kinetics of zinc oxide nanoparticles in aqueous media. Nanotechnology. 27(32):324001

Weber CI. Methods for measuring the acute toxicity of effluents and receiving waters to freshwater and marine organisms Fifth Edition October 2002. Environ Prot. 2002;232(October):266. Availabkle from: http://www.epa.gov/waterscience/WET/disk1/ctm.pdf

Zeng S, Yong KT, Roy I, Dinh XQ, Yu X, Luan F (2011) A review on functionalized gold nanoparticles for biosensing applications. Plasmonics. 6(3):491–506

4.2 Paper 2

This second article entitled “Dissolution kinetics of silver nanoparticles: Behaviour in simulated biological fluids and synthetic environmental media” has been published in Toxicology Reports. The article investigated the dissolution behaviour of silver nanoparticles in simulated biological fluids and environmental media to predict their behaviour in real-life situations. Additionally, the aim was also to determine whether silver nanoparticles cause long-term or short-term health effects on humans and the environment.

Toxicology Reports (2022)
https://doi.org/10.1016/j.toxrep.2022.03.044

Odwa Mbanga- Principal author

Ewa Cukrowska- Supervisor

Mary Gulumian- Supervisor

Toxicology Reports 9 (2022) 788–796

Contents lists available at ScienceDirect

Toxicology Reports

journal homepage: www.elsevier.com/locate/toxrep

Dissolution kinetics of silver nanoparticles: Behaviour in simulated biological fluids and synthetic environmental media

Odwa Mbanga [a,b], Ewa Cukrowska [a], Mary Gulumian [b,c,*]

[a] Molecular Sciences Institute, School of Chemistry, University of Witwatersrand, Private Bag X3, Johannesburg, 2050, South Africa
[b] Toxicology and Biochemistry Department, National Institute for Occupational Health, A divisionof National Health Laboratories, Johannesburg 2000, Gauteng, South Africa
[c] Water research group, Unit for Environmental Sciences and Management, Northwest University, Private Bag X6001, Potchefstroom, 2520, South Africa

ARTICLE INFO

Handling Editor: Dr. Lawrence Lash

Keywords:
Silver nanoparticles
Agglomeration
Dissolution kinetics
PH
Synthetic
Biological & Environmental media

ABSTRACT

Silver nanoparticles offer a wide range of benefits including their application in several fields such as medical, food, health care, consumer, and industrial purposes. However, unlocking this potential requires a responsible and co-ordinated approach to ensure that potential challenges emanating from the use of silver nanoparticles are being addressed. In this study body fluids and environmental media were used to investigate the effects of citrate coated silver nanoparticles (cit-coated AgNPs) to mimic their behaviour in real life situations. Understanding the dissolution kinetics and behaviour of cit-coated AgNPs in simulated biological fluids and synthetic environmental media helps us predict their fate and effects on human health and the environment. The cit-coated AgNPs behaviour significantly varied in acidic and alkaline simulated fluids. Low pH and high ionic strength accelerated the rate and degree of dissolution of AgNPs in simulated fluids. Following exposure to simulated fluids cit-coated AgNPs demonstrated significant changes in agglomeration state and particle reactivity however, the morphology remained unaltered. The slow dissolution rates observed for highly agglomerated cit-coated AgNPs in simulated blood plasma, Gamble's and intestinal fluids, and freshwater indicate that there is a greater likelihood that the particles will be the cause of the observed adverse effects. In contrast, the fast dissolution rates observed for cit-coated AgNPs in simulated gastric and phagolysosomal fluid and synthetic seawater, the release of the silver ions at a fast rate, will be the cause of their short-term effects.

1. Introduction

Silver nanoparticles (AgNPs) are extensively used in the nanotechnology industry due to their effective antibacterial activity, high electrical conductivity, and optical properties. They are incorporated in numerous consumer products such as dietary supplements, materials for food packaging, coatings on medical devices, water disinfectants, air filters, electronic appliances, odour-resistant textile fabrics and cosmetic products such as deodorants [3–5]. Application of AgNPs also includes areas such as biosensing, electronics and surface enhanced Raman spectroscopy [4].

There should be a responsible and co-ordinated approach to ensure that the potential occupational, consumer and environmental safety issues regarding the use of AgNPs are being addressed at the same time as the technology is developing. It is these concerns that have led to a need to elucidate the potential harmful effects of AgNPs to human health and the environment. The assessment of the effects of nanoparticles can be investigated through various properties but in this research study dissolution was employed to determine the effects of nanoparticles on human health and the environment. Dissolution can be explained as the release of species from the nanoparticle surface which leads to the subsequent distribution of those released species throughout the bulk fluid surrounding the nanoparticles. Dissolution heavily influences the biodurability and biopersistence of nanoparticles [9,41]. The tendency of a given nanoparticle to cause negative effects on human health and the environment is strongly related to the duration of residence time in these environments. Biodurability and persistence are parameters that influence the behaviour of nanoparticles in the body and environment and are used to predict the particles' duration of residence time under physiological and environmental conditions. For this reason, the dissolution rate is an important property for the assessment of the effects of NPs [8]. Biopersistent nanoparticles are defined as those with the ability

* Corresponding author.
E-mail addresses: odwa.mbanga@students.wits.ac.za (O. Mbanga), ewa.cukrowska@wits.ac.za (E. Cukrowska), Mary.Gulumian@NWU.ac.za (M. Gulumian).

https://doi.org/10.1016/j.toxrep.2022.03.044
Received 8 September 2021; Received in revised form 25 February 2022; Accepted 29 March 2022
Available online 1 April 2022

to persist in the body due to their biodurability and despite physiological clearance mechanisms [23,41]. Resistance to physical clearance may result through their resistance to chemical dissolution. In human particle toxicology, the propensity of a nanoparticle to resist alterations through dissolution or enzymatic degradation in biological media is defined as biodurability and could consequently lead to bioaccumulation of nanoparticles in the body following their translocation and distribution [23,41]. Dissolution also influences the persistence of NPs in the environment. Persistence is defined as the potential of nanoparticles to degrade in the environment. These properties allow for the categorization of nanoparticles between those that are amenable and those resistant to dissolution. For example, particles with slow dissolution rates are expected to elicit long-term effects in human health and the environment. [34,41].

Numerous dissolution studies of AgNPs reported in the literature have investigated the factors affecting the release of ionic silver under biological and environmental conditions [6,20,21,29,33,37,39]. For example, factors such as pH, ionic strength and surface functionalization have been observed to influence the dissolution of AgNPs where a positive correlation could be observed between low pH conditions and higher dissolution [3,13,35,36]. A positive correlation could also be observed between the salinity of the natural estuarine systems and the higher dissolution of AgNPs [25]. There are other studies which highlight the crucial factor that size and shape have on dissolution of nanoparticles [32]. Despite these numerous studies, there is still a need to investigate the dissolution behaviour of AgNPs in a wide range of simulated biological fluids and environmental media. In addition, many researchers have used a time point greater than 10 min to examine the dissolution behaviour of AgNPs thereby missing crucial information within a key window period during which rapid and major modifications occur to the particles. Furthermore, major focus has been on the highly acidic conditions [36] rather than a wide range of pH conditions to elucidate the dissolution behaviour of AgNPs. Different nanomaterials are reported to be biodurable and persistent as they resist dissolution which in turn can lead to bioaccumulation. It is therefore of crucial importance to investigate the dissolution kinetics of AgNPs in a wide range of simulated biological fluids and environmental media in order to predict their behaviour in real life situations.

Therefore, the present study has investigated the dissolution behaviour and dissolution kinetics (dissolution rates, rate constants and half-times) of citrate coated silver nanoparticles (cit-coated AgNPs) in simulated biological fluids and synthetic environmental media with different chemical composition under a wide variety of pH conditions. Body fluids are very rich in essential elements and may play a very significant role in the intake of NPs and interactions with cellular activities while some are destructive. The body fluids included the Gamble's fluid (GF) & phagolysosomal fluid (PSF) representing the lung exposure pathway, oral exposure pathway represented by gastric fluid (GIF) and intestinal fluid (IF) and lastly blood plasma (BP). The synthetic environmental media of interest have included Freshwater (FW) and Seawater (SW).

2. Materials and methods

2.1. Synthesis and characterization of silver nanoparticles

The silver nanoparticles used in this study were purchased from (Sigma Aldrich Johannesburg, South Africa) in the size of 10 nm in diameter suspended in a 1% sodium citrate solution as a stabilizer. Citrate stabilized AgNPs were chosen because citrate is used as a capping agent to maintain the size, monodispersity and stability without irreversible aggregation or decomposition of the silver nanoparticles. Furthermore, citrate stabilized AgNPs are known to be sensitive to changes in pH and the ionic strength of the medium. Therefore, studying their behaviour in vitro would provide an indication of how they would behave in real-life situations. The nanoparticle suspensions were prepared from the stock solution (0.02 mg mL^{-1}) under sterile conditions. Transmission Electron microscope (TEM) (JOEL Ltd. JEM-2100) (Lireweg, The Netherlands) was used to obtain information on the structure, size, agglomeration, and level of dispersion of the AgNPs before and after exposure to different simulated biological and environmental fluids. A Bruker Tensor 27 Fourier transform infrared spectroscopy (FTIR) (Billerica, Massachusetts, USA) was used to identify functional groups on molecules attached to NPs and to monitor if they migrated from the nanoparticle surface to the bulk media during the duration of the experiments. The Varian Ultraviolet-Visible 50 Conc. spectrophotometer (UV-is) was used to determine the agglomeration state of AgNPs in simulated media at 400 nm before and after dissolution experiments. The concentration of dissolved silver ions in simulated fluids was determined using inductively coupled mass spectrometer (ICP-MS) (Agilent Technologies, 7700 series ICP-MS, Santa Clara, California, United States).

2.2 Procedure

2.2.1 Preparation of fluids

The dissolution experiments were assessed through the use of the static dissolution system whereby the nanoparticle suspension is placed inside a dialysis membrane of a smaller pore size [2,11,20,21,31,38]. The sample holder is then submerged in a beaker containing simulated fluids. This methodology employs the fundamental principles of diffusion whereby silver ions will diffuse from a region of high concentration (nanoparticle surface) to that of low concentration (bulk simulated fluid). The rate at which ions are released from the nanoparticle surface is slower than the released ions diffusing out of the dialysis membrane into the bulk media [20,21]. Therefore, it can be assumed that through measuring the concentration of released ions that passed the dialysis membrane in the bulk fluid by ICP-MS, dissolution kinetics of AgNPs could be predicted.

Table 1
Composition of simulated fluids [30].

Synthetic fluid	Ionic strength (mol L^{-1})	pH	Components (g L^{-1})
BP[a]	0.15	7.2	NaCl (8.035), $NaHCO_3$ (0.355), KCl (0.225), $K_2HPO_4{\cdot}3H_2O$ (0.231), $MgCl_2{\cdot}\ 6H_2O$ (0.331), 1 M HCl (39 mL), $CaCl_2$ (0.292), Na_2SO_4 (0.072), $NH_2C(CH_2OH)_3$ (6.118)
GF[b]	0.17	7.4	$MgCl_2$ (0.203), NaCl (6.019), KCl (0.298), Na_2HPO_4 (0.142), Na_2SO_4 (0.017), $CaCl_2{\cdot}2H_2O$ (0.368), CH_3COONa (0.953), $NaHCO_3$ (2.604), $C_6H_9Na_3O_9$ (0.097)
GIF[c]	0.16	2.0	NaCl (2.922), KCl (7.007), $C_8H_5O_4K$) (0.243), Pepsin (1 mL mL^{-1}), Mucin (3 mg mL^{-1})
IF[d]	0.16	6.8	KCl (0.298), $CaCl_2$ (0.499), $MgCl_2$ (0.190), Urea (0.300), Bile salts (9 mL mL^{-1}), Pancreatin (9 mg mL^{-1})
PSF[e]	0.34	4.5	Na_2HPO_4 (0.142), NaCl (6.650), Na_2SO_4 (0.072), $CaCl_2{\cdot}2H_2O$ (0.029), Glycine (0.450), $C_8H_5O_4K$ (4.086)
FW[f]	0.05	6.8	$NaHCO_3$ (0.012), $CaSO_4$ (0.075), $MgSO_4$ (0.0075), KCl (0.0005)
SW[g]	3.5	8.0	NaCl (21.03), Na_2SO_4 (3.52), KCl (0.61), KBr (0.088), Borax (0.034), $MgCl_2$ (9.50), $CaCl_2$ (1.320), $SrCl_2$ (0.02), $NaHCO_3$ (0.17)

Simulated biological fluids and synthetic environmental media are coded as follows:
[a] BF - Blood plasma,
[b] GF - Gamble's fluid,
[c] GIF - Gastric fluid,
[d] IF - Intestinal fluid,
[e] PSF -Phagolysosomal fluid,
[f] FW - freshwater,
[g] SW - seawater

Simulated biological fluids were synthesized following the procedure obtained from [30] using the anaytical grade reagents described in Table 1. Whereas synthetic environmental media were prepared through the guidelines recommended by the United States (U.S) Environmental Protection Agency (EPA) The focus was on simulated biological fluids intended to mimic the lung, stomach, and intravenous exposure pathways. For the lung, the two main compartments considered were Gamble's fluid (GF) representing the extracellular airway lining fluid and phagolysosomal fluid (PSF) of macrophage cells at pH 7.4 & pH 4.5, respectively. For the oral route, particles will encounter gastric fluid (GIF)and intestinal fluids (IF) in the stomach at pH 2.0 & pH 7.5 respectively. Lastly, Blood plasma (BP) at pH 7.2 which is a fluid that carries blood components throughout the body. The analytical grade reagents were dissolved in 700 mL of distilled water with a conductivity of 18.2 MΩcm in the order given in Table 1. After addition of all the components the final volume was then adjusted to 1 L. Then the pH was adjusted accordingly using 1 M hydrochloric acid or Sodium hydroxide. For the preservation of simulated fluids the anti-fungal agent alkylbenzyldimethylammonium chloride (ABDC) was added to the fluids at 13.7 mM concentration of (51 μL).

2.3 Dialysis experiments

Briefly, 5 mL of the cit-coated silver nanoparticle stock suspension (0.02 mg mL^{-1}) was pipetted into centrifuge tubes. The particles were collected by ultracentrifugation at 13,000 xg for 30 min. They were then re-dispersed in 5 mL simulated fluids then transferred into dialysis membranes (SnakeSkin Dialysis tubing, 3.5 K MWCO, 22 mm-dry diameter) which were rinsed with d-H_2O to eliminate any possible contaminants. A smaller pore size membrane was carefully selected to ensure that only released silver ions can migrate from the nanoparticle surface and dialyze out of the tubing. The dialysis experiments were carried out in water baths maintained at 37 °C and 25 °C under slow stirring to mimic physiological conditions and environmental temperature respectively. Furthermore, the experiments were kept under a closed system in an airtight vessel to eliminate background interreferences and from oxidizing species such as oxygen. Therefore, the impact of concentration of dissolved oxygen in the suspensions has not been considered.

The dialysis membranes contained the NP suspensions were submerged in 500 mL beakers containing simulated fluids then placed in a water bath. The dissolution experiments were conducted over a period of 10 days. On the first day samples were collected from the bulk fluid surrounding the dialysis tubing in 30 min intervals for the first four hours, then twice a day for the next 10 days. The pH of the simulated fluids was constantly checked before, during and after each experiment using a Jenway 3510 pH meter. Samples were collected in triplicates and analysed on ICP-MS with a limit of detection of 0.1 ppb. Reported in the results section is an average of the three measurements.

2.4 Kinetic model for dissolution process

The determination of the biodurability of nanoparticles using in vitro acellular tests is based on the calculation of their dissolution kinetics. The investigation and determination of the dissolution kinetics and subsequent calculation of dissolution rates and rate constants are in turn, the necessary parameters for the prediction of the nanoparticle biodurability.

Since the dissolution of AgNPs follows a first order reaction kinetics, in current study we modified and used the Noyes-Whitey Eq. (1) to calculate the dissolution kinetics including the dissolution rate and half-time of AgNPs to predict their biodurability in simulated biological and environmental media [20,21,42].

$$\frac{d[AgNPs]}{dt} = -D\frac{A}{d}([Ag]_T - [Ag]_{dis}) \quad (1)$$

Where $[AgNPs]$ denotes the initial concentration of AgNPs stock solution, $[Ag]_T$ represents the concentration of silver before the commencement of dissolution process and $[Ag]_{dis}$ represents the concentration of dissolved silver ions. D is the diffusion coefficient of silver ions whereas d accounts for the diffusion layer thickness during the dissolution process and, A represents the surface area of AgNPs.

The total mass of Ag in the system is represented by Eq. 2.

$$[Ag]_T = [AgNPs] + [Ag]_{dis} \quad (2)$$

As previously stated, $[Ag]_T$ is the total amount of silver nanoparticles before the dissolution process commences. The $[AgNPs]$ then substituted by Eq. 3 in the formula:

$$[AgNPs] = [Ag]_T - [Ag]_{dis} \quad (3)$$

However, Eq. 3 can also be re-written in the form represented by Eq. 4:

$$[Ag]_T - [Ag]_{dis} = [Ag]_T\left(1 - \frac{[Ag]_{dis}}{[Ag]_T}\right) \quad (4)$$

Such that

$$[AgNPs] = [Ag]_T\left(1 - \frac{[Ag]_{dis}}{[Ag]_T}\right) \quad (5)$$

Eq. 5 is then substituted into Eq. 1 to obtain the following Eq. (6):

$$[Ag]_T\frac{d\left(1 - \frac{[Ag]_{dis}}{[Ag]_T}\right)}{dt} = -D\frac{A}{d}[Ag]_T\left(1 - \frac{[Ag]_{dis}}{[Ag]_T}\right) \quad (6)$$

Eq. 6 transforms into Eq. 7 if we divide by $[Ag]_T$on both sides of the Eq. 6, yielding the following Eq. 7:

$$\frac{d\left(1 - \frac{[Ag]_{dis}}{[Ag]_T}\right)}{dt} = -D\frac{A}{d}\left(1 - \frac{[Ag]_{dis}}{[Ag]_T}\right) \quad (7)$$

For simplicity let $\left(1 - \frac{[Ag]_{dis}}{[Ag]_T}\right) = x$.

Such that Eq. 7 becomes:

$$\frac{dx}{dt} = -D\frac{A}{d}x \quad (8)$$

In order to bring x to the left hand-side of the equation and dt to the right hand-side of the equation, Eq. 8 is divided by x and multiplied by dt on both sides of the equation:

$$\frac{dx}{x} = -D\frac{A}{d}dt \quad (9)$$

Upon integration, the above equation becomes:

$$lnx = c - D\frac{A}{d}t \quad (10)$$

Where $k = -D\frac{A}{d}$ and representative of the dissolution rate constant whereas c is a constant.

Eq. 11 is obtained through the integration of Eq. 7.

$$\ln\left(1 - \frac{[Ag]_{dis}}{[Ag]_T}\right) = c - kt \quad (11)$$

The plot of $\ln\left(1 - \frac{[Ag]_{dis}}{[Ag]_T}\right)$ vs time enables for the determination of the dissolution rate and dissolution rate constant of AgNPs, consequently predicting their biodurability and persistence in biological media and the environment respectively. The half-time for a first order reaction kinetics is calculated using the following formula:

$$t_{1/2} = \frac{ln2}{k} \quad (12)$$

3 Results

3.1 Characterization

TEM, UV-is, FTIR were used to assess the morphological changes and agglomeration state of cit-coated AgNPs to draw a link between their dissolution behaviour and physicochemical properties.

3.1.1 TEM

TEM images of cit-coated AgNPs before and after 10 days dissolution experiments in simulated biological and environmental fluids. are presented in Fig. 1. The average diameters for cit-coated AgNPs were 10.2 ± 2.1 nm. The size measured from the TEM images were comparable to those reported by the manufacturer to be 10 nm. The nanoparticles were spherical in morphology as seen in the TEM images and there were no appreciable changes in shape after exposure to simulated biological fluids and environmental media (Fig. 1). However, the 10 nm particles showed growth in diameter after dissolution experiments in the simulated intestinal and Gamble's fluid, blood plasma and freshwater with diameter changing as large as 11.2 ± 3.1 nm compared with original diameters of 10 nm as shown in the TEM images. This might be indicative of formation of nanoparticle agglomerates. In contrast, there was an observable decrease in the size to a diameter as small as 8 ± 2.1 nm of the nanoparticles exposed to acidic media such as simulated gastric and phagolysosomal fluid. This decrease was also observed for the cit-coated AgNPs exposed to seawater which had the highest ionic strength. This decrease likely depicts dissolution in these simulated fluids. These results were corroborated by [3,29,36,40].

3.1.2 UV-vis

Fig. 2 shows the UV–vis spectra of silver nanoparticle dispersion in various simulated fluids and environmental media before and after dissolution experiments to determine the agglomeration state of the particles. For all the simulated fluids before the dissolution experiments, well-defined LSPR peaks can be seen at the wavelength of 400 nm (Fig. 1). This is consistent with the reported LSPR absorption band of silver nanoparticles (Li et al., 2010). However, as the period of exposure to simulated fluids increased there was an observable shift to higher wavelength (450 nm) and a drop in absorption peak intensity for particles in contact with neutral media such as blood plasma, intestinal fluid, Gamble's fluid and freshwater. For example, a slight shift from 400 nm to 450 nm was observed after dissolution in BP, GF, IF and FW fluids. This indicates that after a prolonged exposure of silver nanoparticles to these simulated fluids the particles physically coalesce to form larger particles. Generally larger particles tend to absorb UV light at higher wavelength than smaller particles hence there was an observable shift to higher wavelengths for the aggregates. This observation is consistent with the TEM images in Fig. 1 that showed formation of larger AgNPs after exposure to these simulated fluids. These results were consistent with those observed by [15]. However, for simulated fluids characterised by low pH (GIF & PSF) and high ionic strength (SW) a decrease in peak intensity and no shift in peak position was observed which could be indicative of particle dissolution. In these fluids, the particles remained dispersed as single NPs hence there was no observable LSPR peak shift to longer wavelengths [45]. These results were consistent with those observed by [1,13,16,17,27,44]. There was an observable discolouration of the nanoparticle suspension inside the dialysis membrane from yellow to colourless after exposure to all the simulated fluids.

3.1.3 FTIR

FTIR was used to identify functional groups on molecules attached to NPs and to monitor if they migrated from the nanoparticle surface to the bulk media. The absorption wavelength focuses on the range between 500 and 4000 cm^{-1}. The cit-coated AgNPs FTIR spectra are shown in Fig. 3. This is the FTIR spectra of silver nanoparticles in the dialysis membrane before exposure to simulated media and after the end of the dissolution experiments, and lastly the bulk fluid outside the dialysis tubing. The absorption peaks bands at 1432 cm^{-1},1619 cm^{-1}, 1716 cm^{-1} and 3451 cm^{-1} are assigned to C—O stretch, O—H bend, C═O asymmetric stretch and O-H stretch, respectively.

These intense absorption bands emanate from the symmetric and asymmetric stretching of the carboxylate functional group of the citrate molecules [14,19,22,43]. When comparing the FTIR spectra of the nanoparticle suspension inside the dialysis (black spectra labelled before and after) with those of the bulk fluid outside the dialysis membrane (BP, GF, GIF, IF, PSF, FW and SW graph), there were noticeable differences. The prominent absorption bands which result due to stretching of the citrate functional group were absent. The only observable intense absorption bands were of the O-H stretching of the water molecules used in the synthesis of biological fluids and environmental media. This indicates that no particles migrated from the dialysis membrane into the bulk fluid.

3.2 Dissolution in biological fluids and environmental media

Fig. 4 shows dissolution curves of cit-coated silver nanoparticles in simulated biological and environmental fluids over a period of 10 days. In all the simulated fluids and synthetic media partial dissolution was observed. This was confirmed by the analysis of the nanoparticle suspension inside the dialysis membrane after the completion of the experiments where nanoparticles were still observed under TEM (Fig. 1). The dissolution of AgNPs increased gradually over time from 4 h then reached a plateau after 120 h. Meaning that it takes less than 24 h for silver ions to interact with the components used in the synthesis of simulated fluids then migrate from the surface of cit-coated AgNPs into the bulk fluid. Significant differences ($p < 0.05$) were observed in the dissolution trends of cit-coated AgNPs. The concentration of dissolved Ag^{+} ions was smallest for the particles exposed to freshwater. For example, the maximum percentage of dissolved Ag^{+} ion was merely 9.8%. The degree of dissolution depended on the pH and ionic strength of the simulated fluids. Meaning dissolution was higher for simulated fluids characterised by low pH and high ionic strength. For example, the percentage of dissolved Ag^{+} ions were higher for the acidic simulated biological fluids such as gastric and phagolysosomal fluid at 55% and 33%, respectively and high ionic strength seawater at 30% (Fig. 4). This is because under acidic conditions AgNPs are highly unstable therefore likely to dissolve into their ions. Furthermore, the high ionic strength of the sea water significantly favoured the dissolution of AgNPs and shortened their lifetime. Consequently, the percentage of dissolved Ag^{+} ions followed the order GIF > PSF > SW > BP > GF > IF > FW at 55%, 33%, 30%, 22%, 18%, 14% and 9% respectively.

3.3 Statistical analysis

The dissolution data shown in Fig. 4 are expressed as mean ± standard deviation of at least three independent measurements. RStudio version 1.2 software was used to process the data and to investigate if there was a statistically significant difference in the dissolution of citrate coated silver nanoparticles in various simulated biological fluids and synthetic environmental media. The p-values are presented in Table 2 and those less than 0.05 were considered statistically significant.

According to multiple variable ANOVA statistical analysis the p values are less than 0.05 in all cases meaning the dissolution of silver nanoparticles differed significantly among the various simulated fluids. Therefore, silver nanoparticles are expected to behave differently in simulated biological fluids and synthetic environmental media.

3.4 Dissolution kinetics

The first order kinetic model shown in the materials and method

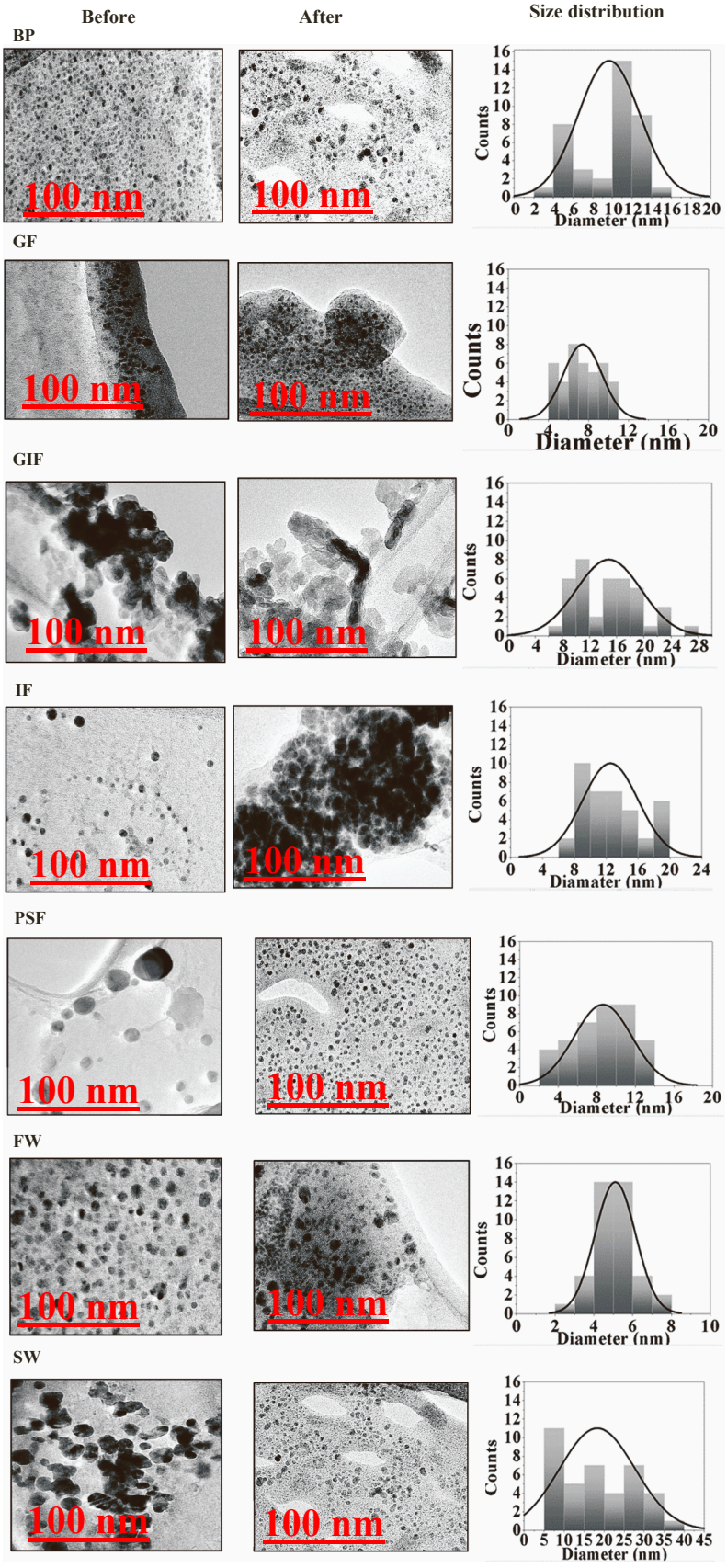

Fig. 1. TEM images of cit-coated AgNPs before and after 10 days dissolution experiments in simulated biological and environmental fluids. Simulated biological fluids are coded as BP, GF, GIF, IF and PSF for blood plasma, Gamble's fluid, gastric fluid, intestinal fluid and phagolysosomal fluid respectively. Whilst synthetic environmental media are denoted as FW and SW are or freshwater and seawater respectively.

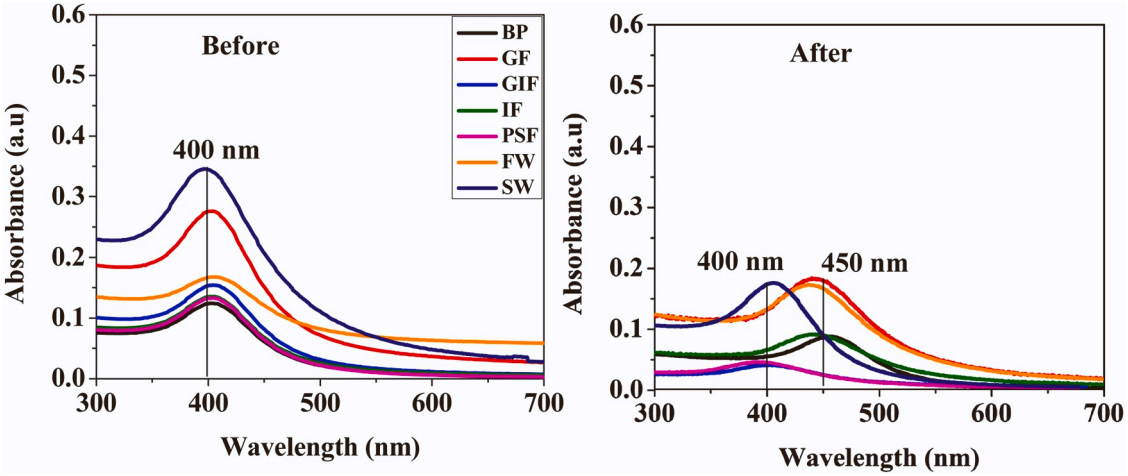

Fig. 2. Citrate-coated silver nanoparticle UV–vis absorption spectra before and after the 10 days dissolution experiments in simulated fluids and synthetic environmental media. Simulated biological fluids are coded as BP, GF, GIF, IF and PSF for blood plasma, Gamble's fluid, gastric fluid, intestinal fluid and phagolysosomal fluid respectively. Whilst synthetic environmental media are denoted as FW and SW are or freshwater and seawater respectively.

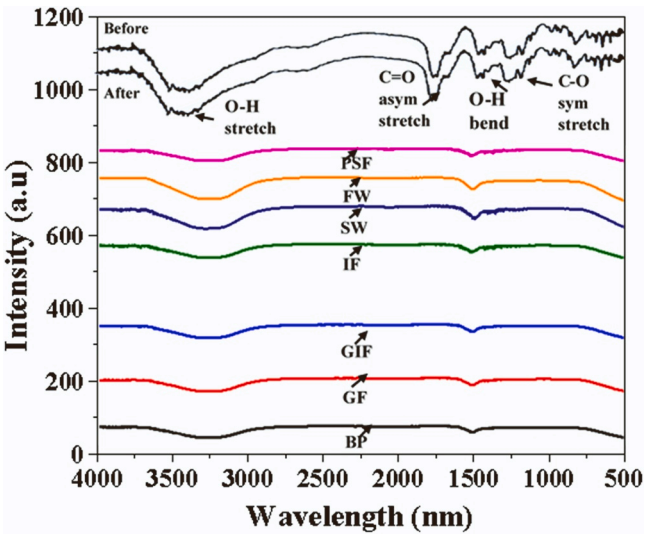

Fig. 3. FTIR spectra of cit-coated AgNPs before and after 10 days dissolution and in the bulk fluid after the dissolution process. Simulated biological fluids are coded as BP, GF, GIF, IF and PSF for blood plasma, Gamble's fluid, gastric fluid, intestinal fluid and phagolysosomal fluid respectively. Whilst synthetic environmental media are denoted as FW and SW are or freshwater and seawater respectively.

section was used to predict the dissolution kinetics of silver nanoparticles. This model enables for the calculation of the dissolution rate constant and half-times of silver nanoparticles in simulated fluids in order to predict their residence time in these biological and environmental surroundings. Therefore, Fig. 5 shows the dissolution rates of citrate coated AgNPs in simulated fluids and synthetic environmental media. The results of dissolution rates k (h^{-1}) and the calculated corresponding half-times $t_{1/2}$ (days) are presented in Table 3.

It was observed that dissolution kinetics depended on the pH and the fastest dissolution was observed for acidic media such as simulated gastric and phagolysosomal fluid whose pH levels are 2.0 and 4.5 respectively. The steeper slope of the linearized model for gastric and phagolysosomal fluid indicate faster dissolution rate (Fig. 5). The dissolution rates were 2.22E-02 $h^{-1}$and 1.68E-02 $h^{-1}$for gastric fluid and phagolysosomal fluid respectively (Table 3). Another factor observed to influence dissolution kinetics was the ionic strength of the media. Comparison of the silver nanoparticle behaviour in environmental media revealed that particles exposed to high ionic strength seawater will dissolve faster than those submerged in freshwater. For example, Table 3 indicates that it will take approximately 3 days for silver nanoparticles to dissolve in sweater whereas the same process would require about 28 days in a freshwater environment. The dissolution half-times followed the order of GIF > PSF > SW > BP > GF > IF > FW at 1, 2, 3, 4, 5, 11 and 28 days, respectively. Lastly, highly agglomerated particles have a reduced surface area thus slow dissolution rates.

Using data obtained from literature the dissolution kinetics of silver nanoparticles were compared with the dissolution rates of various nanoparticles to assess whether silver would elicit short-term or long-term effects on human health and the environment. Table 4.

When comparing the dissolution kinetics of other nanoparticles from literature to that of silver nanoparticles of the present study, it could be observed that zinc oxide nanoparticles have faster dissolution kinetics followed by copper oxide nanoparticles. Barium sulphate nanoparticles also showed faster dissolution because the experiments were carried out in a continuous flow through system which does not reach saturation, and this adds to faster dissolution rates of nanoparticles. Gold nanoparticles were observed to have very low dissolution rates.

4 Discussion

Evident from the TEM images and UV–vis spectra of simulated blood plasma, Gamble's fluid, intestinal fluid and synthetic freshwater was the agglomeration of cit-coated AgNPs after dissolution experiments. Particle agglomeration reduces the surface are to volume ratio of the nanoparticle surface thereby attenuating chances of dissolution. This would explain slow dissolution rates of AgNPs in these simulated fluids. On the other hand, a decrease in the initial particle size of cit-coated AgNPs from 10.2 ± 2.1 nm to 8.1 ± 2.1 submerged in gastric and phagolysosomal fluid and synthetic seawater might have resulted from the dissolution of AgNPs as a result of low pH and high concentration of chloride ions in seawater. According to the Noyes-Whitney equation dissolution of nanoparticles is directly proportional to the particle surface area, as a result monodispersed nanoparticle should dissolved faster than those characterized by agglomeration. Smaller particles have a larger surface area that could release ions faster hence, they provide greater dissolution than larger particles. This might explain the higher dissolution of cit-coated AgNPs immersed in low acidic pH gastric and phagolysosomal fluid and high ionic strength synthetic seawater. These results were consistent with those observed by [7]. [26] investigated dissolution and aggregation of silver nanoparticles in environmental

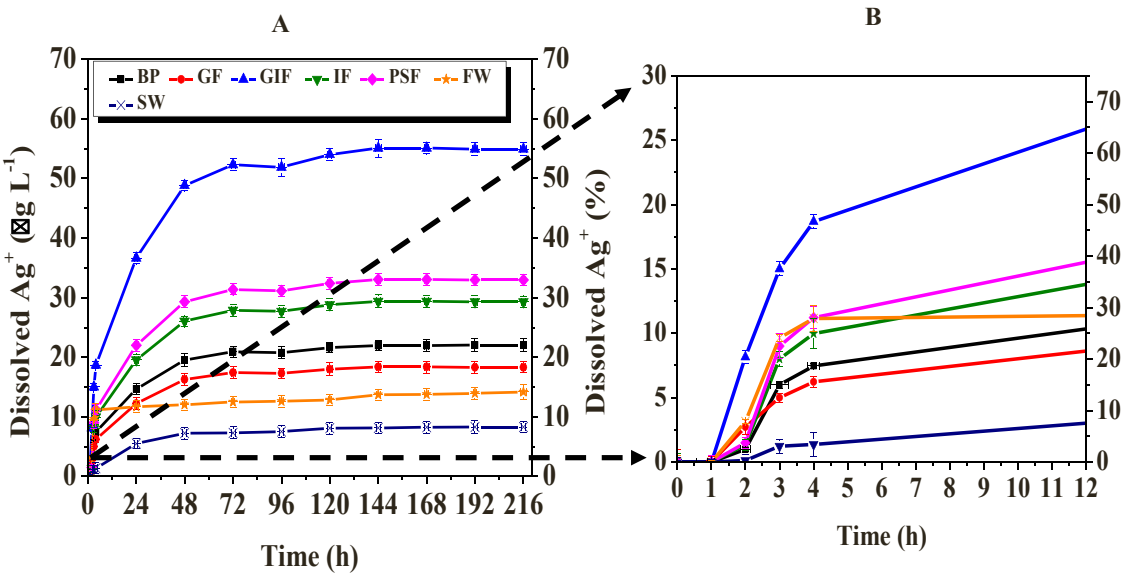

Fig. 4. Dissolution curves of silver ions released from the cit-coated AgNPs after exposure to simulated biological and environmental fluids over a period of 216 h (A). Simulated biological fluids are coded as BP, GF, GIF, IF and PSF for blood plasma, Gamble's fluid, gastric fluid, intestinal fluid and phagolysosomal fluid respectively. Whilst synthetic environmental media are denoted as FW and SW are or freshwater and seawater respectively. Dissolved Ag ions in % was calculated as $[Ag(I)]t/[AgNPs]_T \times 100\%$. Data only for the initial time point up to 12 h (B).

Table 2
Multiple variable ANOVA of the dissolution of citrate coated silver nanoparticles in simulated biological fluids and synthetic environmental media.

Nanoparticles	Simulated fluids	*p-value*
AgNPs	BP	0.0021
AgNPs	GF	0.0008
AgNPs	GIF	0.0144
AgNPs	IF	0.0420
AgNPs	PSF	0.0231
AgNPs	FW	0.0320
AgNPs	SW	0.0231

Table 3
Dissolution rates and half-time of AgNPs in simulated biological and environmental fluids.

Nanoparticles	Sample	k (h^{-1})	$t_{1/2}$ (days)
AgNPs	BP	6.39E-03	4
AgNPs	GF	5.80E-03	5
AgNPs	GIF	2.22E-02	1
AgNPs	IF	2.71E-03	11
AgNPs	PSF	1.68E-02	2
AgNPs	FW	1.02E-03	28
AgNPs	SW	1.09E-02	3

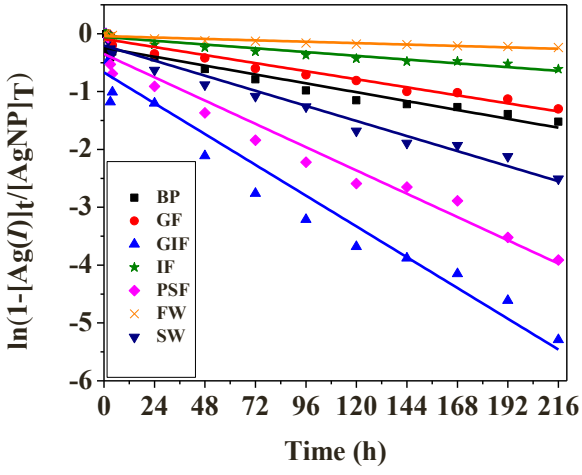

Fig. 5. Dissolution rates of cit-coated AgNPs in simulated biological and environmental fluids. Simulated biological fluids are coded as BP, GF, GIF, IF and PSF for blood plasma, Gamble's fluid, gastric fluid, intestinal fluid and phagolysosomal fluid respectively. Whilst synthetic environmental media are denoted as FW and SW are or freshwater and seawater respectively.

Table 4
Comparison of various nanoparticle dissolution kinetics in simulated fluids.

Nanoparticles	Conditions	k (h^{-1}) From literature	$t_{1/2}$ (days) From literature
Synthesised CuO 7 ± 1 nm	Simulated body fluid	0.644	
	Simulated body fluid	0.469	
Commercial CuO 31 ± 4 nm	pH7.4	[9]	
AgNPs 10 nm (Present study)	Blood plasma		4
	Gamble's fluid		5
	Gastric fluid		1
	Intestinal fluid		11
	Phagolysosomal fluid		2
	Freshwater		28
	Seawater		3
ZnO 63.6 nm	Wastewater effluents		0.12 (h^{-1})
	pH 7.5		[42]
Citrate coated AuNPs 14 nm	Simulated freshwater pH		853
	6.8		[31]
$BaSO_4$ NM-220 32 nm	Simulated phagolysosomal		6.8
	fluid pH 4.5		[18]

media and observed a positive correlation between high dissolution and low acidic pH conditions. Peretyazhko et al. [36] stated that when AgNPs are exposed to media, the formation of silver oxide on the nanoparticle surface initiates dissolution. This in turn releases silver Ag^+ ions into the solution until the silver oxide complex is completely dissolved. Furthermore, low acidic conditions such as gastric and phagolysosomal fluid have a higher abundance of protons which weaken the Ag-O bond resulting in the release of more Ag^+ ions. This might explain

the higher dissolution of cit-coated AgNPs immersed in low acidic pH gastric and phagolysosomal fluid.

Furthermore, the high dissolution of AgNPs in seawater could be due to the high concentration of chloride ions which characterise this synthetic environmental media. Chloride is a hard base ligand with a strong affinity for oxidized silver [24]. Therefore, Li et al. [25] and Li et al. [28] have indicated that the dissolution of AgNPs is highly influenced by the ratio between Ag/Cl in a solution. Meaning if a solution has a high concentration of free Cl^- ions as is the case with seawater, then chances are that the chloride ions will interact with Ag^+ ions forming more soluble complexes (AgCl) thereby encouraging dissolution. Owing to the high concentration of chloride ions in synthetic seawater, the formation of AgCl complexes is more pronounced. Therefore, the AgCl bridging between AgNPs might reduce AgNPs-AgNPs agglomeration leaving the particles monodispersed with a more exposed surface area thus increasing the chances of dissolution [10] corroborates these results. Furthermore, these results are consistent with previous research observation that have suggested that chloride ions might act as a catalyst in the dissolution of AgNPs [10].

It therefore seems that both low acidic solutions and higher ionic strength could result in lower particle agglomeration leading to higher dissolution of cit-coated AgNPs.

5 Conclusion

In this study the potential impact of AgNPs on human health and the environment were investigated through studying their dissolution. It could be shown that Cit-coated AgNPs form agglomerates when introduced to alkaline simulated fluids and this could reduce the surface area thereby lowering chances of dissolution. The rate and degree of the dissolution of cit-coated AgNPs is influenced by pH and ionic strength of simulated fluids. The dissolution rates of particles immersed in simulated gastric fluid, phagolysosomal fluid and seawater were faster compared to the rates of particles exposed to more alkaline biological and environmental media. Meaning that silver nanoparticles in acidic media and fluids characterized by high ionic strength would exhibit short-term effects which could be identical to those of the dissolved ions. However, the potential health and environmental impact of AgNPs in blood plasma, Gamble's & intestinal fluids and freshwater would be expected to be much worse.

CRediT authorship contribution statement

Odwa Mbanga: Conceptualization, Methodology, Validation, Formal analysis, Investigation, Writing – original draft. **Ewa Cukrowska**: Resources, Writing – review & editing, Visualization. **Mary Gulumian**: Resources, Writing – review & editing, Visualization, Supervision, Funding acquisition.

Declaration of Competing Interest

The authors declare that they have no known competing financial interests or personal relationships that could have appeared to influence the work reported in this paper.

Acknowledgements

This work was supported by funding from the European Union's Horizon 2020 research and innovation programme under grant agreement No 814401 (Gov4Nano). Furthermore, we would like to acknowledge the South African Department of Science and Innovation (DSI) and the National Institute for Occupational Health (NIOH) a division of National Health Laboratories, South Africa.

References

[1] Z. Adamczyk, M. Oćwieja, H. Mrowiec, S. Walas, D. Lupa, Oxidative dissolution of silver nanoparticles: A new theoretical approach, J. Colloid Interface Sci. 469 (2016) 355–364, https://doi.org/10.1016/j.jcis.2015.12.051.
[2] M.L. Avramescu, P.E. Rasmussen, M. Chénier, H.D. Gardner, Influence of pH, particle size and crystal form on dissolution behaviour of engineered nanomaterials, Environ. Sci. Pollut. Res. 24 (2) (2017) 1553–1564, https://doi.org/10.1007/s11356-016-7932-2.
[3] J.L. Axson, D.I. Stark, A.L. Bondy, S.S. Capracotta, A.D. Maynard, M.A. Philbert, A. P. Ault, Rapid kinetics of size and pH-dependent dissolution and aggregation of silver nanoparticles in simulated gastric fluid, J. Phys. Chem. C. 119 (35) (2015) 20632–20641, https://doi.org/10.1021/acs.jpcc.5b03634.
[4] A.M. Badawy, T.P. Luxton, R.G. Silva, K.G. Scheckel, M.T. Suidan, T.M. Tolaymat, Impact of environmental conditions (pH, ionic strength, and electrolyte type) on the surface charge and aggregation of silver nanoparticles suspensions, Environ. Sci. Technol. 44 (4) (2010) 1260–1266, https://doi.org/10.1021/es902240k.
[5] R. Behra, L. Sigg, M.J.D. Clift, F. Herzog, M. Minghetti, B. Johnston, B. Rothen-Rutishauser, Bioavailability of silver nanoparticles and ions: From a chemical and biochemical perspective, J. R. Soc. Interface 10 (87) (2013), 20130396, https://doi.org/10.1098/rsif.2013.0396.
[6] P. Bélteky, A. Rónavári, N. Igaz, B. Szerencsés, I.Y. Tóth, I. Pfeiffer, Z. Kónya, Silver nanoparticles: Aggregation behavior in biorelevant conditions and its impact on biological activity, Int. J. Nanomed. 14 (2019) 667–687, https://doi.org/10.2147/IJN.S185965.
[7] S.W. Bian, I.A. Mudunkotuwa, T. Rupasinghe, V.H. Grassian, Aggregation and dissolution of 4 nm ZnO nanoparticles in aqueous environments: Influence of pH, ionic strength, size, and adsorption of humic acid, Langmuir 27 (10) (2011) 6059–6068, https://doi.org/10.1021/la200570n.
[8] S. Chakraborty, S.K. Misra, A comparative analysis of dialysis based separation methods for assessing copper oxide nanoparticle solubility, Environ. Nanotechnol., Monit. Manag. 12 (October) (2019), 100258, https://doi.org/10.1016/j.enmm.2019.100258.
[9] S. Chakraborty, A. Nair, M. Paliwal, A. Dybowska, S.K. Misra, Exposure media a critical factor for controlling dissolution of CuO nanoparticles, J. Nanopart. Res. 20 (12) (2018) 1–14, https://doi.org/10.1007/s11051-018-4428-7.
[10] B.A. Chambers, A.N. Afrooz, S. Bae, N. Aich, L. Katz, N.B. Saleh, M.J. Kirisits, Effects of chloride and ionic strength on physical morphology, dissolution, and bacterial toxicity of silver nanoparticles, Environ. Sci. Technol. 48 (1) (2014) 761–769, https://doi.org/10.1021/es403969x.
[11] M. Chen, C.T. Jafvert, Anion recovery from water by cross-linked cationic surfactant nanoparticles across dialysis membranes, Environ. Sci.: Nano 5 (6) (2018) 1350–1360, https://doi.org/10.1039/c8en00281a.
[13] I. Fernando, Y. Zhou, Impact of pH on the stability, dissolution and aggregation kinetics of silver nanoparticles, Chemosphere 216 (2019) 297–305, https://doi.org/10.1016/j.chemosphere.2018.10.122.
[14] M.S. Frost, M.J. Dempsey, D.E. Whitehead, The response of citrate functionalised gold and silver nanoparticles to the addition of heavy metal ions, Colloids Surf. A: Physicochem. Eng. Asp. 518 (2017) 15–24, https://doi.org/10.1016/j.colsurfa.2016.12.036.
[15] J.M. Gorham, R.I. MacCuspie, K.L. Klein, D.H. Fairbrother, D. Holbrook, UV-induced photochemical transformations of citrate-capped silver nanoparticle suspensions, J. Nanopart. Res. 14 (10) (2012) 1–16, https://doi.org/10.1007/s11051-012-1139-3.
[16] I.L. Gunsolus, M.P.S. Mousavi, K. Hussein, P. Bühlmann, C.L. Haynes, Effects of humic and fulvic acids on silver nanoparticle stability, dissolution, and toxicity, Environ. Sci. Technol. 49 (13) (2015) 8078–8086, https://doi.org/10.1021/acs.est.5b01496.
[17] C.M. Ho, S.K.W. Yau, C.N. Lok, M.H. So, C.M. Che, Oxidative dissolution of silver nanoparticles by biologically relevant oxidants: A kinetic and mechanistic study, Chem. - Asian J. 5 (2) (2010) 285–293, https://doi.org/10.1002/asia.200900387.
[18] J.G. Keller, U.M. Graham, J. Koltermann-Jülly, R. Gelein, L. Ma-Hock, R. Landsiedel, W. Wohlleben, Predicting dissolution and transformation of inhaled nanoparticles in the lung using abiotic flow cells: The case of barium sulfate, Sci. Rep. 10 (1) (2020) 1–15, https://doi.org/10.1038/s41598-019-56872-3.
[19] B.R. Khalkho, R. Kurrey, M.K. Deb, I. Karbhal, B. Sahu, S. Sinha, V.K. Jain, A simple and convenient dry-state SEIRS method for glutathione detection based on citrate functionalized silver nanoparticles in human biological fluids, New J. Chem. 45 (3) (2021) 1339–1354, https://doi.org/10.1039/d0nj04065g.
[20] S. Kittler, C. Greulich, J. Diendorf, M. Koller, M. Epple, Toxicity of silver nanoparticles increases during storage because of slow dissolution under release of silver ions, Chem. Mater. 22 (16) (2010) 4548–4554, https://doi.org/10.1021/cm100023p.
[21] S. Kittler, C. Greulich, J. Diendorf, M. Köller, M. Epple, Toxicity of silver nanoparticles increases during storage because of slow dissolution under release of silver ions, Chem. Mater. 22 (16) (2010) 4548–4554, https://doi.org/10.1021/cm100023p.
[22] R. Kurrey, M.K. Deb, K. Shrivas, B.R. Khalkho, J. Nirmalkar, D. Sinha, S. Jha, Citrate-capped gold nanoparticles as a sensing probe for determination of cetyltrimethylammonium surfactant using FTIR spectroscopy and colorimetry, Anal. Bioanal. Chem. 411 (26) (2019) 6943–6957, https://doi.org/10.1007/s00216-019-02067-8.
[23] P. Laux, C. Riebeling, A.M. Booth, J.D. Brain, J. Brunner, C. Cerrillo, H. Jungnickel, NanoImpact Biokinetics of nanomaterials: The role of biopersistence, NanoImpact 6 (2017) 69–80, https://doi.org/10.1016/j.impact.2017.03.003.

[24] C. Levard, S. Mitra, T. Yang, A.D. Jew, A.R. Badireddy, G.V. Lowry, G.E. Brown, Effect of chloride on the dissolution rate of silver nanoparticles and toxicity to E. coli, Environ. Sci. Technol. 47 (11) (2013) 5738–5745, https://doi.org/10.1021/es400396f.
[25] P. Li, M. Su, X. Wang, X. Zou, X. Sun, J. Shi, H. Zhang, Environmental fate and behavior of silver nanoparticles in natural estuarine systems, J. Environ. Sci. (China) 88 (2020) 248–259, https://doi.org/10.1016/j.jes.2019.09.013.
[26] X. Li, J.J. Lenhart, Aggregation and dissolution of silver nanoparticles in natural surface water, Environ. Sci. Technol. 46 (10) (2012) 5378–5386, https://doi.org/10.1021/es204531y.
[27] X. Li, J.J. Lenhart, H.W. Walker, Aggregation kinetics and dissolution of coated silver nanoparticles, Langmuir 28 (2) (2012) 1095–1104, https://doi.org/10.1021/la202328n.
[28] Y. Li, J. Zhao, E. Shang, X. Xia, J. Niu, J. Crittenden, Effects of chloride ions on dissolution, ROS generation, and toxicity of silver nanoparticles under UV irradiation, Environ. Sci. Technol. 52 (8) (2018) 4842–4849, https://doi.org/10.1021/acs.est.7b04547.
[29] K. Loza, J. Diendorf, C. Sengstock, L. Ruiz-Gonzalez, J.M. Gonzalez-Calbet, M. Vallet-Regi, M. Epple, The dissolution and biological effects of silver nanoparticles in biological media, J. Mater. Chem. B 2 (12) (2014) 1634–1643, https://doi.org/10.1039/c3tb21569e.
[30] M.R. Marques, R. Loebenberg, M. Almukainzi, Simulated biological fluids with possible application in dissolution testing, Dissolution Technol. 18 (3) (2011) 15–28, https://doi.org/10.14227/DT180311P15.
[31] O. Mbanga, E. Cukrowska, M. Gulumian, Dissolution of citrate-stabilized, polyethylene glycol–coated carboxyl and amine-functionalized gold nanoparticles in simulated biological fluids and environmental media, J. Nanopart. Res. 23 (1) (2021) 1–16, https://doi.org/10.1007/s11051-020-05132-x.
[32] S.K. Misra, S. Nuseibeh, A. Dybowska, D. Berhanu, T.D. Tetley, E. Valsami-Jones, Comparative study using spheres, rods and spindle-shaped nanoplatelets on dispersion stability, dissolution and toxicity of CuO nanomaterials, Nanotoxicology 8 (4) (2014) 422–432, https://doi.org/10.3109/17435390.2013.796017.
[33] M.R. Mulenos, J. Liu, H. Lujan, B. Guo, E. Lichtfouse, V.K. Sharma, C.M. Sayes, Copper, silver, and titania nanoparticles do not release ions under anoxic conditions and release only minute ion levels under oxic conditions in water: Evidence for the low toxicity of nanoparticles, Environ. Chem. Lett. 18 (4) (2020) 1319–1328, https://doi.org/10.1007/s10311-020-00985-z.
[34] T. Oyabu, T. Myojo, B.W. Lee, T. Okada, H. Izumi, Y. Yoshiura, M. Kubo, Biopersistence of NiO and TiO2 nanoparticles following intratracheal instillation and inhalation, Int. J. Mol. Sci. 18 (12) (2017) 2757, https://doi.org/10.3390/ijms18122757.
[35] P. Pallavicini, L. Preti, L.De Vita, G. Dacarro, Y.A. Diaz Fernandez, D. Merli, B. Vigani, Fast dissolution of silver nanoparticles at physiological pH, J. Colloid Interface Sci. 563 (2020) 177–188, https://doi.org/10.1016/j.jcis.2019.12.081.
[36] T.S. Peretyazhko, Q. Zhang, V.L. Colvin, Size-controlled dissolution of silver nanoparticles at neutral and acidic pH conditions: Kinetics and size changes, Environ. Sci. Technol. 48 (20) (2014) 11954–11961, https://doi.org/10.1021/es5023202.
[37] L. Pinďáková, V. Kašpárková, K. Kejlová, M. Dvořáková, D. Krsek, D. Jírová, L. Kašparová, Behaviour of silver nanoparticles in simulated saliva and gastrointestinal fluids, Int. J. Pharm. 527 (1–2) (2017) 12–20, https://doi.org/10.1016/j.ijpharm.2017.05.026.
[38] M. Probst, M. Schmidt, K. Tietz, S. Klein, W. Weitschies, A. Seidlitz, In vitro dissolution testing of parenteral aqueous solutions and oily suspensions of paracetamol and prednisolone, Int. J. Pharm. 532 (1) (2017) 519–527, https://doi.org/10.1016/j.ijpharm.2017.09.052.
[39] V.K. Sharma, K.M. Siskova, R. Zboril, J.L. Gardea-Torresdey, Organic-coated silver nanoparticles in biological and environmental conditions: Fate, stability and toxicity, Adv. Colloid Interface Sci. 204 (2014) 15–34, https://doi.org/10.1016/j.cis.2013.12.002.
[40] M. Tejamaya, I. Römer, R.C. Merrifield, J.R. Lead, Stability of citrate, PVP, and PEG coated silver nanoparticles in ecotoxicology media, Environ. Sci. Technol. 46 (13) (2012) 7011–7017, https://doi.org/10.1021/es2038596.
[41] W. Utembe, K. Potgieter, A.B. Stefaniak, M. Gulumian, Dissolution and biodurability: Important parameters needed for risk assessment of nanomaterials, Part. Fibre Toxicol. 12 (1) (2015) 11, https://doi.org/10.1186/s12989-015-0088-2.
[42] N. Wang, T. Tong, M. Xie, J.F. Gaillard, Lifetime and dissolution kinetics of zinc oxide nanoparticles in aqueous media, Nanotechnology 27 (32) (2016), 324001, https://doi.org/10.1088/0957-4484/27/32/324001.
[43] P. Wulandari, T. Nagahiro, N. Fukada, Y. Kimura, M. Niwano, K. Tamada, Characterization of citrates on gold and silver nanoparticles, J. Colloid Interface Sci. 438 (2015) 244–248, https://doi.org/10.1016/j.jcis.2014.09.078.
[44] X. Yang, A.P. Gondikas, S.M. Marinakos, M. Auffan, J. Liu, H. Hsu-Kim, J.N. Meyer, Mechanism of silver nanoparticle toxicity is dependent on dissolved silver and surface coating in Caenorhabditis elegans, Environ. Sci. Technol. 46 (2) (2012) 1119–1127, https://doi.org/10.1021/es202417t.
[45] J.M. Zook, S.E. Long, D. Cleveland, C.L.A. Geronimo, R.I. MacCuspie, Measuring silver nanoparticle dissolution in complex biological and environmental matrices using UV–visible absorbance, Anal. Bioanal. Chem. 401 (6) (2011) 1993–2002, https://doi.org/10.1007/s00216-011-5266-y.

4.3 Paper 3

This third article entitled “Dissolution of titanium dioxide nanoparticles in synthetic biological and environmental media to predict their biodurability and persistence” has been published in Toxicology in Vitro. In this research article we investigated the biodurability and persistence of titanium dioxide nanoparticles (TiO_2 NPs) in simulated biological and environmental media because these parameters influence the particles’ impact on human health and the environment.

Toxicology in Vitro (2022)
https://doi.org/10.1016/j.tiv.2022.105457

Odwa Mbanga- Principal author

Ewa Cukrowska- Supervisor

Mary Gulumian- Supervisor

Toxicology in Vitro 84 (2022) 105457

Contents lists available at ScienceDirect

Toxicology in Vitro

journal homepage: www.elsevier.com/locate/toxinvit

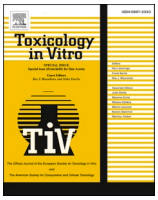

Dissolution of titanium dioxide nanoparticles in synthetic biological and environmental media to predict their biodurability and persistence

Odwa Mbanga [a,b], Ewa Cukrowska [a], Mary Gulumian [b,c,*]

[a] Molecular Sciences Institute, School of Chemistry, University of Witwatersrand, Private Bag X3, Johannesburg 2050, South Africa
[b] Toxicology and Biochemistry Department, National Institute for Occupational Health, A Division of National Health Laboratories, Johannesburg, South Africa
[c] Water Research Group, Unit for Environmental Sciences and Management, Northwest University, Private Bag X6001, Potchefstroom 2520, South Africa

ARTICLE INFO

Editor: Dr. J Davila

Keywords:
Titanium dioxide nanoparticles
Biodurability
Persistence
Dissolution
Dissolution kinetics
Simulated fluids

ABSTRACT

Investigating the biodurability and persistence of titanium dioxide nanoparticles (TiO_2 NPs) is of paramount importance because these parameters influence the particles' impact on human health and the environment. Contrary to most research conducted so far, the present study elucidates the dissolution kinetics, namely the dissolution rates, rate constants, order of reaction and half-times of TiO_2 NPs in five different simulated biological fluids and two synthetic environmental media to predict their behaviour in real life situations. Results have shown that the dissolution of TiO_2 NPs in all simulated fluids was limited. Of all the simulated biological media tested, acidic media such as phagolysosomal and gastric fluid produced the highest dissolution of TiO_2 NPs compared to alkaline media such as blood plasma, Gamble's fluid, and intestinal fluid. Furthermore, when the particles were exposed to simulated environmental conditions, the dissolution was higher in high ionic strength seawater compared to freshwater. The dissolution kinetics of titanium dioxide nanoparticles followed first order reaction kinetics and were generally characterized by low dissolution rates and long half-times. These findings indicate that TiO_2 NPs are very insoluble and will remain unchanged in the body and environment over long periods of time. Therefore, these particles are most likely to cause both short and long-term health effects and will remain persistent following release into the environment.

1. Introduction

Titanium dioxide nanoparticles (TiO_2 NPs) have a wide range of innovative application due to their physicochemical properties. They have the ability to filter UV radiation, have antimicrobial properties, and are excellent inhibitors of corrosion (Musial et al., 2020; Nia et al., 2015; Shi et al., 2013; Syngouna et al., 2022). As a result, they are incorporated in a wide variety of commercial products including preservatives, colourants, paint coatings, sunscreen, solar-cells and photo-catalysts (Freyre-Fonseca et al., 2016; Hulla et al., 2015; Kao and Cheng, 2020; Yu et al., 2017). Additionally, TiO_2 NPs can be used as an adsorbent for the removal of organic compounds from wastewater (Stefanarou and Chrysikopoulos, 2021; Syngouna and Chrysikopoulos, 2017, 2019). As the use of TiO_2 NPs increases exponentially so does their potential to be released into the environment and cause adverse health effects to humans and the environment.

Biopersistence is defined as the extent to which nanomaterials are able to resist chemical, physical, and other physiological clearance mechanisms in the body and therefore is considered to be one of the main contributors to their toxicity and hence pathogenicity. Biodurability, defined as the ability of nanomaterials to resist chemical/biochemical alteration, is a significant contributor to biopersistence. Dissolution, defined as release of molecules and/or ions of nanomaterials, is used as a measure of their biodurability and therefore the determination of dissolution rates has provided an insight on how nanomaterials may interact with different biological and environmental surroundings. Subsequently, if nanomaterials release ions at a fast rate, their short-term toxic effect could be identical to those of the dissolved ions. On the other hand, if they release ions at a slow rate, there is a greater likelihood that they will be the cause of the observed adverse effects (Utembe et al., 2015). The application of nanoparticles is most likely to involve the particle being in contact with biological and environmental media and therefore, it is of utmost importance to elucidate the dissolution of TiO_2 NPs in these different media to investigate their

* Corresponding author at: Water Research Group, Unit for Environmental Sciences and Management, Northwest University, Private Bag X6001, Potchefstroom 2520, South Africa.
E-mail addresses: odwa.mbanga@students.wits.ac.za (O. Mbanga), ewa.cukrowska@wits.ac.za (E. Cukrowska), Mary.Gulumian@NWU.ac.za (M. Gulumian).

https://doi.org/10.1016/j.tiv.2022.105457
Received 24 May 2022; Received in revised form 11 August 2022; Accepted 13 August 2022
Available online 18 August 2022

dissolution kinetics to predict their behaviour in real-life conditions.

Generally, TiO_2 NPs are considered chemically stable and undergo negligible dissolution under usual biological and environmental media (Nam et al., 2012; Shinohara et al., 2017). Even though these particles are thought of as stable, there is sizable research that has been conducted which elucidates titanium dioxide nanoparticle dissolution in media (Schmidt and Vogelsberger, 2006, 2009; Shkol'nikov, 2016; Wang et al., 2014). Several factors have been identified which affect TiO_2 NP dissolution. These factors include the pH, chemical composition and ionic strength of simulated fluids, particle size and crystal form of the nanoparticles (Nia et al., 2015). For example, Avramescu et al. (2017) investigated how the effects of the pH of physiological fluids, particle size and crystal form of titanium dioxide nanoparticles affects their solubility. It was observed that when the particles were exposed to media characterized by low pH conditions the higher the chances of particle solubility. Furthermore, the crystalline form in which TiO_2 NPs existed in was also found to influence solubility where nano-anatase was observed to be more soluble than nano-rutile (Shkol'nikov, 2016). Similar to crystalline form, it was also shown by other investigators that particle size influences the solubility of TiO_2 NPs, and it has been concluded that those smaller in magnitude have a significantly higher solubility than larger particles (Murugadoss et al., 2020). As the formation of aggregates increase the size of TiO_2 NPs it is expected that it will decrease the exposed surface area thereby inhibiting dissolution (Zhong et al., 2017). The chemical composition of simulated fluids has the potential to influence nanoparticle dissolution and thereby the salts containing charged ions interact with the nanoparticle surface thereby promoting or inhibiting dissolution (Larue et al., 2011; Tsai et al., 2016).

Due to the incorporation of these nanoparticles in consumer products their production may lead to their release in the environment. As a result, a study was conducted to assess their accumulation and impact on plants. It was found that TiO_2 NPs do not significantly alter plant germination and root elongation (Larue et al., 2011). Studies have also shown the importance of particle agglomeration in aquatic toxicity testing. For example. It was observed that TiO_2 NPs exposed to aquatic media reach a point of zero charge under neutral pH conditions and become stable thereby increasing the chances of posing toxicity threats to aquatic organisms (Cupi et al., 2016). Yang et al. (2013) investigated the environmental fate and bioavailability of TiO_2 NPs in aquatic invertebrates and the influence of dissolved organic matter. It was concluded that the stability of TiO_2 NPs can be altered by adsorption of dissolved organic matter (Zhong et al., 2017).

Although there has been extensive research on the dissolution of titanium dioxide nanoparticles in simulated media, most studies ignored the importance of determining their dissolution rates, dissolution rate constants, determine their half-times or elucidate the order of reaction. Knowledge of these parameters will assist in assessing their biodurability in different biological and environmental media which in turn will contribute in their biopersistence in these media. In this work we elucidate the dissolution kinetics of titanium dioxide nanoparticles in a wide pH range of simulated physiological fluids and synthetic environment to predict their biodurability in real life situations.

2. Materials and method

2.1. Characterization of TiO_2 NP powder

A unit of standard reference material (SRM) 1898 was purchased from the National Institute of Standards and Technology (NIST). The initial stock suspensions nanoparticles of were prepared from this dry agglomerated powder SRM under sterile conditions. Morphological alterations of the nanoparticles were monitored using the Transmission Electron microscope (TEM) (JOEL Ltd. JEM-2100) (Lireweg, The Netherlands. Nanoparticle suspensions were deposited onto TEM grid (200 mesh size Cu-grid) coated with a lacey carbon film. The images of the nanoparticles were verified using a digital charge coupled device (CCD) camera connected to the TEM. The PANayltical X'Pert Pro powder diffractometer instrument was used to determine the crystalline structure of TiO_2 NPs and to confirm whether they existed in the anatase or rutile crystal phase. This instrument was fitted with 1D X'Celerator detector, 10 mm programmable divergence slit and sample spinner (Spinner PW3064) with a rotation time of 1 s. The X-ray radiation source was Cu Kα ($\lambda = 0.15405$ nm) tube, operating at 40 kV and 40 mA conditions. The measurement was carried out under Gonio scan axis with continuous scan type, step size, scan step time and 2θ range of 0.0170^0, 2θ, 87 s and (5 to 90^0), respectively. The P-XRD sample was transferred onto the low background silicon sample holder. After the X-ray measurements, raw data was interpreted by using High Score (Plus) software with ICDD PDF-4^+ 2019 database. The particles were further characterized by the Varian Ultraviolet-Visible 50 Conc. spectrophotometer (UV–vis) (Agilent Technologies, California, United States). The concentration of dissolved Ti ions was obtained using inductively coupled mass spectrometer (ICP-MS) (Agilent Technologies, 7700 series ICP-MS, Santa Clara, California, United States).

2.2. Experimental procedure

Composition of body fluids and environmental media.

Nanoparticles can enter the human body via various routes, but the focus of this present research study was inhalation, ingestion, intravenous and environmental exposure through waste disposal. Therefore, simulated phagolysosomal fluid (PSF) and Gamble's fluid (GF) were chosen to represent lung fluids found in cellular lysosomes and deep within the lungs at pH 4.5 & pH 7.4, respectively. Whereas gastric fluid (GIF) and intestinal fluid (IF) were representative of stomach fluids at pH 2.0 and pH 7.5 respectively. Lastly, blood plasma (BP) at pH 7.2 which is a fluid that carries blood components throughout the body. The synthetic environmental media of choice were freshwater (FW) and seawater (SW). The preparation of all the simulated fluids was adopted from the procedure presented by Marques et al. (2011) using the reagents listed in Table 1. Synthetic environmental media were prepared following the procedure recommended by the United States (U·S) Environmental Protection Agency (EPA). These reagents were dissolved in 700 mL of d-H_2O in the order given in Table 1, and the pH was adjusted with either 1 M hydrochloric acid or 1 M Sodium hydroxide. The final volume was then adjusted to 1 L with d-H_2O. A 51 μL alkylbenzyldimethylammonium chloride (ABDC) the anti-fungal agent was added to each beaker to preserve the simulated biological fluids and synthetic environmental media.

2.3. Dissolution tests

In vitro acellular tests were used to assess the dissolution of TiO_2 NPs in simulated biological fluids and environmental media. The simulated fluids were prepared in a simplified way such that the influence of certain biological compounds like organic chelators, enzymes, proteins and organic matter was eliminated. A 1 mg TiO_2 NP powder was weighed and transferred into centrifuge tubes each containing 5 ml of simulated biological fluids and environmental media to make nanoparticle suspensions. The murky white nanoparticle suspensions were sonicated at room temperature for 15 min to re-disperse the particles. The stock suspensions were then transferred into decontaminated dialysis membranes (SnakeSkin Dialysis tubing, 3.5 K MWCO, 22 mm-dry diameter) sealed and submerged in beakers filled with 500 mL simulated biological fluids and synthetic environmental media. A dialysis membrane with a significantly smaller pore size was chosen such that titanium in the particle form typically will be fully retained in the dialysis membrane, and species such as charged ions from the nanoparticle surface will dialyze out of the tubing. The beakers were kept in water baths maintained at physiological temperature (37 °C) while synthetic environmental media were kept at 25 °C. Furthermore, the experiments were kept under a closed system in an airtight vessel to eliminate

Table 1
Components and extrinsic properties of simulated biological fluids and synthetic environmental media.

Simulated fluid	Ionic strength (mol L^{-1})	pH	Chemical composition (g L^{-1})
Blood plasma	0.15	7.2	Sodium chloride (NaCl) (8.035), Sodium hydrogen carbonate ($NaHCO_3$) (0.355), Potassium chloride (KCl) (0.225), Potassium phosphate dibasic trihydrate ($K_2HPO_4.3H_2O$) (0.231), Magnesium chloride hexahydrate ($MgCl_2 \cdot 6H_2O$) (0.331), 1 M HCl (39 ml), Calcium chloride ($CaCl_2$) (0.292), Sodium sulphate (Na_2SO_4) (0.072), Tris(hydroxymethyl) aminomethane ($NH_2C(CH_2OH)_3$) (6.118)
Gamble's fluid	0.17	7.4	Magnsium chloride ($MgCl_2$) (0.203), Sodium chloride (NaCl) (6.019), Potassium chloride (KCl) (0.298), Sodium hydrogen phosphate (Na_2HPO_4) (0.142), Sodium sulphate anhydrous (Na_2SO_4) (0.017), Calcium chloride dihydrate ($CaCl_2.2H_2O$) (0.368), Sodium acetate (CH_3COONa) (0.953), Sodium hydrogen carbonate ($NaHCO_3$) (2.604), Trisodium citrate dihydrate ($C_6H_9Na_3O_9$) (0.097)
Gastric fluid	0.16	2.0	Sodium chloride (NaCl) (2.922), Potassium chloride (KCl) (7.007), Potassium hydrogen phthalate ($C_8H_5O_4K$) (0.243), Pepsin (1 ml mL^{-1}), Mucin (3 mg mL^{-1})
Intestinal fluid	0.16	6.8	Potassium chloride (KCl) (0.298), Calcium chloride ($CaCl_2$) (0.499), Magnesium chloride ($MgCl_2$) (0.190), Urea (0.300), Bile salts (9 ml mL^{-1}), Pancreatin (9 mg mL^{-1})
Phagolysosomal fluid	0.34	4.5	Sodium hydrogen phosphate (Na_2HPO_4) (0.142), Sodium chloride (NaCl) (6.650), Sodium sulphate (Na_2SO_4) (0.072), Calcium chloride dihydrate ($CaCl_2.2H_2O$) (0.029), Glycine (0.450), Potassium hydrogen phthalate ($C_8H_5O_4K$) (4.086)
Freshwater	0.05	6.8	Sodium hydrogen carbonate ($NaHCO_3$) (0.012), Calcium sulphate anhydrous ($CaSO_4$) (0.075), Magnesium sulphate anhydrous ($MgSO_4$) (0.0075), Potassium chloride (KCl) (0.0005)
Seawater	3.5	8.0	Sodium chloride (NaCl) (21.03), Sodium sulphate (Na_2SO_4) (3.52), Potassium chloride (KCl) (0.61), Potassium bromide (KBr) (0.088), Borax (0.034), Magnesium chloride ($MgCl_2$) (9.50), Calcium chloride anhydrous ($CaCl_2$) (1.320), Strontium chloride ($SrCl_2$) (0.02), Sodium hydrogen carbonate ($NaHCO_3$) (0.17)

background interreferences. The simulated fluids were stirred using magnetic stirrers and experiments were conducted in the dark over a period of 10 days. Samples were collected from the bulk fluid outside the dialysis membrane in 30 min intervals for the first 4 h and twice a day for the next 10 days. Throughout the duration of the dissolution experiments, the pH of simulated fluids was monitored and maintained using a Jenway 3510 pH meter. Samples were collected in triplicates and analysed on ICP-MS with a limit of detection of 0.1 ppb to determine the concentration of dissolved Ti ions. Reported in the results section is an average of the three measurements.

2.4. Kinetic model for dissolution process

Nanoparticle biodurability and persistence can be predicted by calculating the nanoparticle dissolution rate including half-time. In general, the dissolution of most nanoparticles follows the first order reaction kinetics as predicted by the Noyes-Whitney equation. In this present research study, the Noyes-Whitney equation was modified into eq. 1 to determine the dissolution rate and half-time of TiO_2 NPs exposed to simulated body fluids and synthetic environmental media in order to predict their biodurability and persistence (Wang et al., 2016).

$$\frac{d[Ti0_2NPs]}{dt} = -D\frac{A}{d}\left([Ti]_T - [Ti]_{dis}\right) \quad (1)$$

where $[TiO_2\ NPs]$, $[Ti]_T$ and $[Ti]_{dis}$ represent the initial concentration of the titanium dioxide nanoparticle suspension, the concentration of titanium ions during the dissolution process and lastly the amount of dissolved titanium ions at the end of the dissolution experiments, respectively.

A denotes the surface area of TiO_2NPs powder, D is the diffusion coefficient of titanium ions, and d is the diffusion layer thickness.

The total mass balance of titanium ions in the system is represented by eq. 2.

$$[Ti]_T = [TiO_2\ NPs] + [Ti]_{dis} \quad (2)$$

The $[TiO_2NPs]$ then substituted by eq. 3 in the formula:

$$[TiO_2NPs] = [Ti]_T - [Ti]_{dis} \quad (3)$$

However, $[Ti]_T - [Ti]_{dis}$ can be re-written in the following form represented by eq. 4:

$$[Ti]_T - [Ti]_{dis} = [Ti]_T\left(1 - \frac{[Ti]_{dis}}{[Ti]_T}\right) \quad (4)$$

$$\text{So that } [TiO_2NPs] = [Ti]_T\left(1 - \frac{[Ti]_{dis}}{[Ti]_T}\right) \quad (5)$$

If we substitute eqs. 5 into eq. 1 we obtain the following eq. 6:

$$[Ti]_T\frac{d\left(1 - \frac{[Ti]_{dis}}{[Ti]_T}\right)}{dt} = -D\frac{A}{d}[Ti]_T\left(1 - \frac{[Ti]_{dis}}{[Ti]_T}\right) \quad (6)$$

Upon dividing by $[Ti]_T$on both sides of the equation, eq. 6 is transformed into eq. 7:

$$\frac{d\left(1 - \frac{[Ti]_{dis}}{[Ti]_T}\right)}{dt} = -D\frac{A}{d}\left(1 - \frac{[Ti]_{dis}}{[Ti]_T}\right) \quad (7)$$

If we let $\left(1 - \frac{[Ti]_{dis}}{[Ti]_T}\right) = x$.

Then eq. 7 becomes:

$$\frac{dx}{dt} = -D\frac{A}{d}x \quad (8)$$

To re-arrange the variables and bring x and dt to the left hand-side & right hand-side of the equation respectively, the above equation is divided by x and multiplied by dt on both sides of the equation:

$$\frac{dx}{x} = -D\frac{A}{d}dt \tag{9}$$

Upon integration, the above equation becomes:

$$lnx = c - D\frac{A}{d}t \tag{10}$$

where $k = -D\frac{A}{d}$ and c is a constant and therefore, k is the slope representative of the dissolution rate constant.

Ultimately the integration of Eq. 7 yields Eq. 11

$$ln\left(1 - \frac{[Ag]_{dis}}{[Ag]_T}\right) = c - kt \tag{11}$$

By plotting $\ln\left(1 - \frac{[Ti]_{dis}}{[Ti]_T}\right)$ vs time we are able to calculate the dissolution kinetics of titanium dioxide nanoparticles and predict how long they would remain unchanged in the body and the environment.

Consequently, dissolution predicted by this kinetic model follows first order reaction kinetics and half-time of a first order reaction can be obtained by the following equation:

$$t_{½} = \frac{ln2}{k} \tag{12}$$

2.5. Statistical analysis

The dissolution data are expressed as mean ± standard deviation of at least three independent measurements. A multiple variable ANOVA analysis using RStudio version 1.2 software was performed to determine significant differences between the dissolution behaviour of TiO_2 NPs in various simulated body fluids and synthetic environmental media. Statistical significance was accepted at $P < 0.05$.

3. Results

3.1. Characterization

3.1.1. TEM

The TiO_2 NPs were characterized by using TEM, UV–vis and XRD to monitor their dissolution behaviour in simulated body and environmental fluids and link their changes to physicochemical properties. Fig. 1 shows size distribution curves and TEM images of TiO_2 NPs immediately after having been suspended in simulated biological fluids and synthetic environmental media (marked as before) and after the end of the 10-day dissolution experiments.

The particles size diameter was analysed using image J software (National Institute of Health, version no Java1.8.0_172) by measuring individual particles. Despite the differences in pH and chemical

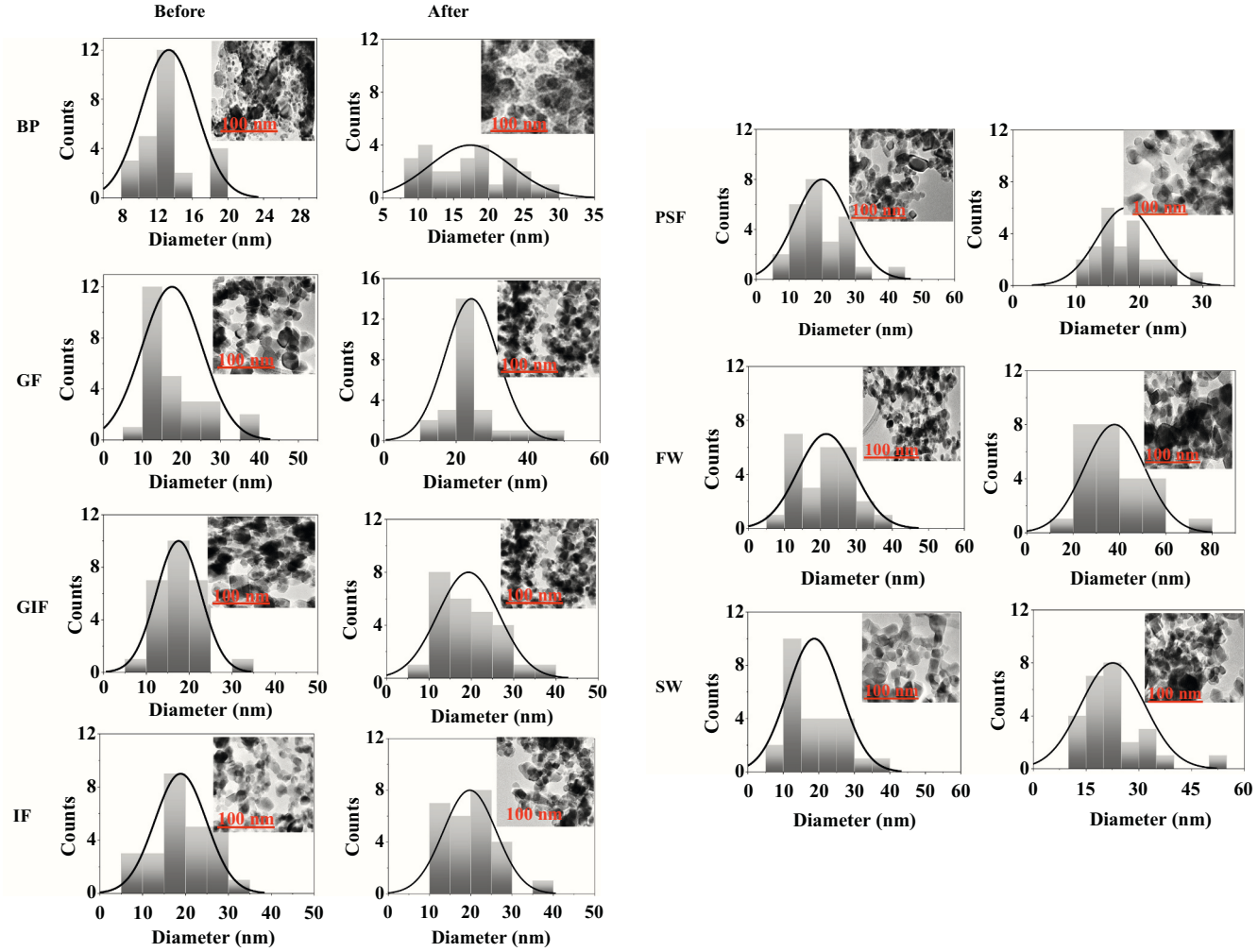

Fig. 1. Size distribution curves and TEM images of TiO_2 NPs in simulated body fluids and environmental media before and after dissolution experiments. Simulated biological fluids are BP- Blood plasma, GF- Gamble's fluid, GIF-Gastric fluid, IF- Intestinal fluid & PSF- Phagolysosomal fluid. Synthetic environmental media are FW- Freshwater and SW- Seawater.

composition of all the simulated biological and environmental media, there was an observable particle aggregation in all fluids with the surface area changing to larger particles after the dissolution experiments as indicated by the size distribution curves and TEM images presented in Fig. 1. During aggregation, particles form a union of nanoparticles through weak van der Waals forces thereby reducing the surface area. All particles showed marked increase in surface area which was more pronounced after the end of the 10-day experiments. It appears that the media composition promotes interactions on the nanoparticle surface thereby encouraging formation of aggregates (Taurozzi et al., 2013). These data indicate that particles will change surface area regardless of the chemical composition and pH of the surrounding media. Particles were partly irregular and semi spherical in shape. There were no observable changes in morphology before and after dissolution experiments. These results were comparable to those observed by other studies Anandgaonker et al. (2019); Korábková et al. (2021); Zhong et al. (2017).

3.1.2. UV–vis

The UV–vis absorption spectra of TiO_2 NPs suspended in simulated biological fluids and synthetic environmental media before and after dissolution experiments are shown in Fig. 2. The surface plasmon resonance of titanium dioxide nanoparticles is usually centred around 300 nm as can be seen in Fig. 2. However, there was a shift to higher wavelengths (320 nm) after exposure to simulated fluids indicative of particle aggregation as the time of exposure to simulated fluids increased. During aggregation smaller particles come together to form a union of nanoparticles with weak van der Waals forces. The number of plasmons as a result of contact decreases, because the specific surface of nanoparticles in the aggregate decreases. This explains the drop in absorption intensity after the particles were in contact with simulated physiological fluids and synthetic environmental media. These results were in agreement with those observed by researchers such as Zhong et al. (2017) whereby metal oxides nanoparticles showed high degrees of aggregation as soon as they were in contact with simulated physiological media. This increase in absorbance intensity at longer wavelengths also has been reported by other studies and has been attributed to the formation of larger NPs through either particle aggregation (De Matteis et al., 2016; H. Wang et al., 2014). Studies have shown that larger particles scatter ultra-violet light at longer wavelengths compared to smaller particles (De Matteis et al., 2016). These results are in strong agreement with the TEM images in Fig. 1 which show nanoparticle aggregation. The NP suspension did not change colour after dissolution experiments, it remained murky white before and after exposure to simulated fluids. There were no observable changes in absorption intensity for all fluids.

3.1.3. XRD

The powder was characterized to determine the crystal phase in which TiO_2 NPs existed in, whether it was rutile or anatase or a mixture of both. The XRD pattern of the TiO_2 nanoparticles is shown in Fig. 3 together with the peak positions at 2θ and their corresponding Miller indices. Research has shown anatase to be more toxic than rutile therefore, in this present research study it was crucial to determine the crystal phase of TiO_2 nanoparticle powder (Endo et al., 1986).

The TiO_2 XRD data demonstrated very sharp peaks. The strong diffraction peaks exhibited by the XRD pattern at angles 25°, 37°, 47°, 55°, 62°, 68°, 70°, 75° and 82° correspond to Miller indices of (101), (004), (200), (211), (204), (116), (220), (215) and (224) plane respectively. The major component of the TiO_2 NPs sample was confirmed to be anatase. However, there was a minor presence of rutile which is represented by the peaks corresponding to (110) and (211) planes. These results are in strong agreement with the standards reported by Endo et al. (1986). Other research have also used SRM NIST 1898 NP reference material and found the composition to be made up of both anatase and rutile (Salou et al., 2020).

3.2. Dissolution in simulated fluids

The dissolution curves of the dissolved titanium ions in various simulated biological fluids and synthetic environmental media are presented in Fig. 4. The dissolution curves are expressed in the amount of dissolved titanium ions (ug L^{-1}) and as a percentage of dissolved ions to the total mass added to the reaction vessel vs time. This method was adopted from these researchers De Matteis et al. (2016); Keller et al.

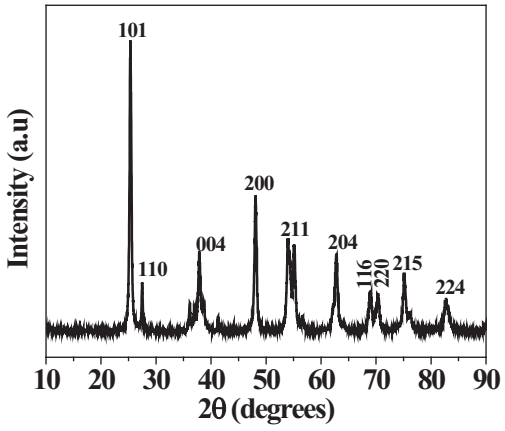

Fig. 3. X-ray diffraction pattern of TiO_2 NPs powder.

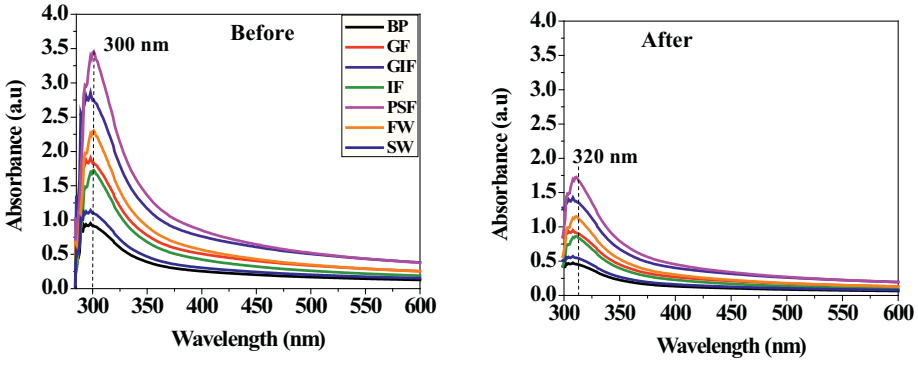

Fig. 2. UV–vis spectra of TiO_2 NPs in simulated body fluids and environmental media before and after dissolution experiments. Simulated biological fluids are BP- Blood plasma, GF- Gamble's fluid, GIF-Gastric fluid, IF- Intestinal fluid & PSF- Phagolysosomal fluid. Synthetic environmental media are FW- Freshwater and SW- Seawater.

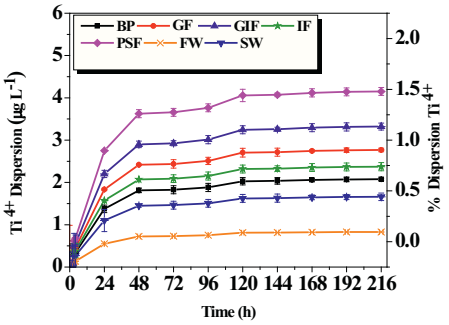

Fig. 4. Concentration of Ti ions dissolved in simulated body fluids and environmental media over a period of 10 days. Simulated biological fluids are BP- Blood plasma, GF- Gamble's fluid, GIF-Gastric fluid, IF- Intestinal fluid & PSF- Phagolysosomal fluid. Synthetic environmental media are FW- Freshwater and SW- Seawater.

(2020); Mbanga et al. (2021).

Very low amount of Ti ions was detected in all simulated fluids meaning TiO_2 NPs did no readily release titanium ions in all the simulated fluids. These low dissolution levels are corroborated by Endo et al. (1986); Murugadoss et al. (2020); Schmidt and Vogelsberger (2006); Taurozzi et al. (2013). A steady increase in the concentration of Ti ions between 0 h to 120 h was observed and reached a plateau after 120 h. These results indicate long-term dissolution is required to get to equilibrium. Under simulated biological conditions, TiO_2 NPs showed significantly higher dissolution in acidic media namely PSF and GIF compared to alkaline media such as BP, GF, IF. In simulated alkaline biological fluids, TiO_2 NPs had higher dissolution in Gamble's fluid but was not statistically significant compared to dissolution in blood plasma and intestinal fluid. Furthermore, when the particles were exposed to simulated environmental conditions, the dissolution was higher in high ionic strength sweater compared to freshwater. Freshwater reaches a point of zero charge whereas the presence of divalent ions in seawater promoted the formation of charged complexes of Ti NPs thereby weakening the metal oxygen bond thus releasing titanium ions (Raza et al., 2016).

3.3. Dissolution kinetics

The kinetic model for dissolution shown in the materials and method section was used to calculate the dissolution kinetics including the dissolution rates and half-times of TiO_2 NPs. Table 2 summarizes the dissolution parameters of TiO_2 NPs in simulated biological fluids and synthetic environmental media.

Titanium dioxide nanoparticles displayed significantly higher dissolution rates in simulated biological media characterized by low pH than at neutral pH. As a result, these nanoparticles released titanium ions significantly faster in phagolysosomal and gastric fluids compared to all other fluids and would take 259 days and 307 days respectively for this process to occur. However, this process would occur at a much slower rate for Gamble's fluid, intestinal fluid and blood plasma taking about 400 days, 400 days, and 409 days respectively before any form of dissolution can occur. Freshwater had the least capacity to dissolve these particles as a result they would take about 881 days for titanium ions to be released from the nanoparticle surface. The half-times of TiO_2 NPs followed the order PSF > GIF > GF=IF> BP > SW > FW.

Table 2
Dissolution kinetics of TiO_2 NPs in simulated biological fluids and synthetic environmental media.

Nanoparticles	Simulated fluids	DF	k (h^{-1})	$t_{1/2}$ (days)	*p-value*
		8			
TiO_2	BP	1	1.69E-03	409	0.0578
TiO_2	GF	1	1.73E-03	400	0.0598
TiO_2	GIF	1	2.25E-03	307	0.0055
TiO_2	IF	1	1.73E-03	400	0.0594
TiO_2	PSF	1	2.26E-03	259	0.0142
TiO_2	FW	1	7.86E-04	881	0.0029
TiO_2	SW	1	8.12E-04	853	0.0042

4. Discussion

These results were comparable to those obtained by other researchers such as Vogelsberger et al. (2008) who investigated the solubility of various oxides in aqueous solution as a function of time. Initially they observed a dissolution maximum which reaches a point of saturation towards the end of the experiments. This phenomenon is known as the kinetic size effect and is inversely related to particle size, meaning that the kinetic size effect decreases with increasing particle size (Vogelsberger et al., 2008). The steady increase in the concentration of Ti ions at the beginning of the dissolution studies, is because for the first few hours the degree of aggregation is not pronounced therefore there still exists enough surface area for the nanoparticle surface to interact with the components of the biological media. Research has indicated that monodispersed particles are more prone to dissolution than particles which combine to form a union via van der Waals forces because monodispersed particles have a larger surface-area-to-volume ratio compared to aggregates. Therefore, this difference in surface area causes monodispersed particles to have a greater ability for dissolution due to the availability of the surface area (León-Silva et al., 2016; Schmidt and Vogelsberger, 2009; Yang et al., 2013).

However, as the period of exposure to simulated fluids and synthetic environmental increased, TiO_2 NPs formed aggregates. The degree of aggregation was more pronounced for all simulated fluids especially towards the end of the dissolution experiments. High concentration of electrolytes in simulated fluids encourage the formation of particle aggregates by reducing the electrostatic forces between the individual particles. Therefore, this causes a reduction in the surface area of the particles thereby inhibiting dissolution. Consequently, this leads to slow dissolution rates of titanium dioxide nanoparticles. This explains the longer half-times of TiO_2 NPs in simulated blood plasma, Gamble's fluid, intestinal fluid, freshwater and more especially seawater. Other researchers have observed that the greater the degree of nanoparticle aggregation, the slower the dissolution rates (Murugadoss et al., 2020).

Similar to particle aggregation, the pH of simulated fluids is a factor that influences the dissolution kinetics of nanoparticles. In this present research study, it was observed that titanium dioxide nanoparticles suspended in simulated acidic media namely phagolysosomal and gastric had significantly higher dissolution rates and shorter half-times. This is because under acidic conditions titanium exists in these charged complexes $[Ti(OH)_2]^+$ and $[Ti(OH)_3]^+$ which facilitate the breakage of the metal – oxygen bond thereby liberating the titanium ions leading to dissolution. However, the higher the pH of simulated fluids the less charged the nanoparticle surface becomes. Schmidt and Vogelsberger (2009) state that the dissolution of oxide nanoparticles is greatly influenced by the surface charge of the respective nanoparticle. Therefore, under alkaline conditions titanium complexes reach a point of zero charge and generally low amounts of Ti ions get released under these circumstances (Xu et al., 2018). This would explain the low dissolution of TiO_2 NPs when exposed to simulated Gamble's fluid, intestinal fluid, blood plasma and freshwater.

Cupi et al. (2016) states that the presence of divalent cations and high ionic strength encourages formation of soluble complexes. When the components of simulated fluids are able to form soluble complexes with the released ions from the nanoparticle's dissolution is enhanced. This could explain high dissolution rate observed for synthetic seawater compared to freshwater. From these results it could be deduced that the dissolution of TiO_2 NPs is strongly influenced by pH and ionic strength of the simulated fluids whereby higher pH resulted in low dissolution whereas high ionic strength encouraged the dissolution of TiO_2 NPs.

There is a lack of research investigating the dissolution of titanium dioxide nanoparticles because they are assumed to be insoluble. This research demonstrate that they are most likely to remain persistence in the environment and under biological conditions and further confirms that are most likely to cause long terms health effects. A study conducted by Zhu et al. (2010) confirm these conclusions.

5. Conclusion

Dissolution is a significant factor that determines the biodurability and persistence of nanoparticles. It can be used to investigate the behaviour of nanoparticles and predict their potential effects on human health and the environment. Significant differences in dissolution behaviour were observed among the studied simulated fluids, which could be connected to pH effects, the ionic strength, and the chemical composition of the simulated media. In all the simulated body fluids and environmental media, the dissolved Ti ions were present in very low concentrations. Furthermore, most of the titanium dioxide nanoparticles remained in particulate form after having been exposed to simulated fluids for a period of 10 days. This is indicative of insoluble particles. The dissolution kinetics of titanium dioxide nanoparticles follow first order reaction kinetics and are generally characterized by low dissolution rates and long half-times. Therefore, these nanoparticles are resistant to dissolution and will most like accumulate in the body, remain persistent in the environment, and cause both short- & long-term health effects and show high environmental persistency.

Declaration of Competing Interest

The authors declare that they have no conflict of interest.

The authors declare that they have no known competing financial interests or personal relationships that could have appeared to influence the work reported in this paper.

Acknowledgements

We thank the European Union's Horizon 2020 research and innovation programme grant number 814401 (Gov4Nano) for funding. For additional support we thank the South African Department of Science and Innovation (DSI) and the National Institute for Occupational Health (NIOH) a division of National Health Laboratories, South Africa.

References

Anandgaonker, P., Kulkarni, G., Gaikwad, S., Rajbhoj, A., 2019. Synthesis of TiO2 nanoparticles by electrochemical method and their antibacterial application. Arab. J. Chem. 12 (8), 1815–1822. https://doi.org/10.1016/j.arabjc.2014.12.015.

Avramescu, M.L., Rasmussen, P.E., Chénier, M., Gardner, H.D., 2017. Influence of pH, particle size and crystal form on dissolution behaviour of engineered nanomaterials. Environ. Sci. Pollut. Res. 24 (2), 1553–1564. https://doi.org/10.1007/s11356-016-7932-2.

Cupi, D., Hartmann, N.B., Baun, A., 2016. Influence of pH and media composition on suspension stability of silver, zinc oxide, and titanium dioxide nanoparticles and immobilization of Daphnia magna under guideline testing conditions. Ecotoxicol. Environ. Saf. 127, 144–152. https://doi.org/10.1016/j.ecoenv.2015.12.028.

De Matteis, V., Cascione, M., Brunetti, V., Toma, C.C., Rinaldi, R., 2016. Toxicity assessment of anatase and rutile titanium dioxide nanoparticles: the role of degradation in different pH conditions and light exposure. Toxicol. in Vitro 37, 201–210. https://doi.org/10.1016/j.tiv.2016.09.010.

Endo, S., Akai, T., Akahama, Y., Wakatsuki, M., Nakamura, T., Tomii, Y., Tokonami, M., 1986. High temperature X-ray study of single crystal stishovite synthesized with Li2WO4 as flux. Phys. Chem. Miner. 13 (3), 146–151. https://doi.org/10.1007/BF00308155.

Freyre-Fonseca, V., Téllez-Medina, D.I., Medina-Reyes, E.I., Cornejo-Mazón, M., López-Villegas, E.O., Alamilla-Beltrán, L., Gutiérrez-López, G.F., 2016. Morphological and physicochemical characterization of agglomerates of titanium dioxide nanoparticles in cell culture media. J. Nanomater. 2016, 1–19. https://doi.org/10.1155/2016/5937932.

Hulla, J.E., Sahu, S.C., Hayes, A.W., 2015. Nanotechnology: history and future. Hum. Exp. Toxicol. 34 (12), 1318–1321. https://doi.org/10.1177/0960327115603588.

Kao, J.Y., Cheng, W.T., 2020. Study on dispersion of TiO2 Nanopowder in aqueous solution via near supercritical fluids. ACS Omega 5 (4), 1832–1839. https://doi.org/10.1021/acsomega.9b03101.

Keller, J.G., Graham, U.M., Koltermann-Jülly, J., Gelein, R., Ma-Hock, L., Landsiedel, R., Wohlleben, W., 2020. Predicting dissolution and transformation of inhaled nanoparticles in the lung using abiotic flow cells: the case of barium sulfate. Sci. Rep. 10 (1), 1–15. https://doi.org/10.1038/s41598-019-56872-3.

Korábková, E., Kašpárková, V., Jasenská, D., Moricová, D., Daďová, E., Truong, T.H., Humpolíček, P., 2021. Behaviour of titanium dioxide particles in artificial body fluids and human blood plasma. Int. J. Mol. Sci. 22 (19), 10614. https://doi.org/10.3390/ijms221910614.

Larue, C., Khodja, H., Herlin-Boime, N., Brisset, F., Flank, A.M., Fayard, B., Carrière, M., 2011. Investigation of titanium dioxide nanoparticles toxicity and uptake by plants. J. Phys. Conf. Ser. 304 (1), 012057 https://doi.org/10.1088/1742-6596/304/1/012057.

León-Silva, S., Fernández-Luqueño, F., López-Valdez, F., 2016. Silver nanoparticles (AgNP) in the environment: a review of potential risks on human and environmental health. Water Air Soil Pollut. 227 (9), 1–20. https://doi.org/10.1007/s11270-016-3022-9.

Marques, M.R., Loebenberg, R., Almukainzi, M., 2011. Simulated biological fluids with possible application in dissolution testing. Dissol. Technol. 18 (3), 15–28. https://doi.org/10.14227/DT180311P15.

Mbanga, O., Cukrowska, E., Gulumian, M., 2021. Dissolution of citrate-stabilized, polyethylene glycol–coated carboxyl and amine-functionalized gold nanoparticles in simulated biological fluids and environmental media. J. Nanopart. Res. 23 (1), 1–16. https://doi.org/10.1007/s11051-020-05132-x.

Murugadoss, S., Brassinne, F., Sebaihi, N., Petry, J., Cokic, S.M., Van Landuyt, K.L., Van Den Brule, S., 2020. Agglomeration of titanium dioxide nanoparticles increases toxicological responses in vitro and in vivo. Particle Fibre Toxicol. 17 (1), 1–14. https://doi.org/10.1186/s12989-020-00341-7.

Musial, J., Krakowiak, R., Mlynarczyk, D.T., Goslinski, T., Stanisz, B.J., 2020. Titanium dioxide nanoparticles in food and personal care products—what do we know about their safety? Nanomaterials 10 (6), 1110. https://doi.org/10.3390/nano10061110.

Nam, S.H., Kim, S.W., An, Y.J., 2012. No evidence of the genotoxic potential of gold, silver, zinc oxide and titanium dioxide nanoparticles in the SOS chromotest. J. Appl. Toxicol. 33 (10), 1061–1069. https://doi.org/10.1002/jat.2830.

Nia, H.M., Rezaei-Tavirani, M., Nikoofar, A.R., Masoumi, H., Nasr, R., Hasanzadeh, H., Shadnush, M., 2015. Stabilizing and dispersing methods of TiO 2 nanoparticles in biological studies. J. Paramed. Sci. (JPS) 6 (2), 96–105 doi:https://pesquisa.bvsalud.org/portal/resource/pt/emr-186271.

Raza, G., Amjad, M., Kaur, I., Wen, D., 2016. Stability and aggregation kinetics of Titania nanomaterials under environmentally realistic conditions. Environ. Sci. Technol. 50 (16), 8462–8472. https://doi.org/10.1021/acs.est.5b05746.

Salou, S., Cirtiu, C.M., Larivière, D., Fleury, N., 2020. Assessment of strategies for the formation of stable suspensions of titanium dioxide nanoparticles in aqueous media suitable for the analysis of biological fluids. Anal. Bioanal. Chem. 412 (7), 1469–1481. https://doi.org/10.1007/s00216-020-02412-2.

Schmidt, J., Vogelsberger, W., 2006. Dissolution kinetics of titanium dioxide nanoparticles: the observation of an unusual kinetic size effect. J. Phys. Chem. B 110 (9), 3955–3963. https://doi.org/10.1021/jp055361l.

Schmidt, J., Vogelsberger, W., 2009. Aqueous long-term solubility of titania nanoparticles and titanium(IV) hydrolysis in a sodium chloride system studied by adsorptive stripping voltammetry. J. Solut. Chem. 38 (10), 1267–1282. https://doi.org/10.1007/s10953-009-9445-9.

Shi, H., Magaye, R., Castranova, V., Zhao, J., 2013. Titanium dioxide nanoparticles: a review of current toxicological data. Particle Fibre Toxicol. 10 (1), 1–33. https://doi.org/10.1186/1743-8977-10-15.

Shinohara, N., Zhang, G., Oshima, Y., Kobayashi, T., Imatanaka, N., Nakai, M., Gamo, M., 2017. Kinetics and dissolution of intratracheally administered nickel oxide nanomaterials in rats. Particle Fibre Toxicol. 14 (1), 1–14. https://doi.org/10.1186/s12989-017-0229-x.

Shkol'nikov, E.V., 2016. Thermodynamics of the dissolution of amorphous and polymorphic TiO2 modifications in acid and alkaline media. Russ. J. Phys. Chem. A 90 (3), 567–571. https://doi.org/10.1134/S0036024416030286.

Stefanarou, A.S., Chrysikopoulos, C.V., 2021. Interaction of titanium dioxide with formaldehyde in the presence of quartz sand under static and dynamic conditions. Water (Switzerland) 13 (10). https://doi.org/10.3390/w13101420.

Syngouna, V.I., Chrysikopoulos, C.V., 2017. Inactivation of MS2 bacteriophage by titanium dioxide nanoparticles in the presence of quartz sand with and without ambient light. J. Colloid Interface Sci. 497, 117–125. https://doi.org/10.1016/j.jcis.2017.02.059.

Syngouna, V.I., Chrysikopoulos, C.V., 2019. Bacteriophage MS2 and titanium dioxide heteroaggregation: effects of ambient light and the presence of quartz sand. Colloids Surf. B: Biointerfaces 180 (February), 281–288. https://doi.org/10.1016/j.colsurfb.2019.04.052.

Syngouna, V.I., Kourtaki, K.I., Georgopoulou, M.P., Chrysikopoulos, C.V., 2022. The role of nanoparticles (titanium dioxide, graphene oxide) on the inactivation of co-existing bacteria in the presence and absence of quartz sand. Environ. Sci. Pollut. Res. 29 (13), 19199–19211. https://doi.org/10.1007/s11356-021-17086-1.

Taurozzi, J.S., Hackley, V.A., Wiesner, M.R., 2013. A standardised approach for the dispersion of titanium dioxide nanoparticles in biological media. Nanotoxicology 7 (4), 389–401. https://doi.org/10.3109/17435390.2012.665506.

Tsai, W.-B., Kao, J.-Y., Wu, T.-M., Cheng, W.-T., 2016. Dispersion of titanium oxide nanoparticles in aqueous solution with anionic stabilizer via ultrasonic wave. J. Nanoparticl. 2016, 1–9. https://doi.org/10.1155/2016/6539581.

Utembe, W., Potgieter, K., Stefaniak, A.B., Gulumian, M., 2015. Dissolution and biodurability: important parameters needed for risk assessment of nanomaterials. Particle Fibre Toxicol. 12 (1), 1–12. https://doi.org/10.1186/s12989-015-0088-2.

Vogelsberger, W., Schmidt, J., Roelofs, F., 2008. Dissolution kinetics of oxidic nanoparticles: the observation of an unusual behaviour. Colloids Surf. A Physicochem. Eng. Asp. 324 (1–3), 51–57. https://doi.org/10.1016/j.colsurfa.2008.03.032.

Wang, H., Burgess, R.M., Cantwell, M.G., Portis, L.M., Perron, M.M., Wu, F., Ho, K.T., 2014. Stability and aggregation of silver and titanium dioxide nanoparticles in seawater: role of salinity and dissolved organic carbon. Environ. Toxicol. Chem. 33 (5), 1023–1029. https://doi.org/10.1002/etc.2529.

Wang, N., Tong, T., Xie, M., Gaillard, J.F., 2016. Lifetime and dissolution kinetics of zinc oxide nanoparticles in aqueous media. Nanotechnology 27 (32), 324001. https://doi.org/10.1088/0957-4484/27/32/324001.

Xu, N., Cheng, X., Wang, D., Xu, X., Huangfu, X., Li, Z., 2018. Effects of *Escherichia coli* and phosphate on the transport of titanium dioxide nanoparticles in heterogeneous porous media. Water Res. 146, 264–274. https://doi.org/10.1016/j.watres.2018.09.047.

Yang, S.P., Bar-Ilan, O., Peterson, R.E., Heideman, W., Hamers, R.J., Pedersen, J.A., 2013. Influence of humic acid on titanium dioxide nanoparticle toxicity to developing zebrafish. Environ. Sci. Technol. 47 (9), 4718–4725. https://doi.org/10.1021/es3047334.

Yu, Q., Wang, H., Peng, Q., Li, Y., Liu, Z., Li, M., 2017. Different toxicity of anatase and rutile TiO2 nanoparticles on macrophages: involvement of difference in affinity to proteins and phospholipids. J. Hazard. Mater. 335, 125–134. https://doi.org/10.1016/j.jhazmat.2017.04.026.

Zhong, L., Yu, Y., Lian, H. Zhen, Hu, X., Fu, H., Chen, Y. Jun, 2017. Solubility of nano-sized metal oxides evaluated by using in vitro simulated lung and gastrointestinal fluids: implication for health risks. J. Nanopart. Res. 19 (11), 1–10. https://doi.org/10.1007/s11051-017-4064-7.

Zhu, X., Chang, Y., Chen, Y., 2010. Toxicity and bioaccumulation of TiO2 nanoparticle aggregates in Daphnia magna. Chemosphere 78 (3), 209–215. https://doi.org/10.1016/j.chemosphere.2009.11.013.

4.4 Paper 4

This fourth article entitled “A comparative study of the biodurability and persistence of gold, silver and titanium dioxide nanoparticles using the continuous flow through system” has been published in Nanomaterials. In this study, dissolution testing using the continuous flow through system was used to investigate the biodurability and persistence of gold nanoparticles (AuNPs), silver nanoparticles (AgNPs), and titanium dioxide nanoparticles (TiO_2 NPs) in five different simulated biological fluids and two synthetic environmental media to predict their behaviour in real life situations.

Nanomaterials 2023
https://doi.org/10.3390/nano13101653

Odwa Mbanga- Principal author

Ewa Cukrowska- Supervisor

Mary Gulumian- Supervisor

nanomaterials

MDPI

Article

A Comparative Study of the Biodurability and Persistence of Gold, Silver and Titanium Dioxide Nanoparticles Using the Continuous Flow through System

Odwa Mbanga [1], Ewa Cukrowska [1] and Mary Gulumian [2,*]

[1] Molecular Sciences Institute, School of Chemistry, University of Witwatersrand, Private Bag X3, Johannesburg 2050, South Africa; 367076@students.wits.ac.za (O.M.); ewa.cukrowska@wits.ac.za (E.C.)
[2] Water Research Group, Unit for Environmental Sciences and Management, Northwest University, Private Bag X6001, Potchefstroom 2520, South Africa
* Correspondence: mary.gulumian@nwu.ac.za

Abstract: The potential for nanoparticles to cause harm to human health and the environment is correlated with their biodurability in the human body and persistence in the environment. Dissolution testing serves to predict biodurability and nanoparticle environmental persistence. In this study, dissolution testing using the continuous flow through system was used to investigate the biodurability and persistence of gold nanoparticles (AuNPs), silver nanoparticles (AgNPs) and titanium dioxide nanoparticles (TiO_2 NPs) in five different simulated biological fluids and two synthetic environmental media to predict their behaviour in real life situations. This study examined the physicochemical properties and agglomeration state of gold, silver and titanium dioxide nanoparticles before and after dissolution tests using three different techniques (UV-vis, XRD and TEM). The UV-vis spectra revealed that all three nanoparticles shifted to higher wavelengths after being exposed to simulated fluids. The titanium powder was found to be mixed with both rutile and anatase, according to XRD examination. The average diameter of gold nanoparticles was 14 nm, silver nanoparticles were 10 nm and titanium dioxide nanoparticles were 25 nm, according to TEM images. The gold and silver nanoparticles were observed to be spherical, but the titanium dioxide nanoparticles were irregular in shape, with some being spherical. The level of dissolved nanoparticles in simulated acidic media was higher in magnitude compared to that dissolved in simulated alkaline media. The results obtained via the continuous flow through dissolution system also displayed very significant dissolution rates. For TiO_2 NPs the calculated half-times were in the range of 13–14 days, followed by AuNPs ranging between 4–12 days, significantly longer if compared to the half-times of AgNPs ranging between 2–7 days. AuNPs and TiO_2 NPs were characterized by low dissolution rates therefore are expected to be (bio)durable in physiological surroundings and persistent in the environment thus, they might impose long-term effects on humans and the environment. In contrast, AgNPs have high dissolution rates and not (bio)durable and hence may cause short-term effects. The results suggest a hierarchy of biodurability and persistence of TiO_2 NPs > AuNPs > AgNPs. It is recommended that nanoparticle product developers should follow the test guidelines stipulated by the OECD to ensure product safety for use before it is taken to the market.

Keywords: gold and silver nanoparticles; titanium dioxide nanoparticles; biodurability; persistence; dissolution kinetics; simulated fluids

Citation: Mbanga, O.; Cukrowska, E.; Gulumian, M. A Comparative Study of the Biodurability and Persistence of Gold, Silver and Titanium Dioxide Nanoparticles Using the Continuous Flow through System. *Nanomaterials* **2023**, *13*, 1653. https://doi.org/10.3390/nano13101653

Academic Editor: Joachim Clement

Received: 18 April 2023
Revised: 12 May 2023
Accepted: 12 May 2023
Published: 16 May 2023

1. Introduction

The manufacturing, production and application of nanoparticles is ever increasing and making a profound impact [1,2]. For example, gold nanoparticles (AuNPs) are used in the medical field as drug delivery agents since they are biocompatible, easy to manipulate in size and shape and are chemically stable [3–6]. Whereas silver nanoparticles

(AgNPs) owing to their antimicrobial properties are used in the food and cosmetics industries [7,8]. Titanium dioxide nanoparticles (TiO_2 NPs) are extensively used as food colourants, nutritional supplements and for food packaging materials [9]. This is due to their ability to filter UV radiation, have antimicrobial properties and are excellent inhibitors of corrosion [10]. Their extensive use in consumer products has resulted in humans being increasingly exposed and they are also released to the environment in many ways including waste disposal [11]. However, much is still unknown about the effects of nanoparticles on human health and the environment. Many discussions are currently ongoing as to whether exposure of NPs to the ecosystem (i.e., plants and animals, humans and the environment) may be conceived as harmful or not [1].

The application of nanoparticles offers a wide range of benefits; however, unlocking this potential requires a responsible and co-ordinated approach to ensure that potential challenges are being addressed in parallel with the development and use of nanotechnology [12]. The traditional testing and assessment methods used to determine the safety of traditional chemicals are not necessarily applicable to NPs [13,14]. The concept of safe by design has been used in a variety of industries to identify potential risks and minimize those risks early in the technological development process. Biotechnology, crop breeding and drug design are examples of industries [15]. To ensure that safety and sustainable usage of nanoparticles is a key priority, safe by design concepts and methodologies used in these industries should also be used in nanotechnology and the development of advanced and smart materials [15]. In this study dissolution was used to assess the biodurability and persistence of AuNPs, AgNPs and TiO_2 NPs to gain a better understanding of their effects on human health and the environment. This is because many studies are concerned mostly with the assessment of toxicity, a challenging but yet unaddressed issue of nanoparticles is their biodurability, which is the tendency to resist dissolution and biodegradation within biological and environmental surroundings [16]. Whereas persistence is the capacity of a substance, particle or fibre to remain unchanged in the environment for a very long time [17,18]. Dissolution tests provide a measure of nanoparticles biodurability and persistence, which can provide useful information about their acute and long-term toxicity as well as the particles' pathogenicity [16]. For example, if a particle dissolves rapidly, it is more likely to cause short-term health effects and its impact on the environment can manifest faster [19]. However, particles that dissolves slow are biodurable and hence may cause both short-term and long-term health effects and show high environmental persistency [12]. For metal-containing nanomaterials, the release of metal ions is thought to be the primary cause of any induced toxicity [12,16,18]. Therefore, it is of utmost importance to study dissolution to better understand the behaviour of nanoparticles in real life situations.

A proper understanding of the safety of nanoparticles requires information on their biodurability in physiological surroundings and persistence in the environment. Currently, several research studies have been conducted on the risk assessment and safety of nanoparticles. For example, a study conducted by Avellan et al. [20] predicted the fate of AuNPs in mesocosms freshwater wetland to simulate aquatic environments and found that some plants can oxidize AuNPs thereby releasing Au^+ ions. Other data in the literature have reported on the biodistribution and accumulation of AuNPs in several cell lines and models and the factors identified to influence their toxicity are surface charge and functionalization, size and shape of AuNPs [3,21–23]. Furthermore, long-term and short-term dissolution studies of AgNPs have been conducted by numerous researchers [1,24–27]. Factors which influence dissolution include agglomeration state of nanoparticles, ionic strength of the media and particle surface functionalization [24,28–31]. Even though TiO_2 NPs are considered insoluble therefor undergo negligible dissolution in biological and environmental media, there is sizable research that has been conducted which elucidates their dissolution in media [32–35].

However, a lot of these studies do not thoroughly elucidate the dissolution kinetics of particles. Little is known about how long it would take for nanoparticles to disintegrate in the body and the environment, and how fast that process occurs. This current research

study is concerned with addressing these issues. Therefore, there is a need to elucidate the biodurability and persistence of nanoparticles to gain a better understanding of their safety and predict their behaviour in real life situations. In this work we predicted the biodurability and persistence of AuNPs, AgNPs and TiO_2 NPs in a wide range of in five different simulated biological fluids and two synthetic environmental media to predict their behaviour in real life situations. These parameters were predicted by studying the dissolution kinetics, including the dissolution rates, rate constants, order of reaction and half-times of AuNPs, AgNPs and TiO_2 NPs to predict their behaviour in physiological and environmental conditions.

It is hypothesized that since nanoparticles are utilised in a wide variety of consumer products, there is concern regarding potential exposure. If these nanoparticles are released into the environment, they may cause negative effects on both the environment and biological organisms. It is expected that when subjected to simulated acidic fluids, the nanoparticles will release ions, whereas in neutral simulated fluid, the nanoparticles will be stable. Short-term toxicity could be due to either the particles or the ions released by them. Longer half-time nanoparticles, on the other hand, will have more severe long-term consequences.

2. Materials and Methods

2.1. Characterization of Gold, Silver and Titanium Dioxide Nanoparticles

The three different types of nanoparticles namely AuNPs, AgNPs and TiO_2 NPs were tested for their biodurability and persistence through investigating their dissolution behaviour and dissolution kinetics. The dissolution tests were conducted using the continuous flow-through system in simulated biological fluids and synthetic environmental media to mimic body fluids and environmental media. The 14 nm in diameter AuNPs were obtained in three different types and provided by MINTEK (Randburg, South Africa). The first type was the citrate stabilized gold nanoparticle (AuNPs-cit) with the concentration of about 3.8 nM, followed by PEGylated carboxyl functionalized gold nanoparticle (AuNPs-COOH) whose concentration was 4.0 nM and the last one was the PEGylated amine functionalized gold nanoparticles (AuNPs-NH_2) whose stock solution had a concentration of 3.0 nM. AgNPs were purchased from (Sigma Aldrich Johannesburg, South Africa) in the size of 10 nm in diameter with the concentration of 0.02 mg $mL^{\times 1}$ suspended in a 1% sodium citrate solution as a stabilizer. For TiO_2 NPs, a unit of standard reference material (SRM) 1898 was purchased from the National Institute of Standards and Technology (NIST, Gaithersburg, MD, USA). All the nanoparticle suspensions were prepared under sterile conditions. Transmission electron microscope (TEM) (JOEL Ltd. JEM-2100) (Lireweg, The Netherlands) analyses were performed before and after dissolution studies to monitor the morphological changes in the nanoparticles upon exposure to simulated fluids. The Specord 50 Analytik Jena Ultraviolet-Visible spectrophotometer (UV-is) (Analytik Jena GmbH+Co. KG, Jena/Germany) was used to determine the agglomeration and aggregation state of NPs in simulated media at various wavelengths before and after dissolution experiments. Titanium dioxide nanoparticles were further characterized with an X-ray diffractometer the PANayltical X'Pert Pro powder diffractometer instrument (Malvern, United Kingdom) was used to determine their crystalline structure and to confirm whether they existed in the anatase or rutile crystal phase. This instrument was fitted with 1D X'Celerator detector, 10 mm programmable divergence slit and sample spinner (Spinner PW3064) with a rotation time of 1 s. The X-ray radiation source was Cu Kα (λ = 0.15405 nm) tube, operating at 40 kV and 40 mA conditions. The measurement was carried out under Gonio scan axis with continuous scan type, step size, scan step time and 2θ range of 0.0170°, 2θ, 87 s and (5 to 90°), respectively. The P-XRD sample was transferred onto the low background silicon sample holder. After the X-ray measurements, raw data were interpreted by using High Score (Plus) software with ICDD PDF-4^+ 2019 database. The concentrations of dissolved Au, Ag and Ti ions were obtained using inductively coupled mass spectrometer (ICP-MS) (Agilent Technologies, 7700 series ICP-MS, Santa Clara, CA, USA).

2.2. Preparation of Simulated Fluids

Nanoparticles can enter the human body via various routes, the focus of this present research study was therefore exposure via inhalation, ingestion, intravenous and environmental exposure through waste disposal. Subsequently, simulated phagolysosomal fluid (PSF) and Gamble's fluid (GF) were chosen to represent lung fluids found in cellular lysosomes and deep within the lungs at pH 4.5 and pH 7.4, respectively. Whereas gastric fluid (GIF) and intestinal fluid (IF) were representative of stomach fluids at pH 2.0 and pH 7.5, respectively. Lastly, blood plasma (BP) at pH 7.2 which is a fluid that carries blood components throughout the body. The synthetic environmental media of choice were freshwater (FW) and seawater (SW). The preparation of all the simulated fluids was adopted from the procedure presented by Innes et al. [16] and Marques et al. [36] using the reagents listed in Table 1. Synthetic environmental media were prepared following the procedure recommended by the United States (U.S) Environmental Protection Agency (EPA). These reagents were dissolved in 5 L of ultrapure milli-Q water with a resistivity of 18.2 MΩ·cm in the order given in Table 1, and the pH was adjusted with either 1 M hydrochloric acid or 1 M sodium hydroxide. A 25 µL alkylbenzyldimethylammonium chloride (ABDC) the anti-fungal agent was added to each 5 L container to preserve the simulated biological fluids and synthetic environmental media.

Table 1. Chemical composition, pH and ionic strength of simulated fluids (Marques et al., 2011).

Chemical Composition (g 5 L^{-1})	BP	GF	GIF	IF	PSF	FW	SW
Bile salts	-	-	-	45 mL	-	-	-
Borax	-	-	-	-	-	-	0.17
Calcium chloride	1.46	-	-	2.49	-	-	-
Calcium chloride anhydrous	-	-	-	-	-	-	1.320
Calcium chloride dihydrate	-	1.84	-	-	0.14	-	-
Calcium sulphate anhydrous	-	-	-	-	-	0.37	-
Glycine	-	-	-	-	2.25	-	-
Magnesium chloride	-	1.015		0.95			47.5
Magnesium chloride hexahydrate	1.65		-	-	-	-	-
Magnesium sulphate anhydrous	-	-	-	-	-	0.037	-
Mucin	-	-	15 mg	-	-	-	-
Pancreatin	-	-	-	45 mL	-	-	-
Pepsin	-	-	5 mL	-	-	-	-
Potassium bromide	-	-	-	-	-	-	0.44
Potassium chloride	1.12	1.49	35	1.49		0.0025	3.05
Potassium hydrogen phthalate	-	-	1.215	-	20.43	-	-
Potassium phosphate dibasic trihydrate	1.15	-	-	-	-	-	-
Sodium acetate	-	4.76	-	-	-	-	-
Sodium chloride	40.17	30.09	14.61		33.25		105.1
Sodium hydrogen carbonate	1.77	13.02	-	-	-	0.06	0.85
Sodium hydrogen phosphate	-	0.71	-	-	0.171	-	-
Sodium sulphate	0.36				0.36		17.6
Sodium sulphate anhydrous	-	0.085	-	-	-	-	-
Strontium chloride	-	-	-	-	-	-	0.1

Table 1. *Cont.*

Chemical Composition (g 5 L^{-1})	BP	GF	GIF	IF	PSF	FW	SW
Tris(hydroxymethyl) aminomethane	30.59	-	-	-	-	-	-
Trisodium citrate dihydrate	-	0.485	-	-	-	-	-
Urea	-	-	-	1.5	-	-	-
1 M HCl	195 mL	-	-	-	-		-
Ionic strength (mol L^{-1})	0.15	0.17	0.16	0.16	0.34	0.05	3.5
pH	7.2	7.4	2.0	6.8	4.5	6.8	8.0

BP—Blood plasma; GF—Gamble's fluid; GIF—Gastric fluid; IF—Intestinal fluid; PSF—Phagolysosomal fluid; FW—Freshwater; SW—Seawater.

2.3. Continuous Flow-Through Dissolution Procedure

The continuous flow-through dynamic method of dissolution testing protocol shown in Figure 1 used in this study was adapted from Keller et al. [37] and Koltermann-Jülly et al. [38] with minor changes to match the specifications of nanoparticles. This dissolution protocol was specifically selected because it is regarded to be more reflective of dissolution occurring in biological and environmental surroundings. It is therefore recommended to avoid achieving an equilibrium that would restrict dissolution. A volume of 2 mL of gold and silver nanoparticles were drawn from the nanoparticle stock solutions and transferred into small centrifuge tubes. These were centrifuged at 13,000 times gravity for 30 min to pre-concentrate the samples which formed pellets. The pellets were transferred separately into the lower chamber of the flow through units. The flow through units containing the pellets were then filled with simulated fluids to create a nanoparticle suspension. TiO_2 NPs were in a powder form therefore, a mass of 1 mg of titanium dioxide nanoparticle powder was weighed onto a membrane and was also transferred into the lower chamber of the flow through unit which was also filled with simulated fluid forming a nanoparticle suspension. An o-ring membrane holder was placed on top of the flow through unit containing the NP suspensions which was then sealed with the 3.5 kD membrane. The three separate flow through units containing AuNP, AgNP and TiO_2 NP suspensions were then closed with a membrane (Spectrum/Por 3—Standard RC Discs—MWCO: 3.5 kD–33 mm^2) pore size to only permit the movement of dissolved ions. A small pore size membrane was carefully selected to ensure that all the nanoparticles were kept inside the flow through units whilst only permitting the dissolved ions to diffuse into the bulk fluid. A second flow through unit (upper chamber) was placed on top of the membrane sealed lower chamber and tightly closed to only permit the movement of dissolved ions into the fraction collectors. The three separate flow through units were simultaneously submerged in a water bath maintained at 37 °C to mimic physiological conditions and room temperature 25 °C for synthetic environmental fluids. The simulated fluids from the fluid reservoir were pumped through the flow through units using the peristaltic pump at 8 mL/h and the eluate containing dissolved ions were continuously collected by the fraction collectors. The concentration of released ions from the eluate were analysed by ICP-MS to determine the level of dissolved ions of gold, silver and titanium. The programmable sampler drew 8 mL/h of the eluate. The dissolution experiments were conducted over a period of 10 days and triplicate samples were taken and measured. Samples were collected in 30 min interval for the first 4 h and once a day for the next 10 days. Sampling times were 0 h, 0.5 h, 1 h, 1.5 h, 2 h, 2.5 h, 3 h, 3.5 h and 4 h. From day 2 to day 10 samples were collected at 24 h, 48 h, 72 h, 96 h, 120 h, 144 h, 168 h, 192 h and 2016 h. Reported in the results section is an average of the three measurements.

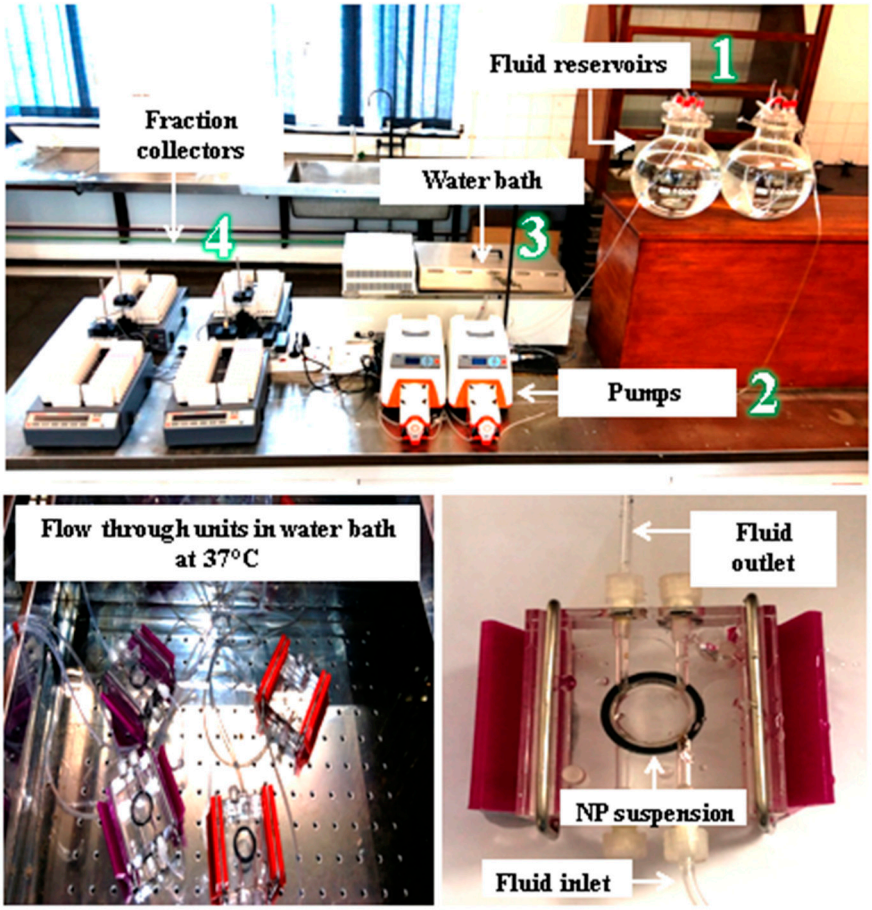

Figure 1. Continuous flow-through dissolution system protocol.

2.4. Determination of the Kinetic Parameters

The dissolution of nanoparticles follows the first order reaction kinetics and involves the mass transfer rate process whereby the solute is transported from the nanoparticle surface to the bulk fluid surrounding the nanoparticles. The rate of solute liberation and transport from the nanoparticle surface is calculated using the dissolution kinetics model described below. To determine the dissolution rate constant and half-time of nanoparticles in the current research, the dissolution data were fit to a first order kinetic model previously described by Keller et al. [39] and Koltermann-Jülly et al. [38] using the following equation:

$$M_{dissolved}(T) = \frac{m(ENM)}{m(metal\ ion)} \times \sum_{i=0}^{T} c_i(ion) \times V_i \times \Delta t_i \quad (1)$$

where $M_{dissolved}(T)$ is the mass of the dissolved nanoparticles, $m(ENM)$ is the initial mass of the nanoparticles weighed before the commencement of the dissolution experiments, $m(metal\ ion)$ is the mass of dissolved nanoparticles obtained at different sampling time points, $c_i(ion)$ is the concentration of dissolved ions obtained at a specific sampling time point, V_i is the volume sampled at different times and Δt_i is the different time interval where samples were collected to determine the amount of dissolved ions. Equation (1) gives us the rate of mass removal and the dissolution rate k is obtained using Equation (2) which is calculated as follows:

$$M_{solids}(T) = M_0 - M_{dissolved}(T) \quad (2)$$

From Equation (2) the mass of nanoparticles remaining can be determined where $M_{solids}(T)$ is the mass remaining after dissolution has occurred, M_0 represents the initial

mass of the before dissolution and $M_{dissolved}(T)$ is the mass dissolved at different sampling time points. Equation (2) allows us to determine the dissolution rate k which is calculated using the following equation:

$$k = \ln\{M_0 / M_{solids}(T)\} / (SSA(T) \times T) \quad (3)$$

where k is the dissolution rate, SSA represents the initial surface area of the nanoparticles before dissolution and T is the time taken for the duration of the dissolution experiments. The initial surface area provided in Table 2 was used to calculate the half-time of nanoparticles to predict their duration in biological and environmental surroundings using the following equation:

$$t_{1/2} = \frac{\ln 2}{k * SSA} \quad (4)$$

Table 2. Physical–chemical description of AuNPs, AgNPs and TiO_2 NPs.

Nanoparticles	Simulated Fluids	UV-Vis Absorption Wavelength		Surface Area	Particle Size Diameter	Crystallinity (XRD)
		[nm]		[m^2/g]	[nm]	[%]
		Before	After			
Citrate-AuNPs	BP	520	549	25	14	None
Citrate-AuNPs	GF	520	549	21	14	None
Citrate-AuNPs	GIF	520	549	23	14	None
Citrate-AuNPs	IF	520	549	21	14	None
Citrate-AuNPs	PSF	520	549	20	14	None
Citrate-AuNPs	FW	520	549	22	14	None
Citrate-AuNPs	SW	520	549	20	14	None
COOH-AuNPs	BP	520	547	24	14	None
COOH-AuNPs	GF	520	547	23	14	None
COOH-AuNPs	GIF	520	547	24	14	None
COOH-AuNPs	IF	520	547	26	14	None
COOH-AuNPs	PSF	520	547	26	14	None
COOH-AuNPs	FW	520	547	24	14	None
COOH-AuNPs	SW	520	547	25	14	None
NH_2-AuNPs	BP	520	540	22	14	None
NH_2-AuNPs	GF	520	540	23	14	None
NH_2-AuNPs	GIF	520	540	22	14	None
NH_2-AuNPs	IF	520	504	22	14	None
NH_2-AuNPs	PSF	520	504	20	14	None
NH_2-AuNPs	FW	520	540	18	14	None
NH_2-AuNPs	SW	520	540	20	14	None
AgNPs	BP	400	450	22	10	None
AgNPs	GF	400	450	22	10	None
AgNPs	GIF	400	400	18	10	None
AgNPs	IF	400	450	15	10	None
AgNPs	PSF	400	400	15	10	None
AgNPs	FW	400	450	26	10	None
AgNPs	SW	400	400	20	10	None
TiO_2 NPs	BP	300	320	57	25	Mix rutile/anatase
TiO_2 NPs	GF	300	320	58	25	Mix rutile/anatase
TiO_2 NPs	GIF	300	320	56	25	Mix rutile/anatase
TiO_2 NPs	IF	300	320	55	25	Mix rutile/anatase
TiO_2 NPs	PSF	300	320	55	25	Mix rutile/anatase
TiO_2 NPs	FW	300	320	59	25	Mix rutile/anatase
TiO_2 NPs	SW	300	320	58	25	Mix rutile/anatase

To calculate the mass of dissolved ions and account for the molar masses of the nanoparticles and detectable metal ions, we multiplied the measured ion concentration of each eluate by the eluted volume. This allowed us to calculate the percentage mass of remaining nanoparticles during the sampling time intervals.

2.5. Statistical Analysis

The data on dissolution are presented as the mean standard deviation of at least three independent measurements. To determine significant differences in the dissolution kinetics of AuNPs, AgNPs and TiO_2 NPs in various simulated body fluids and synthetic environmental media, a multiple variable ANOVA analysis was performed using RStudio version 1.2 software. $p < 0.05$ was considered statistically significant.

3. Results

3.1. Physichichemical Properties of AuNPs, AgNPs and TiO_2NPs

Investigating the biodurability and persistence of nanoparticles requires a thorough and accurate characterization of the particles' physicochemical properties which can in turn be linked to their dissolution behaviour. In the present study, UV-vis, XRD and TEM were used to characterize, assess and monitor morphological changes and agglomeration states of AuNPs, AgNPs and TiO_2 NPs before and after the dissolution experiments. Table 2 shows the physicochemical characterization of AuNPs, AgNPs and TiO_2 NPs.

Generally, the UV-vis spectra of gold, silver and titanium dioxide nanoparticles have a localized surface plasmon resonance peaks at 520 nm, 400 nm and 300 nm, respectively [40–43]. This was confirmed by the UV-vis characterization of these nanoparticles before the dissolution experiments as shown in Table 2. After exposure to simulated fluids there was an observable shift to higher wavelengths for all the three nanoparticles. Interestingly this red shift for AuNPs was functional group specific. For example, -AuNPs-cit shifted to 547 nm followed by AuNPs-COOH at 540 nm then lastly AuNPs-NH_2 shifted to 540 nm. These subtle differences are likely due to that the functionalized AuNPs are coated with polyethylene glycol (PEG) then functionalized with the carboxyl and amine functional groups. Consequently, PEG provides electro steric stabilizing thereby preventing the particles from combining to form agglomerates as a result, they remain monodispersed [44,45]. However, the citrate on the citrate stabilized AuNPs is just a stabilizing agent which can be easily displaced from the NP surface as a result it is easier to from agglomerates once the stabilizing agent is removed. For AgNPs there was an observable shift to higher wavelength (450 nm) for particles in contact with neutral media such as blood plasma, intestinal fluid, Gamble's fluid and freshwater. This indicates that after a prolonged exposure of silver nanoparticles to these simulated fluids the particles physically coalesce to form larger particles. Generally larger particles absorb light at higher wavelength than smaller particles hence there was an observable shift to higher wavelengths for the agglomerates. TiO_2 NPs exhibited a similar trend whereby there was a shift to higher wavelengths (320 nm) after exposure to simulated fluids indicative of particle aggregation as the time of exposure to simulated fluids increased. For AuNPs and AgNPs this red shift in wavelength was due to particle agglomeration whereas, for TiO_2 NPs the major cause of the shift was formation of particle aggregates. Particle aggregation leads to a reduced surface area because particles combine to form a union of larger particles through weak Van der Waal forces [35,46,47]. As a result, the nanoparticle absorbs UV-light at a much higher wavelength as shown in Table 2 after dissolution experiments.

3.2. XRD Characterization of TiO_2 NP Powder

The TiO_2 nanoparticle powder was examined using XRD to assess its crystallographic phase, whether it was rutile, anatase, or a combination of both. The XRD pattern of the nanoparticles can be seen in Figure 2, with the peak positions at 2θ and their Miller indices. The TiO2 XRD data demonstrated very sharp peaks. The strong diffraction peaks exhibited by the XRD pattern at angles 25°, 37°, 47°, 55°, 62°, 68°, 70°, 75° and 82° correspond to Miller indices of (101), (004), (200), (211), (204), (116), (220), (215) and (224) plane, respectively. The major component of the TiO2 NPs sample was confirmed to be anatase. However, there was a minor presence of rutile which is represented by the peaks corresponding to (110) and (211) planes.

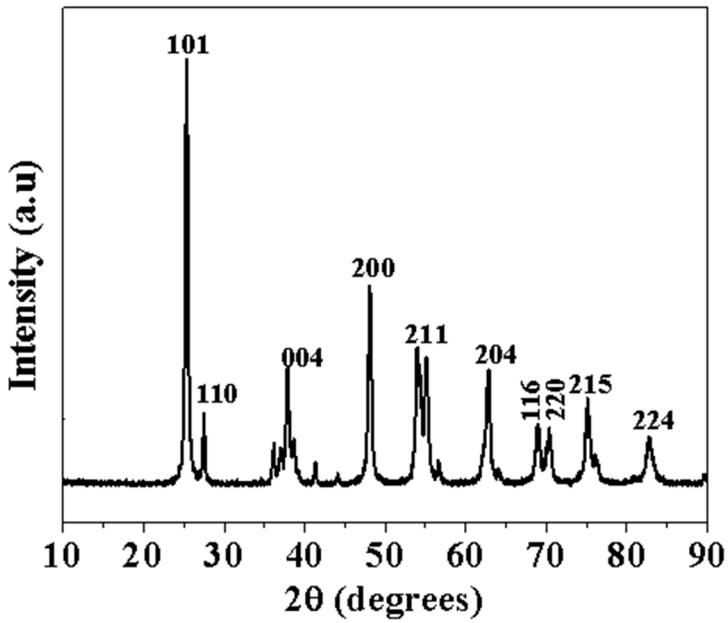

Figure 2. X-ray diffraction pattern of TiO_2 NPs powder.

3.3. TEM Characterization of AuNPs, AgNPs and TiO_2 NPs

TEM was used to investigate the morphological changes in AuNPs, AgNPs and TiO_2 NPs in simulated fluids before and after the dissolution experiments. The TEM images of AuNPs-cit, AuNPs-COOH, AuNPs-NH_2, AgNPs and TiO_2 NPs in simulated fluids are shown in Figure 3a–e respectively.

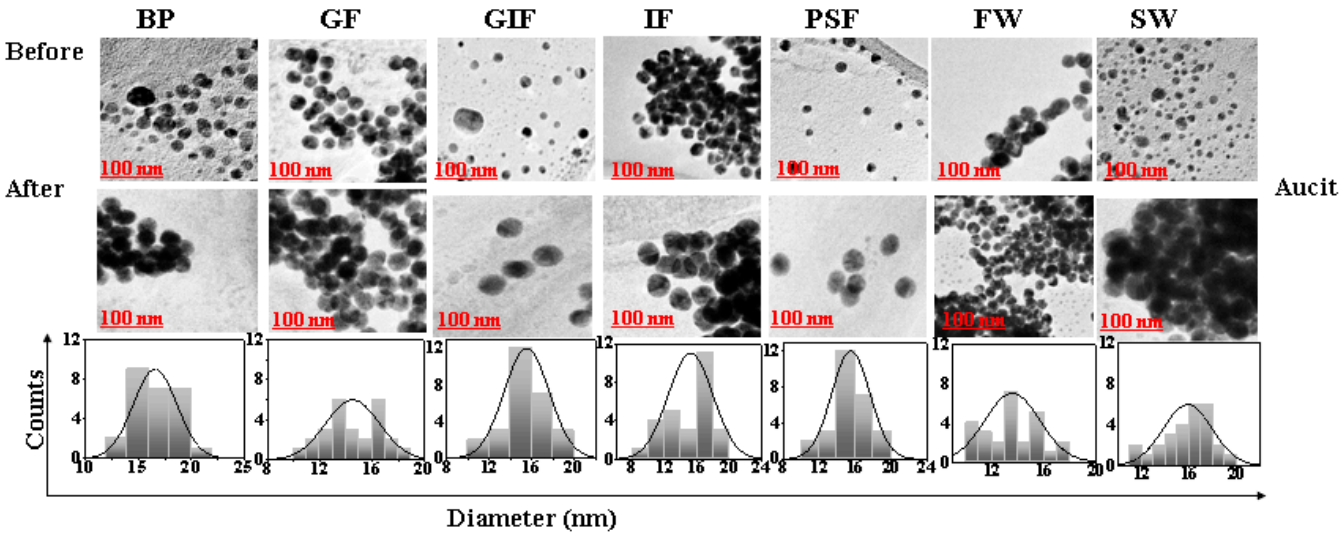

(**a**)

Figure 3. *Cont.*

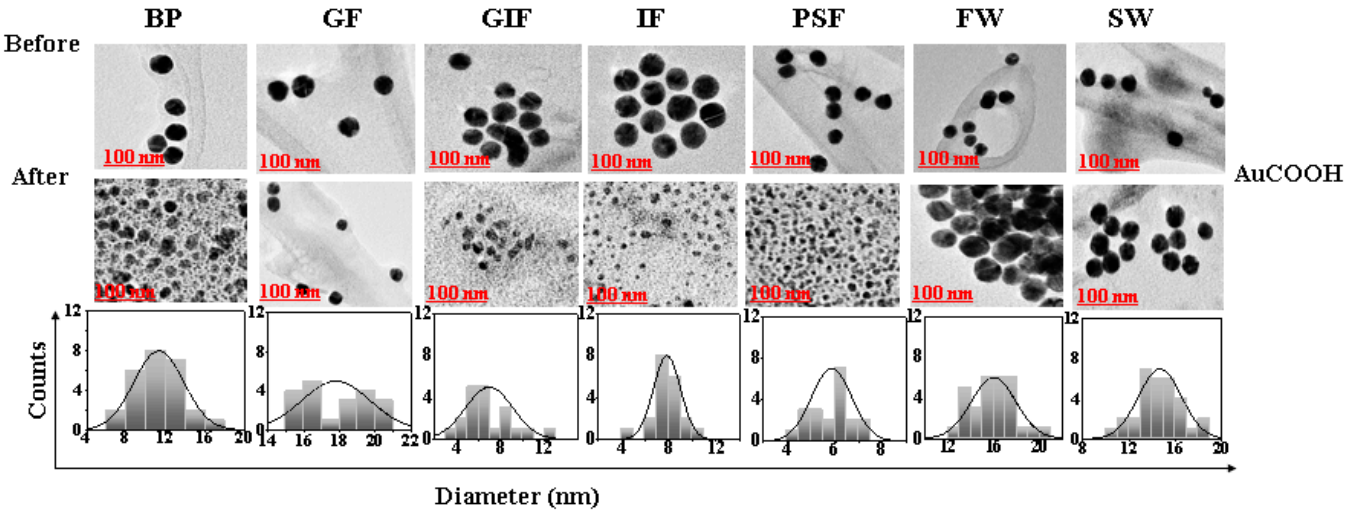

(**b**)

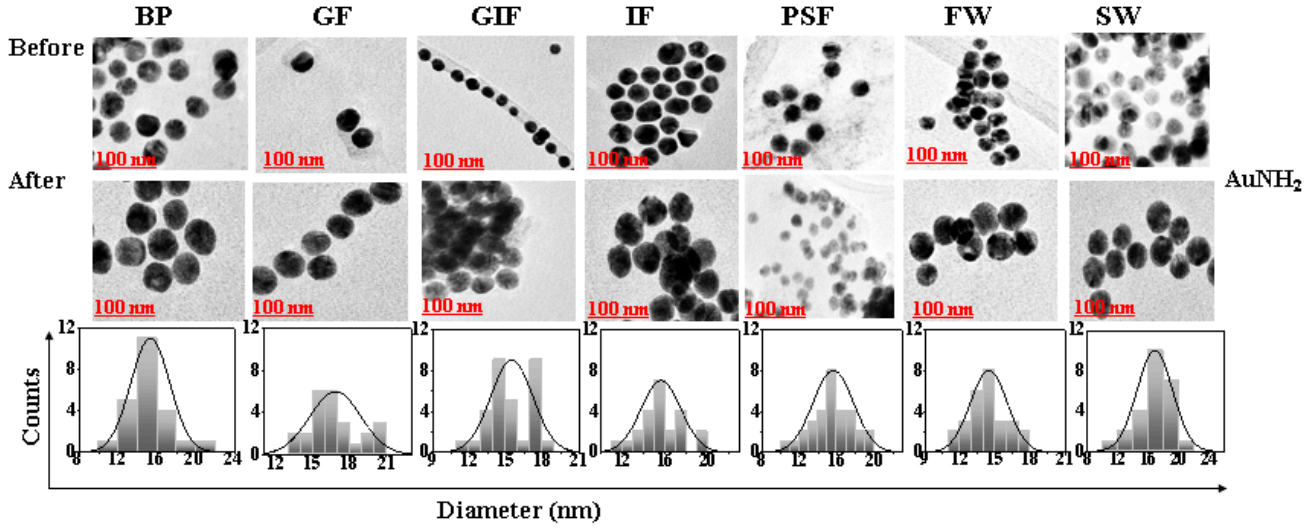

(**c**)

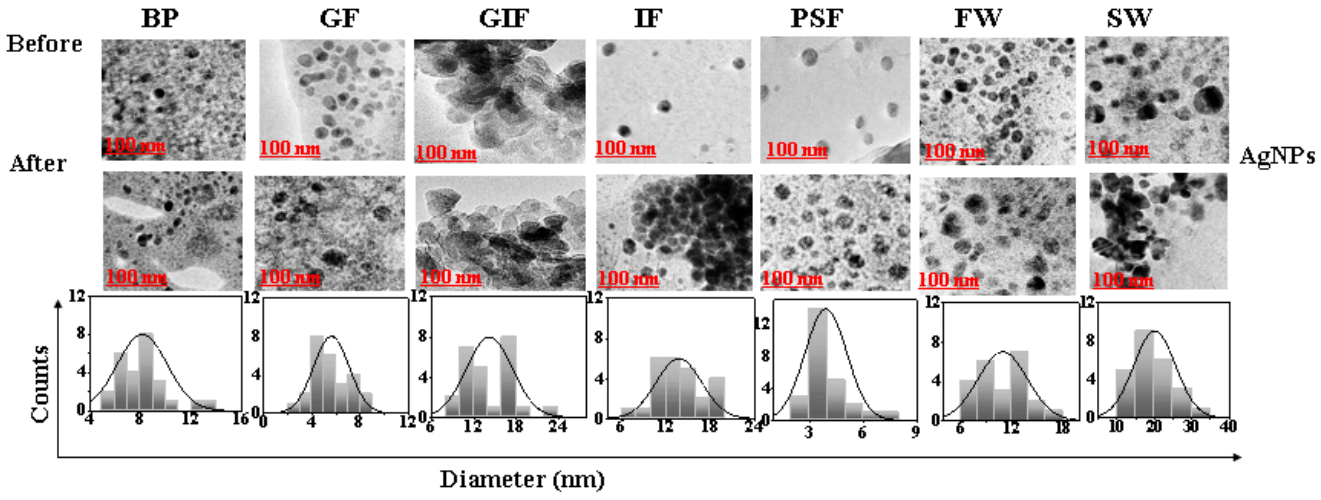

(**d**)

Figure 3. *Cont.*

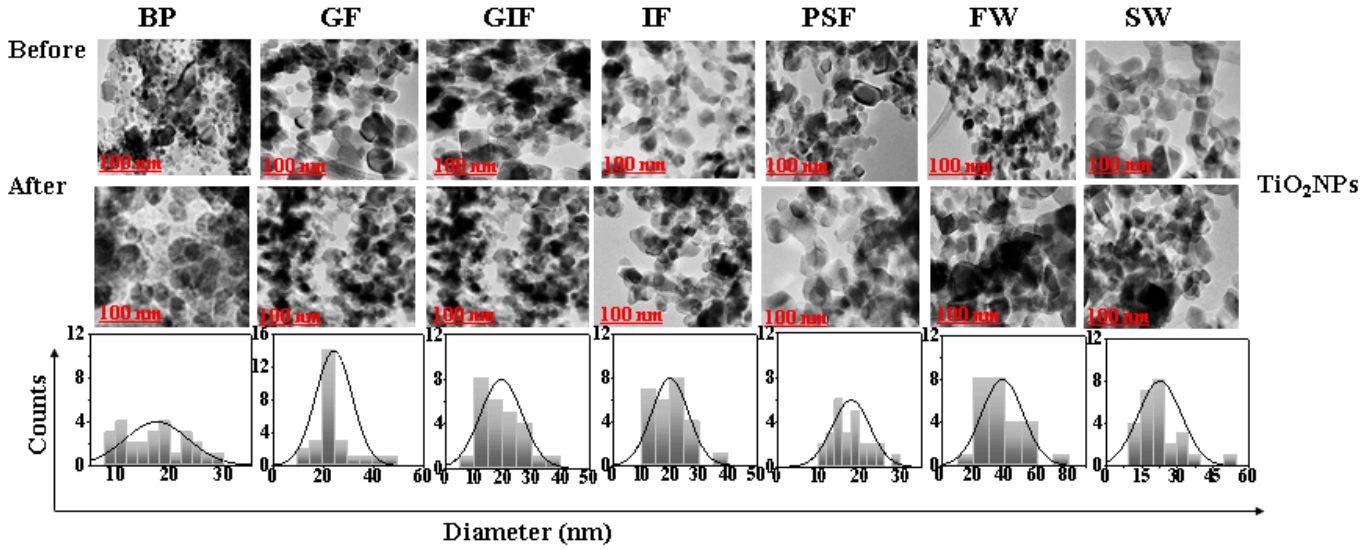

(**e**)

Figure 3. TEM images of cit-stabilized AuNPs (**a**); COOH-AuNPs (**b**) NH_2-AuNPs (**c**), AgNPs (**d**) and TiO_2 NPs (**e**) in simulated biological and environmental fluids before and after dissolution tests. BP, GF, GIF, IF and PSF are simulated biological fluids for blood plasma, Gamble's fluid, gastric fluid, intestinal fluid and phagolysosomal fluid, respectively. FW and SW are synthetic environmental fluids for freshwater and seawater, respectively.

The average nanoparticle diameter measured using Image J software (National Institute of Health, version no Java1.8.0_172) were 14 ± 2.8 nm for citrate stabilized AuNPs, 14 ± 2.3 nm for COOH-AuNPs and 14 ± 1.7 nm for NH_2-AuNPs. Whereas the AgNPs had a size diameter of about 10 ± 0.8 nm which was smaller than that of TiO_2 NPs with the size of 25 ± 3.1 nm. The gold and silver nanoparticles were spherical in shape as shown in Figure 3a–d. However, TiO_2 NPs were irregular in morphology, and some were spherical as seen in Figure 3e. Among the AuNPs the citrate stabilized AuNPs tended to form multiple single particle clusters after exposure to simulated fluids. In contract, the pegylated carboxyl and amine functionalized gold nanoparticles (AuCOOH) and ($AuNH_2$) remained monodispersed throughout the duration of the dissolution experiments. The Peg polymer coating present on the surface of functionalized gold nanoparticles provides steric stability which prevents the particles from colliding together to form clusters. Additionally, polymers are always present in the suspension system for steric stabilization, and they adsorb onto the particle surface, resulting in an additional steric repulsive force. Silver nanoparticles were spherical in shape and monodispersed. The morphological analysis of the TiO_2 nanopowder by TEM (Figure 3e) showed high degrees of particle aggregation in all simulated fluids despite the differences in chemical composition, pH and ionic strength of the simulated fluids [48,49]. The formation of nanoparticle aggregates is due to Van der Waals interactions on the nanoparticle surface. During particle–particle interactions, if the force of attraction far exceeds the repulsive forces, then particles will tend to stick together to form aggregates [29,50]. The formation of nanoparticle aggregates can hinder the dissolution process by reducing the exposed surface area of the particle [51]. Additionally, particle aggregation can introduce a kinetic hindrance effect to the diffusion process thereby significantly reducing chances of dissolution [52].

3.4. Dissolution Curves of AuNPs, AgNPs and TiO_2 NPs

Figure 4 presents the dissolution curves of AuNPs, AgNPs and TiO_2 NPs in various simulated biological fluids and synthetic environmental media. The dissolution curves are reported as a percentage mass of nanoparticles that remained undissolved in the reaction

vessel over a period of 10 days expressed as time in hours. This method was adopted from these researchers Koltermann-Jülly et al. [38] and Keller et al. [39].

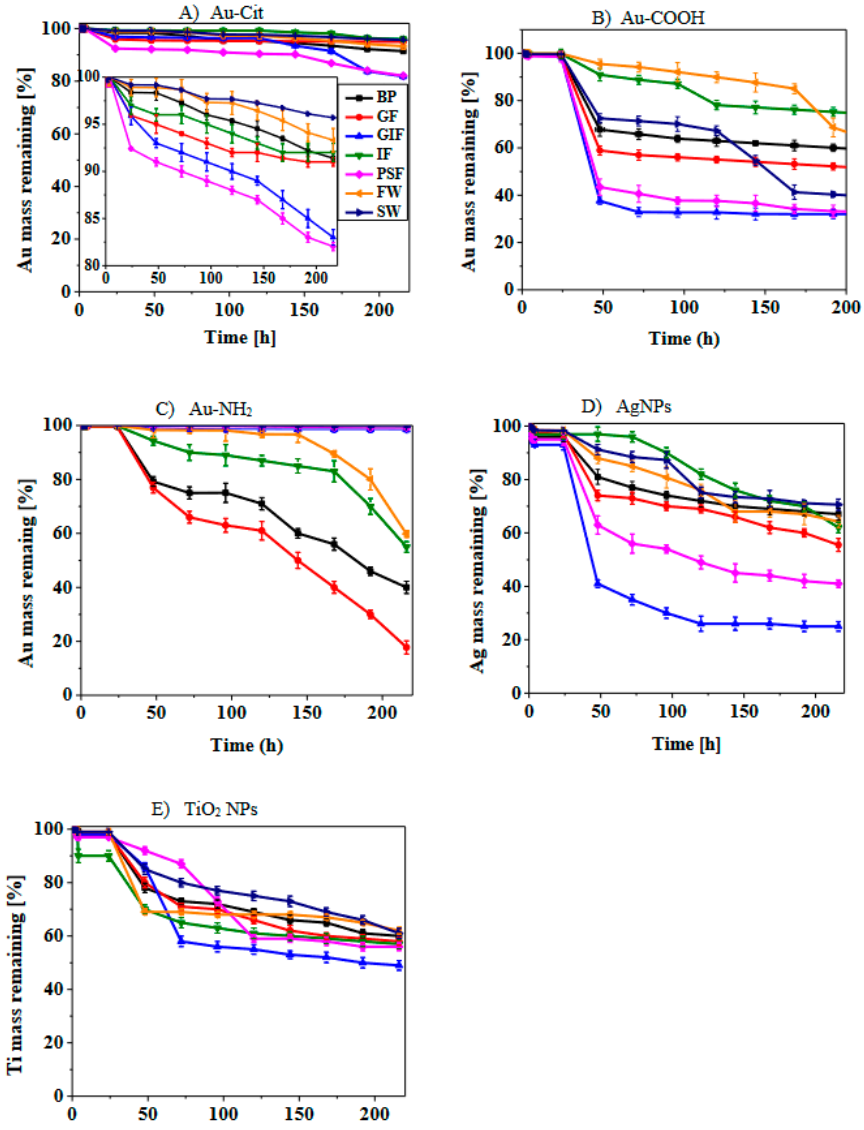

Figure 4. Dissolution profiles for cit-AuNPs (**A**); COOH-AuNPs (**B**); NH_2-AuNPs (**C**); AgNPs (**D**) and TiO_2 NPs (**E**) in simulated fluids. Simulated biological fluids are BP—Blood plasma, GF—Gamble's fluid, GIF—Gastric fluid, IF—Intestinal fluid and PSF—Phagolysosomal fluid. Synthetic environmental media are FW—Freshwater and SW—Seawater.

There was no complete dissolution of all the nanoparticles in all the simulated fluids. Additionally, dissolution was gradual in all cases meaning the release of ions from all the nanoparticle surfaces commenced after 24 h. Of the three types of AuNPs, COOH-AuNPs showed the highest amount of dissolved Au^+ ions with the maximum found in acidic media such as gastric fluid and phagolysosomal fluid. For example, from the starting mass of 1 mg, only 32% and 33% mass remained undissolved in simulated gastric fluid and phagolysosomal fluid, respectively. Over the period of 10 days, cit-AuNPs exhibited the lowest dissolution whereby the maximum dissolution occurred in simulated phagolysosomal fluid. In addition, 81% mass of the particles remained undissolved. However, for NH_2-AuNPs, the dissolution was higher in alkaline media such as simulated blood plasma and Gamble's fluid. The reason for high dissolution of these nanoparticles could be due to the presence of this compound in the simulated fluid which acts as a solubilizing agent

and encourages formation of more soluble complexes [53]. This occurs via the complexation of the nanoparticles with these compounds thereby facilitating the liberation of these nanoparticle ions which ultimately diffuse into the bulk fluid [53]. Interestingly, cit-AuNPs showed limited dissolution compared to functionalized COOH-AuNPs and NH_2-AuNPs. This demonstrates the effect of surface functionalization on dissolution.

AgNPs showed significantly higher dissolution compared to both AuNPs and TiO_2 NPs. TEM images of AgNPs revealed a decrease in size diameter after the end of the dissolution experiments and this is evidence of dissolution. The nanoparticles started releasing ions after 24 h of exposure to simulated fluids. AgNPs dissolved in acidic simulated gastric fluid and phagolysosomal fluid within 48 h but took longer to dissolve in alkaline media such as Gamble's fluid, intestinal fluid and blood plasma. Generally, when particles were exposed to simulated fluids, the dissolution was significantly lower in alkaline media than in acidic media. There was no observable plateau reached during dissolution because under continuous flow through conditions the equilibrium is not reached therefore, the particles keep releasing ions till the end of the dissolution experiments. These results are in agreement with those obtained by Keller et al. [39] where barium sulphate dissolved in phagolysosomal fluid after two years.

For TiO_2 NPs the amount of dissolved Ti ions did not even reach 50% of the initial mass in all simulated fluids regardless of the differences in chemical composition and pH of simulated fluids. The dissolution profile of TiO_2 NPs showed low dissolution in both alkaline and acidic media. From the physicochemical properties data provided and the TEM images in Figure 3, it can be observed that the surface area of TiO_2 NPs is larger compared to that of AuNPs and AgNPs. Research has shown that particles with a larger surface area are less reactive than those with smaller surface area [54,55].

When comparing the dissolution profiles of the synthetic environmental fluids, synthetic seawater had lower dissolution of all three nanoparticles compared to freshwater. However, COOH-AuNPs submerged in seawater dissolved faster than those exposed to freshwater. Even though COOH-AuNPs dissolved faster in seawater, the dissolution of particles in seawater and freshwater was not statistically significant except AgNPs. Particles showed degrees of agglomeration in both waters, but in seawater this was enhanced by the high ionic strength of the media. This could be attributed to the high ionic strength of seawater and the presence of divalent cations in high concentrations [30,56]. The influence of ionic strength is further explained in the discussion section.

3.5. Dissolution Kinetics of AuNPs, AgNPs and TiO_2 NPs

Dissolution kinetics are a crucial factor in determining the safety of nanoparticles, which affect the biodurability and persistence of particles in biological and environmental surroundings. The kinetic model presented in the materials and methodology section was used to determine the dissolution kinetics. Additionally, the biodurability and persistence of AuNPs, AgNPs and TiO_2 NPs were estimated using the dissolution rates and half-times. The data are presented in Table 3. The dissolution rates were determined over a period of 10 days in different simulated biological fluids and synthetic environmental media. From Table 3 it was observed that the dissolution rates of AgNPs were significantly higher ($p < 0.05$) and half-times were shorter in all media compared to those of AuNPs and TiO_2 NPs. For example, the half-times of AgNPs range between the period of 2–7 days, whereas the half-times of AuNPs and TiO_2 NPs fall within the range of 4–12.5 days and 13.5–14.4 days, respectively. TiO_2 NPs had longer half-times regardless of the pH and chemical composition of simulated fluids. Generally, dissolution rates of particles in simulated gastric fluid and phagolysosomal fluid were higher than those of alkaline media such as blood plasma and intestinal fluid with the exception of NH_2-AuNPs. The dissolution rate constants in Table 3 show that the dissolution rates of AuNPs increase in the rate of COOH > NH_2 > citrate. Accordingly, the aggregation follows the inverse order and is influence by the protection of the gold core by the polyethylene-glycol in the case of COOH and NH_2 functionalized nanoparticles. The high dissolution rate of amine functionalized

nanoparticles in simulated blood plasma, Gamble's fluid and intestinal fluid could be due to the interaction of the amine group and components of simulated fluids leading to the formation of more soluble complexes. In the case of synthetic environmental fluids, dissolution in simulated freshwater was faster than in seawater for all the nanoparticles. This is due to the ionic strength of seawater. Furthermore, the dissolution rates data indicate that the rate and extent of dissolution depends on the pH of simulated fluids, chemical composition of the simulated fluids, nanoparticle surface area and aggregation state and are nanoparticle specific. The observed dissolution rates of the nanoparticles in this study followed the order AgNPs > AuNPs > TiO_2 NPs. These results were corroborated by those obtained by Koltermann-Jülly et al. [38]; Keller et al. [39]; Braun et al. [54]; Shinohara et al. [57].

Table 3. Comparison of the dissolution rates and half-times of AuNPs, AgNPs and TiO_2 NPs in simulated fluids.

Nanoparticles	Simulated Fluids	Dissolution Rate k	Half-Time $t_{1/2}$	*p*-Value
		[ng/cm^2/h]	[days]	
Citrate-AuNPs	BP	0.09	10	0.0621
Citrate-AuNPs	GF	0.08	8.6	0.1138
Citrate-AuNPs	GIF	0.08	8.6	0.2144
Citrate-AuNPs	IF	0.06	12.5	0.0720
Citrate-AuNPs	PSF	0.10	7.3	0.0591
Citrate-AuNPs	FW	0.06	11.5	0.0820
Citrate-AuNPs	SW	0.05	12.5	0.0931
COOH-AuNPs	BP	0.08	6.5	0.0656
COOH-AuNPs	GF	0.08	7	0.0809
COOH-AuNPs	GIF	0.10	5	0.0633
COOH-AuNPs	IF	0.06	9	0.0744
COOH-AuNPs	PSF	0.10	5.7	0.0537
COOH-AuNPs	FW	0.06	10	0.0644
COOH-AuNPs	SW	0.09	7.5	0.0937
NH_2-AuNPs	BP	0.13	4	0.1151
NH_2-AuNPs	GF	0.11	6	0.2413
NH_2-AuNPs	GIF	0.06	10	0.0655
NH_2-AuNPs	IF	0.09	7	0.0594
NH_2-AuNPs	PSF	0.06	10	0.0742
NH_2-AuNPs	FW	0.13	4	0.0894
NH_2-AuNPs	SW	0.06	10	0.0942
AgNPs	BP	0.15	4	0.0021
AgNPs	GF	0.15	4	0.0008
AgNPs	GIF	0.18	2	0.0144
AgNPs	IF	0.10	7	0.0420
AgNPs	PSF	0.2	2	0.0231
AgNPs	FW	0.12	6	0.0320
AgNPs	SW	0.10	7	0.0231
TiO_2NPs	BP	3.70×19^{-05}	13.6	0.0778
TiO_2NPs	GF	3.47×10^{-05}	14.3	0.0898
TiO_2NPs	GIF	3.63×10^{-05}	14.1	0.0755
TiO_2NPs	IF	3.67×10^{-05}	14.2	0.0894
TiO_2NPs	PSF	3.65×10^{-05}	14.3	0.0842
TiO_2NPs	FW	3.40×10^{-05}	14.3	0.2329
TiO_2NPs	SW	3.43×10^{-05}	14.4	0.1142

4. Discussion

The high dissolution rates of silver nanoparticles can be attributed to the nanoparticle surface exposed in the simulated fluids. From the TEM images it is evident that these silver nanoparticles are monodispersed and not agglomerated meaning there is a larger particle surface area exposed and this results in enhanced interaction between the components of the simulated fluids and silver nanoparticles thereby encouraging dissolution. However, this is not the case for titanium dioxide nanoparticles, as most of the particles are highly aggregated thereby minimizing the exposed surface area. The effect of poor dissolution because of particle aggregation is dramatically enhanced for poorly soluble particles such as TiO_2 NPs [53,57]. This is because smaller particles have many reactive atoms on the nanoparticle surface and ready to interact with the components of the simulated fluids. In addition, for this reason, TiO_2 NPs take longer to release Ti ions, therefore have low dissolution. Additionally, the TEM images in Figure 2e show high degrees of TiO_2 particle aggregation. In addition, particle aggregation has been shown to slow dissolution [17,58]. This is because as the particles combine to form clusters, this significantly reduces the particle surface area available for dissolution. As a result, the diffusion of Ti ions from the surface is inhibited thereby limiting dissolution.

In addition to the surface area, particle size also affects the dissolution of nanoparticles. From the physicochemical properties outlined in Table 1, it can be observed that AgNPs have the smallest size diameter followed by AuNPs and TiO_2 NPs have the largest particle diameter at 10 nm, 14 nm and 25 nm, respectively. The smaller the particle size the greater the availability of the surface area and this leads to increased chances of ion diffusion from the surface to the bulk fluid. It is for this reason that about 70% mass of Ag^+ ions dissolved in simulated gastric fluid. Whereas the highest dissolution of Ti+ ions could only reach a maximum of 55% in simulated gastric fluid. These results are corroborated by those obtained by Hedberg et al. [50] and Murugadoss et al. [58].

Similar to particle size, particle surface functionalization is another factor that influences the dissolution kinetics of nanoparticles. It could be inferred that the addition of functional groups to the gold nanoparticles surface enhanced dissolution because the amine and carboxyl functional groups have better solubilizing properties compared to citrate stabilized AuNPs. Additionally, citrate was present on the AuNP surface as a stabilizing agent therefore can be easily displaced thereby encouraging nanoparticle agglomeration. These authors also concluded that the rate of dissolution depends on the type of functional group attached to the nanoparticle surface [59–61].

Of all the simulated fluids, synthetic seawater had the highest ionic strength and highest concentration of divalent cations such as Ca^{2+} and Mg^{2+} These divalent cations are known to induce particle aggregation by suppressing the electrostatic repulsive forces between the particle–particle interactions [30,56]. This leads to the reduction in the surface area to volume ratio thereby inhibiting dissolution from occurring. This would explain the low dissolution rates of nanoparticles exposed to synthetic seawater. In so far as particle functionalization is concerned, the presence of Polyethylene glycol (PEG) as a coating agent on the surface of functionalized gold nanoparticles (COOH-AuNPs) and (NH_2-AuNPs) reduces particle agglomeration and this is attributed to the steric repulsive forces imparted by PEG on the nanoparticle surface. These results were corroborated by Botha et al. [44] and Breitner et al. [45].

Generally, when particles were exposed to simulated fluids, the dissolution was significantly lower in alkaline media than in acidic media. This is because acidic conditions, as evidenced by low pH values in gastric and phagolysosomal fluids, enable the oxidation of nanoparticles into ions, increasing their solubility and thus the likelihood of dissolution [24,62]. As a result, nanoparticles exposed to acidic media would be less stable and dissolve more readily than in alkaline media. This could explain why citrate stabilized gold nanoparticles, carboxyl functionalized gold nanoparticles and silver nanoparticles dissolved faster in highly acidic simulated gastric fluid and phagolysosomal fluid. Other researchers corroborate these results and have observed that particles exposed to simulated

fluids characterized by alkaline conditions reach a point of zero charge and generally low amounts of ions get released under these circumstances [53,63].

5. Conclusions

This study investigated the biodurability and persistence of gold, silver and titanium dioxide nanoparticles using the continuous flow-through system. The dissolution kinetics of the nanoparticles were affected by pH, ionic strength, particle aggregation and agglomeration state, as well as surface functionalization. Results showed that all three types of nanoparticles had varying levels of biodurability/persistence; however, silver nanoparticles had the highest rate of dissolution in all simulated biological fluids and synthetic environmental media. This suggests that silver nanoparticles are more likely to have short-term health and environmental effects, which could be similar to those caused by dissolved Ag ions. Gold nanoparticles on the other hand may have the potential to cause both short-term and long-term health and environmental effects depending on their surface functionalization. PEGylated gold nanoparticles are more resistant to agglomeration than citrate-stabilized gold nanoparticles due to ligand-promoted processes that increase dissolution rates. Citrate-stabilized gold nanoparticles have low dissolution rates and can cause long-term health effects as they are more stable and persistent. Titanium dioxide nanoparticles have low dissolution rates, high stability and form agglomerates, making them particularly biodurable and biopersistent in aquatic environments and likely to cause long-term toxicity. To ensure the safety of workers, consumers and the environment, it is critical to study the biodurability and persistence of nanoparticles.

Author Contributions: O.M.: Conceptualization, Methodology, Validation, Formal analysis, Investigation, Writing—Original draft E.C.: Resources, Writing—Review and Editing, Visualization M.G.: Resources, Writing—Review and Editing, Visualization, Supervision, Funding. All authors have read and agreed to the published version of the manuscript.

Funding: This research was funded by the European Union's Horizon 2020 research and innovation program grant number 814401 (Gov4Nano) and the Department of Science and Innovation South Africa.

Data Availability Statement: Data will be made freely available on request, it can be requested from mary.gulumian@NWU.ac.za.

Acknowledgments: We gratefully acknowledge funding from the European Union's Horizon 2020 research and innovation program grant number 814401 (Gov4Nano). We also would like to acknowledge the South African Department of Science and Innovation (DSI) and the University of Northwest for their assistance.

Conflicts of Interest: The authors declare no conflict of interest.

References

1. Bove, P.; Malvindi, M.A.; Kote, S.S.; Bertorelli, R.; Summa, M.; Sabella, S. Dissolution test for risk assessment of nanoparticles: A pilot study. *Nanoscale* **2017**, *9*, 6315–6326. [CrossRef] [PubMed]
2. Landvik, N.E.; Skaug, V.; Mohr, B.; Verbeek, J.; Zienolddiny, S. Criteria for grouping of manufactured nanomaterials to facilitate hazard and risk assessment, a systematic review of expert opinions. *Regul. Toxicol. Pharmacol.* **2018**, *95*, 270–279. [CrossRef] [PubMed]
3. Adewale, O.B.; Davids, H.; Cairncross, L.; Roux, S. Toxicological Behavior of Gold Nanoparticles on Various Models: Influence of Physicochemical Properties and Other Factors. *Int. J. Toxicol.* **2019**, *38*, 357–384. [CrossRef] [PubMed]
4. Elahi, N.; Kamali, M.; Baghersad, M.H. Recent biomedical applications of gold nanoparticles: A review. *Talanta* **2018**, *184*, 537–556. [CrossRef]
5. Fan, J.; Cheng, Y.; Sun, M. Functionalized Gold Nanoparticles: Synthesis, Properties and Biomedical Applications. *Chem. Rec.* **2020**, *20*, 1474–1504. [CrossRef]
6. Kalimuthu, K.; Cha, B.S.; Kim, S.; Park, K.S. Eco-friendly synthesis and biomedical applications of gold nanoparticles: A review. *Microchem. J.* **2019**, *152*, 104296. [CrossRef]
7. Bapat, R.A.; Chaubal, T.V.; Joshi, C.P.; Bapat, P.R.; Choudhury, H.; Pandey, M.; Gorain, B.; Kesharwani, P. An overview of application of silver nanoparticles for biomaterials in dentistry. *Mater. Sci. Eng. C* **2018**, *91*, 881–898. [CrossRef]

8. Burdușel, A.C.; Gherasim, O.; Grumezescu, A.M.; Mogoantă, L.; Ficai, A.; Andronescu, E. Biomedical applications of silver nanopar-ticles: An up-to-date overview. *Nanomaterials* **2018**, *8*, 681. [CrossRef]
9. Irshad, M.A.; Nawaz, R.; Rehman, M.Z.U.; Adrees, M.; Rizwan, M.; Ali, S.; Ahmad, S.; Tasleem, S. Synthesis, characterization and advanced sustainable applications of titanium dioxide nanoparticles: A review. *Ecotoxicol. Environ. Saf.* **2021**, *212*, 111978. [CrossRef]
10. Mbanga, O.; Cukrowska, E.; Gulumian, M. Dissolution of titanium dioxide nanoparticles in synthetic biological and environmental media to predict their biodurability and persistence. *Toxicol. Vitr.* **2022**, *84*, 105457. [CrossRef]
11. Kansara, K.; Bolan, S.; Radhakrishnan, D.; Palanisami, T.; Al-Muhtaseb, A.H.; Bolan, N.; Vinu, A.; Kumar, A.; Karakoti, A. A critical review on the role of abiotic factors on the transformation, environmental identity and toxicity of engineered nanomaterials in aquatic environment. *Environ. Pollut.* **2022**, *296*, 118726. [CrossRef] [PubMed]
12. OECD. *Joint Meeting of the Chemicals Committee and the Working Party on Chemicals, Pesticides and Biotechnology*; OECD: Paris, France, 2018; Volume 86.
13. Klaessig, F.C. Dissolution as a paradigm in regulating nanomaterials. *Environ. Sci. Nano* **2018**, *5*, 1070–1077. [CrossRef]
14. Sauer, U.G.; Werle, K.; Waindok, H.; Hirth, S.; Hachmöller, O.; Wohlleben, W. Critical Choices in Predicting Stone Wool Biodurability: Lysosomal Fluid Compositions and Binder Effects. *Chem. Res. Toxicol.* **2021**, *34*, 780–792. [CrossRef] [PubMed]
15. Gulumian, M.; Cassee, F.R. Safe by design (SbD) and nanotechnology: A much-discussed topic with a prudence? *Part. Fibre Toxicol.* **2021**, *18*, 32. [CrossRef]
16. Innes, E.; Yiu, H.H.P.; McLean, P.; Brown, W.; Boyles, M. Simulated biological fluids—A systematic review of their biological relevance and use in relation to inhalation toxicology of particles and fibres. *Crit. Rev. Toxicol.* **2021**, *51*, 217–248. [CrossRef]
17. Sohal, I.S.; Cho, Y.K.; O'fallon, K.S.; Gaines, P.; Demokritou, P.; Bello, D. Dissolution Behavior and Biodurability of Ingested Engineered Nanomaterials in the Gastrointestinal Environment. *ACS Nano* **2018**, *12*, 8115–8128. [CrossRef]
18. Utembe, W.; Potgieter, K.; Stefaniak, A.B.; Gulumian, M. Dissolution and biodurability: Important parameters needed for risk as-sessment of nanomaterials. *Part. Fibre Toxicol.* **2015**, *12*, 11. [CrossRef]
19. Laux, P.; Riebeling, C.; Booth, A.M.; Brain, J.D.; Brunner, J.; Cerrillo, C.; Creutzenberg, O.; Estrela-Lopis, I.; Gebel, T.; Johanson, G.; et al. Biokinetics of nanomaterials: The role of biopersistence. *Nanoimpact* **2017**, *6*, 69–80. [CrossRef]
20. Avellan, A.; Simonin, M.; McGivney, E.; Bossa, N.; Spielman-Sun, E.; Rocca, J.D.; Bernhardt, E.S.; Geitner, N.K.; Unrine, J.M.; Wiesner, M.R.; et al. Gold nanoparticle biodissolution by a freshwater macrophyte and its associated microbiome. *Nat. Nanotechnol.* **2018**, *13*, 1072–1077. [CrossRef]
21. Boldeiu, A.; Simion, M.; Mihalache, I.; Radoi, A.; Banu, M.; Varasteanu, P.; Nadejde, P.; Vasile, E.; Acasandrei, A.; Popescu, R.C.; et al. Comparative analysis of honey and citrate stabilized gold nanoparticles: In vitro interaction with proteins and toxicity studies. *J. Photochem. Photobiol. B Biol.* **2019**, *197*, 111519. [CrossRef]
22. John, T.; Gladytz, A.; Kubeil, C.; Martin, L.L.; Risselada, H.J.; Abel, B. Impact of nanoparticles on amyloid peptide and protein ag-gregation: A review with a focus on gold nanoparticles. *Nanoscale* **2018**, *10*, 20894–20913. [CrossRef] [PubMed]
23. Nambiar, S.; Osei, E.; Fleck, A.; Darko, J.; Mutsaers, A.J.; Wettig, S. Synthesis of curcumin-functionalized gold nanoparticles and cytotoxicity studies in human prostate cancer cell line. *Appl. Nanosci.* **2018**, *8*, 347–357. [CrossRef]
24. Fernando, I.; Zhou, Y. Impact of pH on the stability, dissolution and aggregation kinetics of silver nanoparticles. *Chemosphere* **2019**, *216*, 297–305. [CrossRef] [PubMed]
25. Loza, K.; Diendorf, J.; Sengstock, C.; Ruiz-Gonzalez, L.; Gonzalez-Calbet, J.M.; Vallet-Regi, M.; Köller, M.; Epple, M. The dissolution and biological effects of silver nanoparticles in biological media. *J. Mater. Chem. B* **2014**, *2*, 1634–1643. [CrossRef]
26. Mbanga, O.; Cukrowska, E.; Gulumian, M. Dissolution kinetics of silver nanoparticles: Behaviour in simulated biological fluids and synthetic environmental media. *Toxicol. Rep.* **2022**, *9*, 788–796. [CrossRef] [PubMed]
27. Zienkiewicz-Strzałka, M.; Deryło-Marczewska, A.; Skorik, Y.A.; Petrova, V.A.; Choma, A.; Komaniecka, I. Silver Nanoparticles on Chitosan/Silica Nanofibers: Characterization and Antibacterial Activity. *Int. J. Mol. Sci.* **2020**, *21*, 166. [CrossRef] [PubMed]
28. Baccaro, M.; Undas, A.K.; De Vriendt, J.; Van Den Berg, J.H.J.; Peters, R.J.B.; Van Den Brink, N.W. Ageing, dissolution and biogenic formation of nanoparticles: How do these factors affect the uptake kinetics of silver nanoparticles in earthworms? *Environ. Sci. Nano* **2018**, *5*, 1107–1116. [CrossRef]
29. Jiang, X.; Wu, Y.; Gray, P.; Zheng, J.; Cao, G.; Zhang, H.; Zhang, X.; Boudreau, M.; Croley, T.R.; Chen, C.; et al. Influence of gastrointestinal environment on free radical generation of silver nanoparticles and implications for their cytotoxicity. *Nanoimpact* **2018**, *10*, 144–152. [CrossRef]
30. de Souza, T.A.J.; Rosa Souza, L.R.; Franchi, L.P. Silver nanoparticles: An integrated view of green synthesis methods, transformation in the environment, and toxicity. *Ecotoxicol. Environ. Saf.* **2019**, *171*, 691–700. [CrossRef]
31. Zhong, L.; Hu, X.; Cao, Z.; Wang, H.; Chen, Y.; Lian, H. Aggregation and dissolution of engineering nano Ag and ZnO pre-treated with natural organic matters in the simulated lung biological fluids. *Chemosphere* **2019**, *225*, 668–677. [CrossRef]
32. Schmidt, J.; Vogelsberger, W. Dissolution Kinetics of Titanium Dioxide Nanoparticles: The Observation of an Unusual Kinetic Size Effect. *J. Phys. Chem. B* **2006**, *110*, 3955–3963. [CrossRef] [PubMed]
33. Schmidt, J.; Vogelsberger, W. Aqueous Long-Term Solubility of Titania Nanoparticles and Titanium (IV) Hydrolysis in a Sodium Chloride System Studied by Adsorptive Stripping Voltammetry. *J. Solut. Chem.* **2009**, *38*, 1267–1282. [CrossRef]
34. Shkol'nikov, E.V. Thermodynamics of the dissolution of amorphous and polymorphic TiO2 modifications in acid and alkaline media. *Russ. J. Phys. Chem. A* **2016**, *90*, 567–571. [CrossRef]

35. Wang, H.; Burgess, R.M.; Cantwell, M.G.; Portis, L.M.; Perron, M.M.; Wu, F.; Ho, K.T. Stability and aggregation of silver and titanium dioxide nanoparticles in seawater: Role of salinity and dissolved organic carbon. *Environ. Toxicol. Chem.* **2014**, *33*, 1023–1029. [CrossRef] [PubMed]
36. Marques, M.R.C.; Loebenberg, R.; Almukainzi, M. Simulated Biological Fluids with Possible Application in Dissolution Testing. *Dissolution Technol.* **2011**, *18*, 15–28. [CrossRef]
37. Keller, J.G.; Peijnenburg, W.; Werle, K.; Landsiedel, R.; Wohlleben, W. Understanding Dissolution Rates via Continuous Flow Systems with Physiologically Relevant Metal Ion Saturation in Lysosome. *Nanomaterials* **2020**, *10*, 311. [CrossRef] [PubMed]
38. Koltermann-Jülly, J.; Keller, J.G.; Vennemann, A.; Werle, K.; Müller, P.; Ma-Hock, L.; Landsiedel, R.; Wiemann, M.; Wohlleben, W. Abiotic dissolution rates of 24 (nano)forms of 6 substances compared to macrophage-assisted dissolution and in vivo pulmonary clearance: Grouping by biodissolution and transformation. *NanoImpact* **2018**, *12*, 29–41. [CrossRef]
39. Keller, J.G.; Graham, U.M.; Koltermann-Jülly, J.; Gelein, R.; Ma-Hock, L.; Landsiedel, R.; Wiemann, M.; Oberdörster, G.; Elder, A.; Wohlleben, W. Predicting dissolution and transformation of inhaled nanoparticles in the lung using abiotic flow cells: The case of barium sulfate. *Sci. Rep.* **2020**, *10*, 458, Correction in *Sci. Rep.* **2021**, *11*, 8813. [CrossRef]
40. Badiah, H.I.; Seedeh, F.; Supriyanto, G.; Zaidan, A.H. Synthesis of Silver Nanoparticles and the Development in Analysis Method. *IOP Conf. Series: Earth Environ. Sci.* **2019**, *217*, 012005. [CrossRef]
41. Dobrucka, R. Synthesis of Titanium Dioxide Nanoparticles Using Echinacea purpurea Herba. *Iran. J. Pharm. Res. IJPR* **2017**, *16*, 756–762.
42. Monfared, A.H.; Jamshidi, M. Synthesis of polyaniline/titanium dioxide nanocomposite (PAni/TiO2) and its application as pho-tocatalyst in acrylic pseudo paint for benzene removal under UV/VIS lights. *Prog. Org. Coat.* **2019**, *136*, 105257. [CrossRef]
43. Pashkov, D.M.; Guda, A.A.; Kirichkov, M.V.; Martini, A.; Soldatov, S.A.; Soldatov, A.V. Quantitative Analysis of the UV–Vis Spectra for Gold Nanoparticles Powered by Supervised Machine Learning. *J. Phys. Chem. C* **2021**, *125*, 8656–8666. [CrossRef]
44. Botha, T.L.; James, T.E.; Wepener, V. Comparative Aquatic Toxicity of Gold Nanoparticles and Ionic Gold Using a Species Sensi-tivity Distribution Approach. *J. Nanomater.* **2015**, *2015*, 986902. [CrossRef]
45. Breitner, E.K.; Hussain, S.M.; Comfort, K.K. The role of biological fluid and dynamic flow in the behavior and cellular interactions of gold nanoparticles. *J. Nanobiotechnology* **2015**, *13*, 2–10. [CrossRef] [PubMed]
46. De Matteis, V.; Cascione, M.; Brunetti, V.; Toma, C.C.; Rinaldi, R. Toxicity assessment of anatase and rutile titanium dioxide nano-particles: The role of degradation in different pH conditions and light exposure. *Toxicol. Vitr.* **2016**, *37*, 201–210. [CrossRef]
47. Zhong, L.; Yu, Y.; Lian, H.; Hu, X.; Fu, H.; Chen, Y. Solubility of nano-sized metal oxides evaluated by using in vitro sim-ulated lung and gastrointestinal fluids: Implication for health risks. *J. Nanoparticle Res.* **2017**, *19*, 375. [CrossRef]
48. Klonos, P.; Dapei, G.; Sulym, I.Y.; Zidropoulos, S.; Sternik, D.; Deryło-Marczewska, A.; Borysenko, M.V.; Gun'ko, V.M.; Kyritsis, A.; Pissis, P. Morphology and molecular dynamics investigation of PDMS adsorbed on titania nanoparticles: Effects of polymer molecular weight. *Eur. Polym. J.* **2016**, *74*, 64–80. [CrossRef]
49. Lin, X.; Li, J.; Ma, S.; Liu, G.; Yang, K.; Tong, M.; Lin, D. Toxicity of TiO2 Nanoparticles to Escherichia coli: Effects of Particle Size, Crystal Phase and Water Chemistry. *PLoS ONE* **2014**, *9*, e110247. [CrossRef]
50. Hedberg, J.; Blomberg, E.; Wallinder, I.O. In the Search for Nanospecific Effects of Dissolution of Metallic Nanoparticles at Freshwater-Like Conditions: A Critical Review. *Environ. Sci. Technol.* **2019**, *53*, 4030–4044. [CrossRef]
51. Pujalté, I.; Dieme, D.; Haddad, S.; Serventi, A.M.; Bouchard, M. Toxicokinetics of titanium dioxide (TiO2) nanoparticles after inha-lation in rats. *Toxicol. Lett.* **2017**, *265*, 77–85. [CrossRef]
52. Borm, P.; Klaessig, F.C.; Landry, T.D.; Moudgil, B.; Pauluhn, J.; Thomas, K.; Trottier, R.; Wood, S. Research Strategies for Safety Evaluation of Nanomaterials, Part V: Role of Dissolution in Biological Fate and Effects of Nanoscale Particles. *Toxicol. Sci.* **2006**, *90*, 23–32. [CrossRef] [PubMed]
53. Avramescu, M.L.; Rasmussen, P.E.; Chénier, M.; Gardner, H.D. Influence of pH, particle size and crystal form on dissolution be-haviour of engineered nanomaterials. *Environ. Sci. Pollut. Res.* **2017**, *24*, 1553–1564. [CrossRef] [PubMed]
54. Braun, K.; Pochert, A.; Beck, M.; Fiedler, R.; Gruber, J.; Lindén, M. Dissolution kinetics of mesoporous silica nanoparticles in different simulated body fluids. *J. Sol-Gel Sci. Technol.* **2016**, *79*, 319–327. [CrossRef]
55. Donovan, A.R.; Adams, C.D.; Ma, Y.; Stephan, C.; Eichholz, T.; Shi, H. Single particle ICP-MS characterization of titanium dioxide, silver, and gold nanoparticles during drinking water treatment. *Chemosphere* **2016**, *144*, 148–153. [CrossRef]
56. Cupi, D.; Hartmann, N.B.; Baun, A. Influence of pH and media composition on suspension stability of silver, zinc oxide, and titanium dioxide nanoparticles and immobilization of Daphnia magna under guideline testing conditions. *Ecotoxicol. Environ. Saf.* **2016**, *127*, 144–152. [CrossRef]
57. Shinohara, N.; Zhang, G.; Oshima, Y.; Kobayashi, T.; Imatanaka, N.; Nakai, M.; Sasaki, T.; Kawaguchi, K.; Gamo, M. Kinetics and dissolution of intratracheally administered nickel oxide nanomaterials in rats. *Part. Fibre Toxicol.* **2017**, *14*, 48. [CrossRef]
58. Murugadoss, S.; Brassinne, F.; Sebaihi, N.; Petry, J.; Cokic, S.M.; Van Landuyt, K.L.; Godderis, L.; Mast, J.; Lison, D.; Hoet, P.H.; et al. Agglomeration of titanium dioxide nano-particles increases toxicological responses in vitro and in vivo. *Part. Fibre Toxicol.* **2020**, *17*, 10. [CrossRef]
59. Bozich, J.S.; Lohse, S.E.; Torelli, M.D.; Murphy, C.J.; Hamers, R.J.; Klaper, R.D. Surface chemistry, charge and ligand type impact the toxicity of gold nanoparticles to Daphnia magna. *Environ. Sci. Nano* **2014**, *1*, 260–270. [CrossRef]
60. Li, Y.; Zhang, W.; Niu, J.; Chen, Y. Surface-coating-dependent dissolution, aggregation, and reactive oxygen species (ROS) gener-ation of silver nanoparticles under different irradiation conditions. *Environ. Sci. Technol.* **2013**, *47*, 10293–10301.

61. Tejamaya, M.; Römer, I.; Merrifield, R.C.; Lead, J.R. Stability of Citrate, PVP, and PEG Coated Silver Nanoparticles in Ecotoxicology Media. *Environ. Sci. Technol.* **2012**, *46*, 7011–7017. [CrossRef]
62. Chambers, B.A.; Afrooz, A.R.M.N.; Bae, S.; Aich, N.; Katz, L.; Saleh, N.B.; Kirisits, M.J. Effects of Chloride and Ionic Strength on Physical Morphology, Dissolution, and Bacterial Toxicity of Silver Nanoparticles. *Environ. Sci. Technol.* **2014**, *48*, 761–769. [CrossRef] [PubMed]
63. Xu, N.; Cheng, X.; Wang, D.; Xu, X.; Huangfu, X.; Li, Z. Effects of Escherichia coli and phosphate on the transport of titanium dioxide nanoparticles in heterogeneous porous media. *Water Res.* **2018**, *146*, 264–274. [CrossRef] [PubMed]

CHAPTER 5

5 Conclusions and recommendations

5.1 Conclusions

The present research determined the dissolution behaviour and dissolution kinetics of gold, silver and titanium dioxide nanoparticles in various simulated body fluids and synthetic environmental media to predict their biodurability and persistence. The study focused on the use of the static dissolution protocol and the continuous flow-through system. Generally, the static dissolution system involves exposing a fixed mass of particles to a relatively confined volume of a synthetic fluid contained in a beaker, followed by storing the particles in a dialysis membrane. However, a limitation of the static dissolution protocol is that the limited volume of the media may reach saturation prior to equilibrium being achieved, thus inhibiting dissolution. In contrast, the continuous flow-through dissolution system is a flow-through chamber that contains particles isolated from the test fluid by a membrane. The particles are suspended in the chamber while test fluid passes over the membrane and through the fraction collector. This allows for the collection of ions or molecules from the particles that have diffused through the membrane. Therefore, the continuous flow-through method of dissolution testing is believed to be more reflective of dissolution that occurs in biological surroundings, therefore, it is recommended to prevent reaching equilibrium, which can inhibit dissolution.

Regarding the behaviour of the three tested nanoparticles, silver nanoparticles dissolved significantly faster compared to gold nanoparticles and titanium dioxide nanoparticles. Titanium dioxide nanoparticles were prone to aggregation as soon as they were immersed in physiological fluids and synthetic environmental media. Whereas polyethylene glycol reduced the propensity of functionalized gold nanoparticles to come together to form clusters. The dissolution of particles was higher in simulated acidic media such as gastric and phagolysosomal fluids compared to simulated alkaline media such as Gamble's fluid, blood plasma and intestinal fluid. Additionally, particles dissolved faster in synthetic seawater compared to freshwater. And this was regulated by the effect of ionic strength on

dissolution which encouraged the formation of more soluble complexes. From the results it was deduced that nanoparticle dissolution is strongly influenced by media pH & ionic strength, surface functionalization and particle aggregation/agglomeration state. The dissolution of all the particles followed the first order reaction kinetics with AgNPs having high dissolution rates and shorter halt-times. Meaning AgNPs would exhibit short-term effects which could be identical to those caused by dissolved ions. This was not the case for AuNPs and TiO_2 NPs which had low dissolution rates and long half-times. The low dissolution of gold nanoparticles and titanium dioxide nanoparticles implies that these particles will have a longer circulation time in the blood and higher accumulation in the body thereby causing long term health effects. The dissolution kinetics indicate that titanium dioxide nanoparticles are more likely to accumulate in the body and cause adverse health effects after long periods of time compared to silver and gold nanoparticles.

5.2 Recommendations

- ✓ Safety assessment of nanoparticles should be incorporated in the early developmental stages of nano-enabled products rather than later where they have reached the market.

- ✓ There should be a standardized protocol/model to be used for the risk assessment of nanoparticles. The protocol should be easily amenable, relatively fast, economically viable, simple to perform and most importantly representative of *in vivo* surroundings in order to accurately predict the behaviour of nanoparticles in real-life situations.

- ✓ It is also highly recommended that dissolution is considered when conducting the risk assessment of nanoparticles.

- ✓ Researchers, regulators, policy makers, public and the private sector should establish a criterion for the classification and labelling of consumer products containing nanomaterials. Additionally, there is a need to develop disposal strategies to minimize the potential risks for undesirable environmental health and safety.